6-25-2020 10:00 AM

Mass spectrometry identification of membrane-type 1 matrix metalloproteinase (MT1-MMP) binding partners following co-immunoprecipitation in MCF-7 cells

Bradley Bork, *The University of Western Ontario*

Supervisor: Damjanovski, Sashko, *The University of Western Ontario*

A thesis submitted in partial fulfillment of the requirements for the Master of Science degree in Biology

Abstract

Membrane-type 1 matrix metalloproteinase (MT1-MMP) is an integral multidomain membrane protease involved in extracellular matrix remodelling. No longer recognized solely as a destructive enzyme, MT1-MMP proteolytic and non-proteolytic activities are involved in a variety of cellular processes. I hypothesized that the diverse functions of MT1-MMP are dependent on domain-specific binding partner interactions that elicit a cellular response. Using a combination of co-immunoprecipitation and mass spectrometry, 248 unique proteins were isolated in MT1-MMP variant expressing MCF-7 cells. Newly identified binding partners suggest potential roles of MT1-MMP in the nucleus, endoplasmic reticulum, cytoplasm, and plasma membrane. Additionally, the cytoplasmic domain of MT1-MMP attenuates canonical transforming growth factor beta (TGF-β) signalling through an unknown mechanism. The results of this proteomic study add proteins to a growing catalogue of binding partners involved in proper localization and function of MT1-MMP.

Keywords

ECM remodelling

matrix metalloproteinase (MMP)

membrane-type 1 matrix metalloproteinase (MT1-MMP)

MCF-7

co-immunoprecipitation

mass spectrometry

transforming growth factor beta (TGF-β)

Summary for Lay Audience

The extracellular matrix (ECM) is an interconnected network of proteins that provides structural support to cells, tissues, and organ systems. For cells, the building blocks of life, to migrate to new places within a growing organism, the ECM needs to be remodelled. It is important to note that migration is necessary for proper development and function, but abnormal cell migration is involved in various pathologies. Matrix metalloproteinases (MMPs) are proteins secreted by the cell into the ECM, where they function to break down the ECM so the cell can move freely. There are many types of MMPs that can collectively degrade all the different parts of the ECM. In my project, I studied membrane-type 1 matrix metalloproteinase (MT1-MMP). Early research deemed MT1-MMP a destructive enzyme observed in cancerous tissue. However, MT1-MMP not only degrades the ECM so the cell can move, but part of this protein extends into the cell (cytoplasmic domain), where it is observed to communicate to the cell when and where to migrate. For this reason, MT1-MMP is described as a multifunctional protease. The purpose of my research was to further investigate the function of MT1-MMP, more specifically through its interaction with other proteins. Here, 248 proteins were identified that associate with MT1-MMP in breast cancer cells. These newly identified proteins point to possible novel interactions and functions of MT1-MMP throughout the cell, not just its role as an enzyme. Additionally, removal of the cytoplasmic domain induces transforming growth factor beta (TGF-β) signalling, an important regulator of cellular processes. TGF-β signalling, in addition to having critical embryonic roles, has dual functions in tumours, acting either as a suppressor or activator. Understanding what MT1-MMP interacts with is critical due to its involvement in many important processes in development, wound healing, and disease.

Acknowledgments

Most importantly, I would like to thank my supervisor, Dr. Sashko Damjanovski, without whom none of this would have been possible. Always insightful, pleasant, and supportive, you've made my time in the Sash Lab a tremendous experience. I never would have thought that starting off as an undergrad volunteer in your lab would have brought me to where I am today. Thank you for believing in me!

Many thanks to all who have helped me along the way. To my advisory committee, Dr. Dean Betts and Dr. Greg Kelly, you have been a source of guidance and support throughout my studies. A huge thanks to Dr. Kelly and Dr. Kohalmi's labs for the use of equipment, lab reagents, and always helping me out in a bind. Additionally, thanks to the Don Rix Protein Identification Facility, especially Paula Pittock, for all their work and insight regarding mass spectrometry.

To my lab family, you've made being a member of the Sash Lab an immensely enjoyable experience. One of which I will never forget. To Dr. Mario Cepeda and Jake Pelling, thank you for the cell lines and opening up new research possibilities in the lab. To Dr. Jessica Willson, you've been my mentor since the beginning. The role you've played in my development as a scientist and person will have an everlasting impact. To Carlie Muir, your support and friendship in and outside of the lab is so great that I cannot express it in words. But I can truly say that no matter where our journeys take us, you will always be a dear friend of mine. To Rachel Wise, I always enjoy your company and know you will succeed in whatever you put your mind to. To all of you, I wish nothing but the best in life!

To all my friends along the way – Bonnie, Chris, Christy, Emily, and Jordan (alphabetical, not in order of favourites) – my most cherished memories of graduate school involve each and every one of you. No matter the circumstance, you were always there for me.

Finally, thank you to my family for their unwavering support and unconditional love. The opportunities I have rest fully on the sacrifices they've made. Although they didn't understand it, they are the driving force I needed in this work.

Table of Contents

List of Tables

List of Figures

List of Appendices

List of Abbreviations

Note: SI units are not listed.

Akt	Protein kinase B
ANOVA	Analysis of variance
AP-MS	Affinity purification – mass spectrometry
BCA	Bicinchoninic acid
BRCA	Breast cancer gene
BSA	Bovine serum albumin
CD	Cytoplasmic domain
CD44	Cluster of differentiation 44
cDNA	Complementary deoxyribonucleic acid
Co-IP	Co-immunoprecipitation
COPII	Coat protein complex 2
DMEM	Dulbecco's modified eagle's medium
DTT	Dithiothreitol
ECM	Extracellular matrix
EDTA	Ethylenediaminetetraacetic acid
EGF	Epidermal growth factor
EGFR	Epidermal growth factor receptor
EMMPRIN	Extracellular matrix metalloproteinase inducer
EMT	Epithelial-mesenchymal transition
ER	Endoplasmic reticulum
ERK	Extracellular regulated kinase
F1,6BP	fructose-1,6-bisphosphate
FBS	Fetal bovine serum
FDR	False discovery rate
FGF	Fibroblast growth factor
FIH	Factor-inhibiting HIF-1α
FMR1	Fragile X mental retardation 1
FXR	Fragile X-related protein
GAPDH	Glyceraldehyde-3-phosphate dehydrogenase
GPI	Glycosylphophatidylinositol

GRASP55	Golgi reassembly and stacking protein 55
GSK	Glycogen synthase kinase
GTP	Guanosine triphosphate
HA	Hyaluronic acid
HIF	Hypoxia-inducing factor
HMMR	Hyaluronan mediated motility receptor
HRP	Horseradish peroxidase
HSP	Heat shock protein
ICAT	Isotope-coded affinity tagging
IgG	Immunoglobin G
IP	Immunoprecipitation
KEGG	Kyoto encyclopedia of genes and genomes
LC-MS/MS	Liquid chromatography-tandem mass spectrometry
LTBP	Latent TGF-β binding protein
LYVE-1	Lymphatic vessel endothelial hyaluronan receptor-1
MAPK	Mitogen-activated protein kinase
MCF-7	Michigan Cancer Foundation 7
MDA-MB-231	MD Anderson Metastatic Breast 231
MMP	Matrix metalloproteinase
mRNA	Messenger ribonucleic acid
MT1-MMP	Membrane-type 1 matrix metalloproteinase
NLS	Nuclear localization sequence
NP-40	Nonidet P-40
PBS	Phosphate-buffered saline
PI3K	Phosphoinositide 3-kinase
PPI	Protein-protein interaction
PVDF	Polyvinylidene fluoride
qPCR	Quantitative (real-time) polymerase chain reaction
Raf	Rapidly accelerated fibrosarcoma
Ras	Rat sarcoma
RECK	Reversion-inducing cysteine-rich protein with Kazal motifs
RIPA	Radioimmunoprecipitation assay buffer
RNA	Ribonucleic acid

SDS	Sodium dodecyl sulphate
SDS-PAGE	Sodium dodecyl sulphate polyacrylamide gel electrophoresis
SEM	Standard error of the mean
SLC	Small latent complex
SMAD	Mothers against decapentaplegic homolog
Src	Proto-oncogene tyrosine-protein kinase
SRP	Signal recognition particle
STRING	Search Tool for the Retrieval of Interacting Genes/Proteins
TBST	Tris buffered saline with Tween
TCA	Trichloroacetic acid
TGF-β	Transforming growth factor beta
TIMP	Tissue inhibitors of metalloproteinases
TRAP	Translocon-associated protein
UPR	Unfolded protein response
VEGF	Vascular endothelial growth factor
VTN	Vitronectin
ZEB	Zinc finger E-box binding homeobox

1 INTRODUCTION

1.1 Extracellular matrix

The extracellular matrix (ECM) is a heterogenous, three-dimensional network of secreted macromolecules that provides structural support to the embedded cells. Composed primarily of water, polysaccharides, and proteins, the composition and structure of the ECM influences the function of cells in tissues (Theocharis et al., 2016). Matrix components bind to each other as well as cell adhesion receptors, typically integrins, with which cells integrate signals from the ECM. It is important to note that cell-ECM interactions are reciprocal. All cell types locally synthesize and secrete ECM macromolecules, which in turn can influence the behaviour of surrounding cells (Kim et al., 2011). For this reason, the ECM is important for cellular growth, migration, differentiation, survival, homeostasis, and morphogenesis (Clause and Barker, 2013; Frantz et al., 2010).

Structurally, the ECM can be classified into two components: the interstitial matrix and basement membrane. These two domains share a basic structure defined by a collagen scaffold, but the types of collagen and resulting three-dimensional structure are drastically different (Bosman and Stamenkovic, 2003). The interstitial matrix is primarily deposited by stromal cells and composed of fibrillar collagens, proteoglycans, and glycoproteins that contribute to the tensile strength of the tissue (Egeblad et al., 2010; Lu et al., 2012). The basement membrane is a sheet-like barrier produced jointly by epithelial, endothelial, and stromal cells. Composed primarily of type IV collagen, laminins, fibronectin, and linker proteins, the basement membrane is much more compact and less porous than the interstitial matrix (Egeblad et al., 2010; Lu et al., 2012). Separating epithelial cells from the surrounding stroma, the basement membrane is a specialized form of ECM that is not only crucial to maintain cell polarity, but also serves to support and inhibit the movement of cells (Kalluri, 2003; Pöschl et al., 2004). The mechanisms involved in the process of cell movement are well understood. In brief, a migrating cell will become polar in which actin-based membrane protrusions will adhere to specific ECM substrate through cell surface integrins, giving polarity to the cell (leading edge). As the cell advances, posterior focal adhesions will detach to facilitate

forward movement of the cell body (trailing edge) (Trepat et al., 2012). Coordinated movement of the cell is primarily guided by cell-ECM and cell-cell cues (Reig et al., 2014). With this in mind, the ECM is not only a physical scaffold supporting the cell, but also a reservoir of biologically active molecules that can modulate cell movement (Chirco et al., 2006; Egeblad and Werb, 2002).

Independent of its structural function, the biochemical properties of the ECM rely on its association with growth factors, cytokines, and chemokines within the matrix that allow cells to sense and interact with their environment through various signal transduction cascades. Signalling molecules that elicit a cellular response can be sequestered within the ECM, limiting diffusion and maintaining homeostasis. Then, at a developmentally or physiologically relevant time, these molecules can be locally released from the matrix through proteolytic processing (Theocharis et al., 2016). For example, vascular endothelial growth factor (VEGF) and fibroblast growth factor (FGF) 2 bind to heparan sulfate proteoglycans, and are sequestered in the ECM (Ortéga et al., 1998; Robinson and Stringer, 2001; Walker et al., 1994). This retention creates a chemical gradient important during development for proper cell differentiation (Hynes, 2009). The interaction between FGF-2 and heparan sulfate is also required for binding to, and stabilization of, the FGF receptors (Rapraeger et al., 1991; Schlessinger et al., 2000; Yayon et al., 1991). Through sequestering and release of signalling molecules, the ECM can indirectly influence cell behaviour. However, ECM proteins themselves can serve as ligands for cell receptors, thus directly affecting cell function. Laminin, an integral ECM glycoprotein, contains multiple epidermal growth factor (EGF)-like domains which may bind to EGF receptors (EGFR) (Engel, 1989). When presented as soluble ligands, laminin EGF-like domains were able to modulate signalling through EGFR (Panayotou et al., 1989; Schenk et al., 2003). Many such domains are found within ECM proteins in various arrangements and combinations so it is hypothesized that these domains can be released by proteolysis to act as soluble ligands (Hynes, 2009).

Cells are constantly remodelling the ECM through synthesis, degradation, and subsequent reassembly of matrix proteins – especially during cell migration and invasion. As described, the basement membrane directly underlies epithelial and endothelial cells

where it functions as a barrier of cell invasion. With a thickness of approximately 100-300 nm, the collagen IV scaffold of the basement membrane is densely compact with a pore size of approximately 50 nm between fibers (Abrams et al., 2000). As the typical permissive size for cell movement is 2 μm, the ECM must be remodelled for migration to occur, a process that includes protease-mediated degradation (Rowe and Weiss, 2009). During embryogenesis, remodelling occurs during large-scale migration events such as gastrulation, neurulation, and other processes in which cells undergo epithelial-mesenchymal transition (EMT). All of these involve disruption of cell-cell and cell-ECM adhesion as well as turnover of the ECM (Ohta et al., 2010). The mechanisms mediating ECM remodelling are also associated with many diseases including breast cancer, in which excessive ECM degradation seemingly allows the invasion of epithelial cells (Bonnans et al., 2014). Important for cell migration and invasion during development, but also unregulated in various pathologies, the ECM is a dynamic structure that is remodelled and degraded by proteases.

The importance of ECM remodelling during development has been studied for decades. The first vertebrate collagenolytic factor was identified by Gross and Lapiere (1962) in tadpole tissues (skin, gut, and gills) undergoing metamorphosis, establishing the field of protease-mediated ECM remodelling research. To date, the MEROPS database has identified over 600 individual peptidases and 1600 inhibitors in the human degradome. Based on the nucleophile involved in catalysis, the degradome can be divided into aspartic proteases, cysteine proteases, metalloproteases, mixed proteases, serine proteases, and threonine proteases (Figure 1) (Rawlings et al., 2014). Cysteine, serine, and threonine proteases utilize their respective amino acid side chains as a nucleophile, while mixed proteases are capable of using a combination of the three (Rawlings et al., 2014). In contrast, aspartic proteases and metalloproteases use an activated water molecule to mediate the nucleophilic attack of a peptide bond (James, 2004; Murphy and Nagase, 2008). Although proteases in each clan contain the same nucleophile in the catalytic site, the molecular structures, catalytic mechanism, and sequence homology can be very different between individual proteases (Rawlings et al., 2014). Proteases are

Figure 1. Classification of proteases in the human degradome

To date, MEROPS database has identified over 600 known and putative peptidases within the human degradome. They can be classified into six groups – aspartic, cysteine, mixed, serine, threonine, and metalloproteases – as based on the nucleophile involved in catalysis. Aspartic proteases and metalloproteases activate a water molecule to cleave a peptide bond. In contrast, serine, cysteine, and threonine proteases utilize their corresponding amino acid side chains, with mixed proteases capable of using a combination of the three (Rawlings et al., 2014).

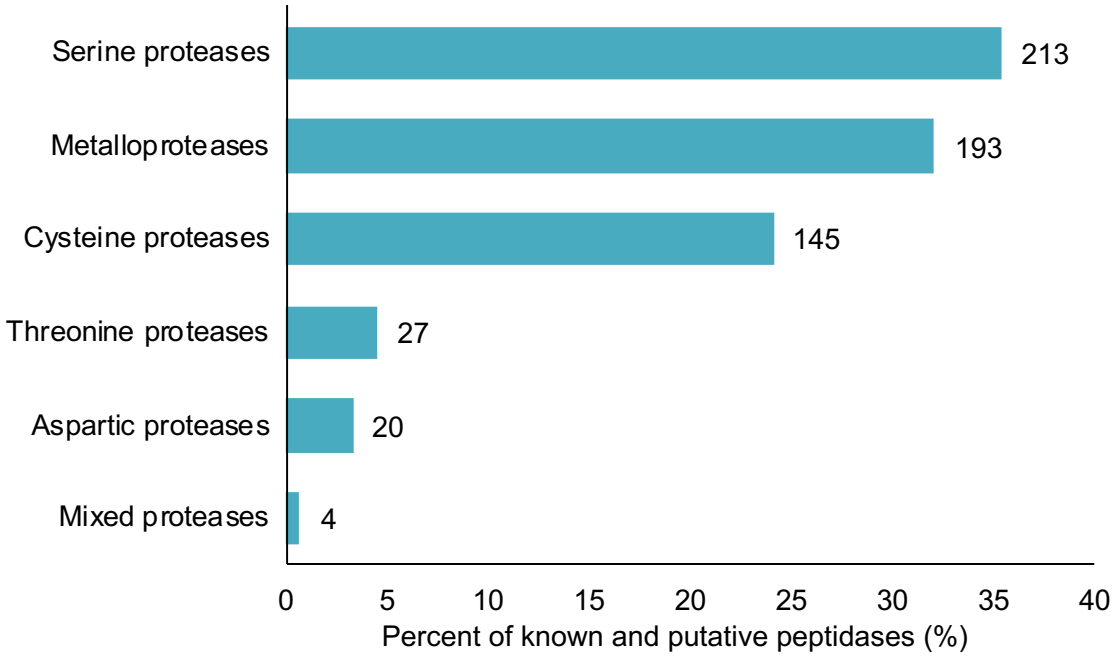
Serine proteases
213
Metalloproteases
193
Cysteine proteases
145
Threonine proteases
27
Aspartic proteases
20
Mixed proteases
4
0
5
10
15
20
25
30
35
40
Percent of known and putative peptidases (%)

further divided into families that share significant sequence homology to a prototypical representative of the family, usually the peptidase that has been most studied (Rawlings et al., 2014). Matrix metalloproteinases are a family of proteases that have been well-studied because they are the primary enzymes involved in ECM remodelling.

1.2 Matrix metalloproteinases

Matrix metalloproteinases (MMPs), or matrixins, are a subfamily of zinc-dependent endopeptidases with amino acid sequence similarity to the catalytic domain of human fibroblast collagenase 1 (MMP-1) (Rawlings et al., 2014). In total, there are 24 matrixin genes in the human genome, but only 23 unique MMP proteins due to a duplication of *MMP23*. As members of the metzincin superfamily of proteases, the catalytic domain contains a zinc-binding motif (HE*XX*H*XX*G*XX*H) and a conserved methionine ("Met-turn") eight residues downstream (Bode et al., 1993; Murphy et al., 1991). This sequence creates an active site in which the three histidines ligated to a catalytic Zn^{2+} ion rest on the conserved "Met-turn" - a hydrophobic base - for further support of the structure. The glutamate within the zinc-binding motif aids in polarizing a Zn^{2+}-bound water molecule. During a series of transition states, the Zn^{2+}-bound water executes a nucleophilic attack of the target peptide's carbonyl carbon, resulting in the breakdown of the peptide bond between the carboxyl group and amino group of two linked amino acids, as well as the release of a water molecule (Bode et al., 1999; Jacobsen et al., 2010; Park et al., 2003; Pelmenschikov and Siegbahn, 2002). MMPs are distinguished from other metzincins by their synthesis as pre-proenzymes with a "cysteine switch" motif (PRCG*X*PD), which maintains the newly translated enzyme in a latent state (Figure 2a) (Van Wart and Birkedal-Hansen, 1990). The signal peptide of a pre-proMMP is removed during translation, but the proMMP remains inactive due to the cysteine sulfhydryl group within the pro-domain chelating the active site Zn^{2+} (Van Wart and Birkedal-Hansen, 1990). Disruption of the zinc-thiol interaction is required for the zymogen to acquire activity, typically by protease-mediated removal of the pro-domain (Ra and Parks, 2007; Van Wart and Birkedal-Hansen, 1990). However, proMMPs can also be activated by various

Figure 2. Classification of matrix metalloproteinases within the human degradome

(a) Due to the diversity of the human degradome, enzymes are categorized following the ranking scheme of clan, subclan, family, and subfamily. **Clan MA:** Clan MA contains a variety of metallopeptidases identified by an HE*XX*H motif. Two histidines stabilize a catalytic Zn^{2+} ion while a nearby glutamic acid polarizes the Zn^{2+}-bound water molecule to cleave the peptide. **Subclan MA(M):** Clan MA is further divided into subclan MA(M) in which these peptidases are synthesized as inactive zymogens. **Family M10:** Metzincins, classified as family M10, contain the motif HE*XX*H*XX*G*XX*H and a methionine located 7 amino acids C-terminal to the last His. Expanding upon the clan MA motif, the third His is involved in stabilizing the catalytic Zn^{2+}. The conserved methionine forms a hydrophobic base - a structure identified as a "Met-turn" - which supports the catalytic site (Bode et al., 1993). The metzincin family includes various subfamilies differing in the mechanism of activation. **Subfamily M10A:** Matrix metalloproteases (MMPs), termed matrixins as part of subfamily M10A, are a mosaic group of 23 unique proteins that remain inactive due to a "cysteine switch" (Van Wart and Birkedal-Hansen, 1990). Synthesized as pre-proenzymes, an inhibitory pro-domain contains a PRCG*X*PD motif in which the cysteine sulfhydryl group chelates the active site Zn^{2+}, preventing interaction with a water molecule. **(b) Structure:** Save for MMP-7, MMP-23, and MMP-26, matrix metalloproteases typically share a common core structure of a propeptide, catalytic domain, linker region, and hemopexin domain.

a.

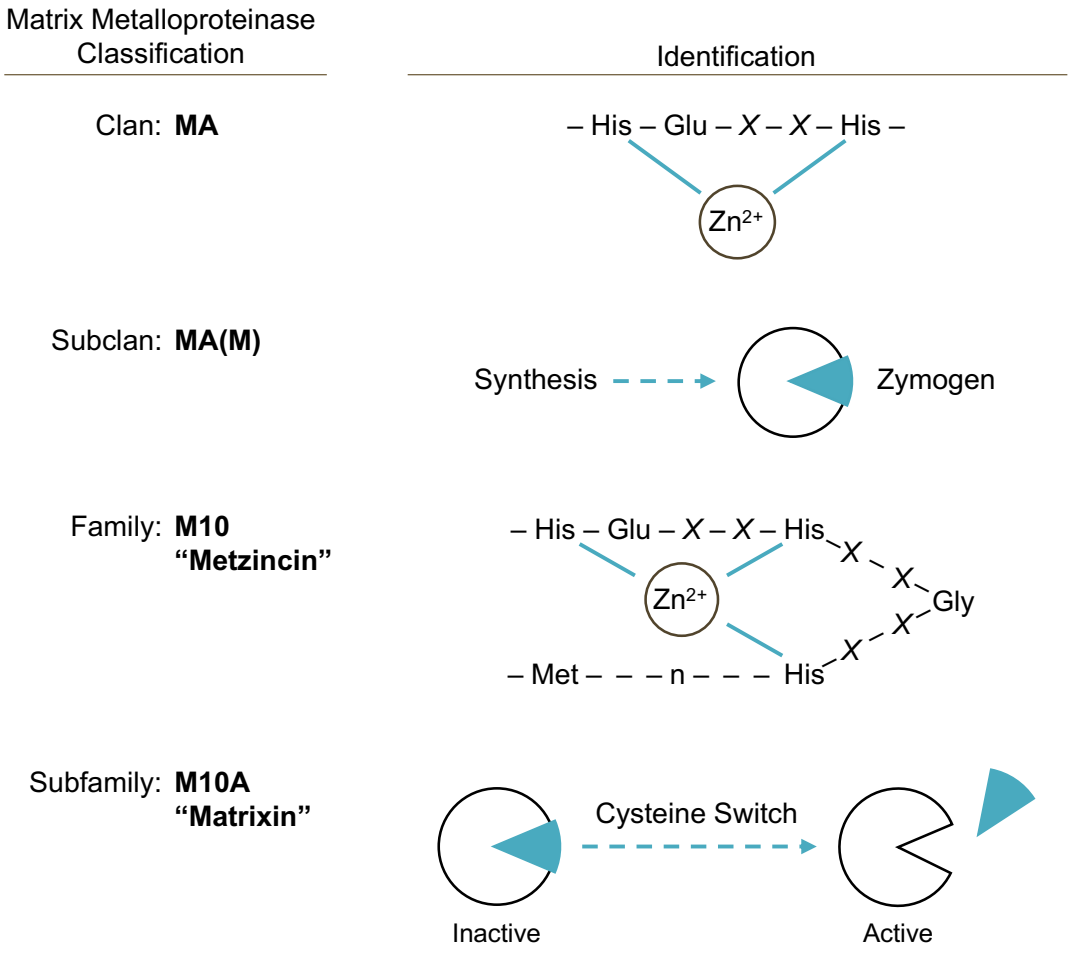
Matrix Metalloproteinase Classification
Identification
Clan: MA
– His – Glu – X – X – His –
Zn2+
Subclan: MA(M)
Synthesis
Zymogen
Family: M10
"Metzincin"
– His – Glu – X – X – His
Zn2+
X
X
Gly
X
– Met – – – n – – – His
Subfamily: M10A
"Matrixin"
Cysteine Switch
Inactive
Active

b.


Propeptide
Linker
Structure:
Catalytic Domain
Hemopexin Domain

ectopic mechanisms that perturb the conformation or free the thiol (Springman et al., 1990; Van Wart and Birkedal-Hansen, 1990).

Matrix metalloproteinases are classified by two independent characteristics: substrate preference and cellular localization. They can be divided into collagenases (MMP-1, -8, and -13), gelatinases (MMP-2 and -9), stromelysins (MMP-3, -10, and -11), matrilysins (MMP-7 and -26), membrane-bound (MMP-14, -15, -16, -17, -24, and -25), and other MMPs (MMP-12, -19, -20, -21, -23, -27, and -28) as based on domain organization and ECM substrate affinity. Each MMP has distinct yet overlapping substrate specificities, but together they can process virtually all ECM proteins (Sternlicht and Werb, 2001). Because of this, a more common classification of MMPs is based on their cellular localization. A majority of MMPs are soluble and commonly secreted into the ECM as zymogens (proMMPs). In contrast, membrane-type MMPs are anchored to the cell membrane after their pro-domains are removed in the Golgi, and thus are proteolytically active. Membrane-type 1, 2, 3, and 5 MMPs contain a type 1 transmembrane domain followed by a cytoplasmic domain, whereas MT4-MMP and MT6-MMP are glycosylphosphatidylinositol-anchored to the plasma membrane (Itoh et al., 1999; Kojima et al., 2000; Sato et al., 1994). Typically, MMPs share a common structure: a propeptide of about 80 amino acids, a catalytic domain of about 170 amino acids, a linker or hinge region of variable length, and a hemopexin domain of about 200 amino acids (Figure 2b). Exceptions include MMP-7, MMP-23, and MMP-26, which lack the linker peptide and hemopexin domain (Murphy and Nagase, 2008; Nagase et al., 2006). MMP-23 uniquely contains a C-terminal cysteine rich immunoglobulin-like domain after the catalytic domain (Gururajan et al., 1998; Park et al., 2000).

1.3 MMP regulation

Due to an overlap in substrate specificity, the biological function of an individual MMP is often dictated by its differential pattern of expression as compared to other similar MMPs (Sternlicht and Werb, 2001). Although expression varies during embryogenesis, MMP transcription in healthy adult tissue is restricted to low levels, save for wound healing or immune response, by a combination of inhibitory mechanisms (Moore and

Crocker, 2012; Sternlicht and Werb, 2001). MMP expression can be influenced by a variety of cytokines, growth factors, hormones, and chemical agents, leading to cell-type specific responses (Mauviel, 1993). For example, transforming growth factor-β (TGF-β) 1 induces MMP-9 expression in oral squamous cell carcinoma (Sun et al., 2008). In contrast, inhibition of TGF-β in mice following myocardial infarction results in increased MMP-9 expression in ventricular myocardium (Frantz et al., 2008). Similar to expression, which can be cell-type specific, growth factor responses can also be MMP-specific; some MMPs have a TGF-β1 inhibitory element in their promoter, whereas others, like MMP-2, do not (Cui et al., 2017). In many cases, stimulatory or suppressive factors modulate the expression/activation of c-*fos* and c-*jun*, which bind activator protein (AP-1) sites within MMP promoters.

Additional to transcriptional regulation, like other proteolytic enzymes, MMPs are synthesized as zymogens and are post-translationally regulated. The inhibitory pro-domain of proMMPs is removed either intra- or extracellularly to expose the catalytic domain. Membrane-type MMPs, as well as MMP-11, -21, -23, and -28, contain a target sequence between the propeptide and catalytic domain, which is commonly cleaved by furin in the trans-Golgi network (Pei and Weiss, 1995; Ra and Parks, 2007). Secreted soluble MMPs that lack the furin-susceptible cleavage site are activated outside of the cell by serine proteases and other MMPs. Treatment with heavy metals, oxidants, disulfide compounds, and sulfhydryl-alkylating agents can also disrupt the inhibitory pro-domain cysteine switch, thus uncovering the catalytic domain (Van Wart and Birkedal-Hansen, 1990).

In addition to pro-domain inhibition of proteolytic function, another level of MMP regulation relies on compartmentalization of MMPs to specific regions of the pericellular environment. Localization to the plasma membrane is straightforward for membrane-type MMPs, but soluble MMPs can also be anchored to maintain a locally high concentration at the cell surface. Protein-protein interactions that compartmentalize soluble MMPs include MMP-1 to $\alpha_2\beta_1$ integrin (Dumin et al., 2001; Stricker et al., 2001), MMP-2 to $\alpha_V\beta_3$ integrin (Brooks et al., 1998) and MMP-9 to cluster of differentiation 44 (CD44) (Yu and Stamenkovic, 2000). Many docking mechanisms have not been definitively

proven, though it is likely that other secreted MMPs are localized in a similar manner (Parks et al., 2004; Ra and Parks, 2007). Confinement of MMPs to the cell surface is also important for pro-enzyme activation by other proteases and increased probability of substrate proteolysis. Additionally, MMPs have a localization to the leading edge of migrating and invading cells. Migrating human colon adenocarcinoma L-10 cells express MT1-MMP and MMP-2 on their leading edges to remodel the gelatin substrate on which they were seeded. This migration was ablated by treatment with BB-94, a broad-spectrum inhibitor of MMP proteolytic function (Nabeshima et al., 2000). Similarly, MT1-MMP as well as MMP-2 and MMP-9 concentrate at invadopodia, specialized actin-based protrusions commonly associated with invasive tumour cells (Bowden et al., 1999; Buccione et al., 2004; Chen, 1989; Clark and Weaver, 2008; Linder, 2007; Nakahara et al., 1997).

A further mechanism of MMP regulation involves blocking proteolytic function by endogenous inhibitors within the ECM. Tissue inhibitors of metalloproteinases (TIMP) are a family of secreted proteins that include TIMP-1, -2, -3, and -4 in humans. The TIMP N-terminal domain binds non-covalently to the active catalytic domain of MMPs, thus inhibiting the proteolytic function of the latter. The C-terminal domain plays a role independent of catalytic inhibition and can bind various ECM and cell-surface proteins to regulate cell survival and migration (Moore and Crocker, 2012; Stetler-Stevenson, 2008; Tuuttila et al., 1998). The four mammalian TIMPs are able to bind each of the 23 different MMPs, but with different efficacies (Bourboulia and Stetler-Stevenson, 2010). This interaction occurs in a 1:1 ratio of TIMP:MMP, but depending on the stoichiometry of these proteins in the ECM, TIMPs can either inhibit or activate MMPs (section 1.4.1). Another endogenous inhibitor shown to negatively regulate MT1-MMP, MMP-2, and MMP-9 proteolytic activity and/or expression is reversion-inducing cysteine-rich protein with Kazal motifis (RECK), a GPI-anchored protein (Chang et al., 2008; Oh et al., 2001; Simizu et al., 2005; Takahashi et al., 1998). The Kazal motifs, for which RECK is named, are serine protease inhibitor-like domains believed to suppress MMP proteolytic function (Takahashi et al., 1998). Interestingly, TIMP-2 can bind $\alpha_3\beta_1$ integrin on the surface of human endothelial cells leading to increased RECK expression, suggesting that these inhibitors may act in a coordinated manner (Oh et al., 2004). While TIMPs and RECK

are the most commonly studied endogenous inhibitors that reversibly bind MMPs, others such as α2-macroglobulin can irreversibly clear MMPs from the ECM (Tchetverikov et al., 2003). MMP•α2-macroglobulin complexes are removed by scavenger receptor-mediated endocytosis (Sternlicht and Werb, 2001). Altogether, MMP proteolytic activity can be regulated by TIMPs, RECK, and other endogenous inhibitors, which too can differ in their transcriptional regulation and tissue-specific expression patterns (Sternlicht and Werb, 2001).

1.4 Membrane-type 1 matrix metalloproteinase

Membrane-type 1 matrix metalloproteinase (MT1-MMP) is the commonly used alias of MMP14 employed by the broader scientific community. Of all MMPs, MT1-MMP is well characterized due to its importance during development as well as many human pathologies. MT1-MMP is indispensable for embryonic development as it is the only MMP that is lethal when knocked out in mice (Holmbeck et al., 1999). These knockout mice exhibit craniofacial dysmorphism, dwarfism, and arthritis due to an ablation in collagenolytic activity crucial during skeletal and extraskeletal tissue development (Holmbeck et al., 1999). As a collagenase, MT1-MMP can degrade integral ECM substrates such as collagen types I, II, and III, as well as vitronectin and laminin 1 (Ohuchi et al., 1997). While *MT1-MMP* expression is common in development, it is low or negligible in healthy adult cells. However, cancerous cells may reactivate the developmental transcriptional programming of MMPs since *MT1-MMP* is present in mesenchymal cancers, sarcomas, and mesotheliomas as well as primary human breast cancers (Li et al., 2015; Lodillinsky et al., 2016; Marchesin et al., 2015; Turunen et al., 2017). As there is no preeminent genetic link between *MT1-MMP* and cancer, this suggests that the role(s) played by MT1-MMP in cancerous tissue is not due to a mutation. For this reason, the extracellular proteolytic activity of MT1-MMP has been well-studied due to its role in ECM remodelling during development as well as cell migration and invasion. However, MT1-MMP functions on multiple levels: the proteolysis of ECM molecules (section 1.4.1), MT1-MMP interaction with various extracellular (section 1.4.2) and intracellular (section 1.4.3) binding partners, proteolysis

of intracellular molecules (section 1.4.4), and as a possible transcription factor (section1.4.5); as summarized in Figure 3 (Knapinska and Fields, 2019).

1.4.1 Proteolysis of ECM molecules

The most well-described proteolytic function of MT1-MMP is not related to degradation of structural ECM molecules, but the activation of proMMP-2 in collaboration with TIMP-2. As mentioned, MT1-MMP is embedded in the plasma membrane in an active form with its pro-domain already removed. Two MT1-MMP molecules homodimerize through their hemopexin and transmembrane domains (Itoh et al., 2001, 2008). A TIMP-2 molecule can then bind via its N-terminal domain to the catalytic domain of one of these MT1-MMP molecules, thus inhibiting its proteolytic activity (Strongin et al., 1995). At this time, the hemopexin domain of a nearby proMMP-2, which has affinity for the exposed TIMP-2 C-terminal domain, binds to it, forming a $(MT1\text{-}MMP)_2$•TIMP-2• proMMP-2 quaternary complex (Itoh and Seiki, 2006). The uninhibited MT1-MMP within this complex is then able to cleave the pro-domain of MMP-2, initiating the activation of this MMP-2 molecule (Will et al., 1996). Once activated, MMP-2 can either be released into the ECM, remain bound to TIMP-2 via its hemopexin domain, or remain bound to TIMP-2, but subsequently inhibited by another TIMP-2 molecule (Itoh et al., 1998b). This activation mechanism is dependent on the precise stoichiometry of MMPs and TIMP-2 in the ECM.

The significance of this mechanism of MT1-MMP-mediated MMP-2 activation is related to their different enzymatic capabilities. MMP-2, but not MT1-MMP, is able to degrade type IV collagen, a major component of the basement membrane (Okada et al., 1990). This MT1-MMP/MMP-2 mediated cleavage of the basement membrane plays a role in the growth and invasion of epithelial cancer cells *in vivo* (Taniwaki et al., 2007). It was hypothesized that the sole function of MT1-MMP in tumour invasion was proMMP-2 activation (Ellerbroek and Stack, 1999; Seiki, 1999). However, MMP-2 deficient mice do not show the same severe developmental defects as MT1-MMP null mice, suggesting MT1-MMP has additional biological functions (Itoh et al., 1998a).

Figure 3. Domain-specific functions of membrane-type 1 matrix metalloproteinase

Research has identified key domains of MT1-MMP necessary for its proper structure, localization, as well as various roles in ECM remodelling and cell signalling. Simplistically, MT1-MMP is composed of an extracellular catalytic domain, a linker region, and a hemopexin domain, followed by a transmembrane domain and intracellular cytoplasmic tail. Altogether, the diverse functions of membrane-type 1 matrix metalloproteinase are highlighted (Knapinska and Fields, 2019).

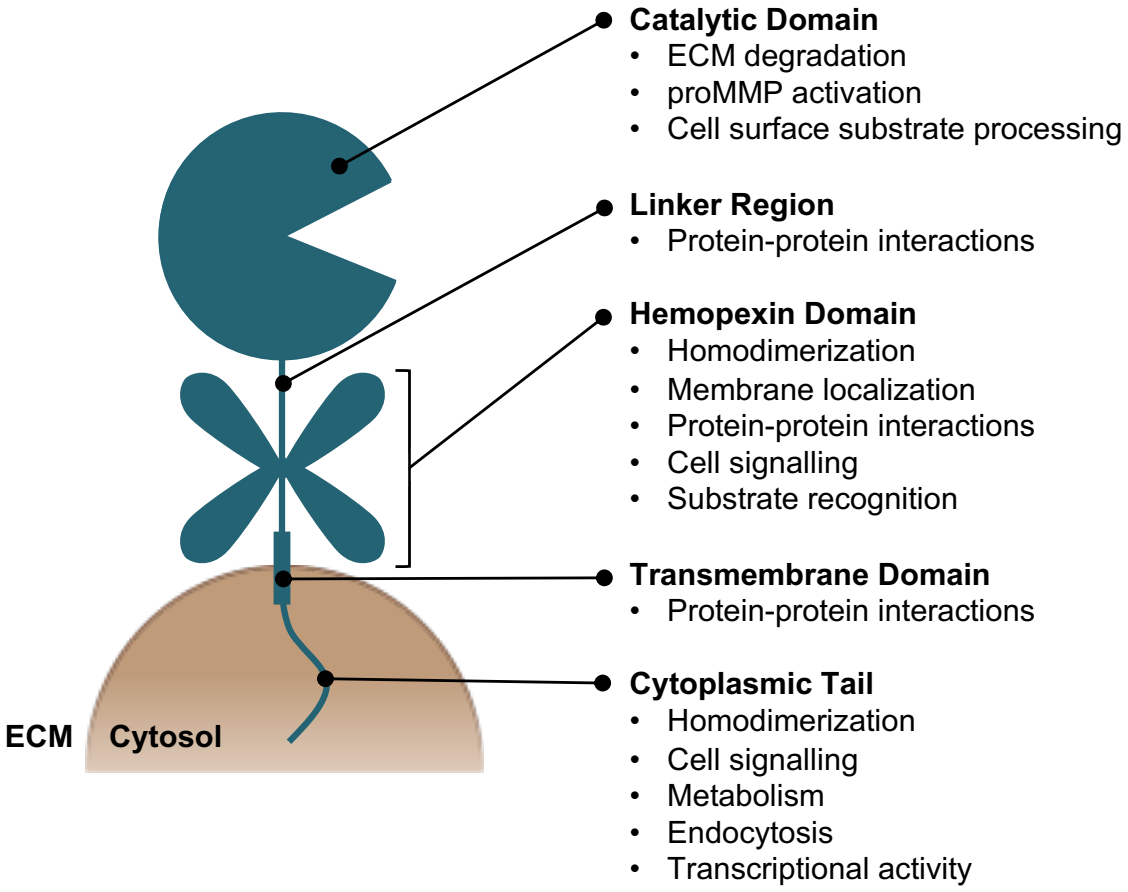
Catalytic Domain
• ECM degradation
• proMMP activation
• Cell surface substrate processing
Linker Region
• Protein-protein interactions
Hemopexin Domain
• Homodimerization
• Membrane localization
• Protein-protein interactions
• Cell signalling
• Substrate recognition
Transmembrane Domain
• Protein-protein interactions
Cytoplasmic Tail
• Homodimerization
• Cell signalling
• Metabolism
• Endocytosis
• Transcriptional activity
ECM
Cytosol

MT1-MMP is not only involved in initiating cell movement through ECM degradation, but also maintaining migration by cleaving ECM molecules that function as ligands in cell signalling. When TGF-β is secreted, it is non-covalently associated with its latency associated peptide, forming the small latent complex (SLC) (Miyazono et al., 1993). Furthermore, the SLC needs to associate with the latent TGF-β binding protein (LTBP) for proper secretion (Miyazono et al., 1991). Ultimately, MT1-MMP mediated cleavage of TGF-β from LTBP plays a role in activating TGF-β signalling. MT1-MMP activation of TGF-β1 has been associated with upregulation of *CUTL1* and *WNT5A* to induce EMT in prostate cancer cells (Nguyen et al., 2016). Furthermore, free TGF-β can increase the expression of *MT1-MMP*, facilitating positive feedback via mothers against decapentaplegic (SMAD) 3/4 induction of *SNAIL* in other cancer phenotypes (Ota et al., 2009; Shields et al., 2011, 2012).

Additionally, MT1-MMP localization at the plasma membrane positions it to cleave various other cell-surface molecules. For example, solubilization of extracellular matrix metalloproteinase inducer (EMMPRIN) – a cell surface glycoprotein – by MT1-MMP not only increases the expression/activation of other MMPs in surrounding cancerous cells, but also from fibroblasts and stromal cells (Egawa et al., 2006; Sameshima et al., 2000). MT1-MMP can shed other biomolecules such as fibronectin, death-receptor 6, pro-tumour necrosis factor (Tam et al., 2004), syndecan-1 (Endo et al., 2003), E-cadherin (Covington et al., 2006), various tetraspanins (Tomari et al., 2009), mucin 16 (Bruney et al., 2014), and heparin-binding epidermal growth factor (Overland and Insel, 2015). All of which have been associated with altered migration and invasion capabilities of cancerous cells. Such observations have resulted in MT1-MMP being described as pro-invasive and pro-migratory. However, MT1-MMP has also been shown to inhibit cancer progression. MT1-MMP-mediated shedding of endoglin and lymphatic vessel endothelial hyaluronan receptor-1 (LYVE-1) inhibits angiogenesis and lymphangiogenesis, respectively (Hawinkels et al., 2010; Wong et al., 2016). Regardless, MT1-MMP functions as a potent modulator of the pericellular environment through its proteolytic activity.

1.4.2 Extracellular binding partners

Although MT1-MMP has been implicated in cell migration, a well-defined mechanism remains elusive since expression of constitutively inactive MT1-MMP still results in increased cell migration (Bonnans et al., 2014; Hara et al., 2011). Recent focus has shifted from the proteolytic to non-proteolytic functions of MT1-MMP with regards to cell migration, specifically focusing on its hemopexin, transmembrane, and cytoplasmic domains.

Migrating cells reorganize their actin cytoskeleton to form lamellipodia on the leading edge, a process regulated by the Rho family of GTPases. These GTPases are also involved in CD44 localization to lamellipodia, and by association MT1-MMP (Mori et al., 2002; Ridley et al., 1992). In the context of CD44 - a hyaluronan receptor - trafficking of MT1-MMP to the leading edge of migrating cells relies on the MT1-MMP hemopexin domain binding to CD44 (Mori et al., 2002). Once localized to the leading edge, MT1-MMP can degrade ECM molecules. Interestingly, the CD44•MT1-MMP complex also activates EGFR. This crosstalk between CD44•MT1-MMP and EGFR induces cell migration through mitogen-activated protein kinase (MAPK) and phosphatidylinositol-3-kinase (PI3K) pathways via phosphorylation of extracellular signal-regulated kinase (ERK) 1/2 and AKT, respectively (Zarrabi et al., 2011). It has been observed that MT1-MMP-mediated shedding of CD44 from the membrane is important for enhanced cell migration (Kajita et al., 2001; Mori et al., 2002; Suenaga et al., 2005). Shedding of CD44 disrupts its weak interaction with the substrate, eventually being replaced with stronger integrin interactions that fortify migration (Cauwe et al., 2007).

Binding of TIMP-2 to the MT1-MMP catalytic domain abolishes its proteolytic activity, but TIMP-2 binding to the hemopexin domain promotes cell migration and tumour growth via MAPK signalling (D'Alessio et al., 2008). The rat sarcoma (RAS) – rapidly accelerated fibrosarcoma (RAF) – ERK1/2 cascade is induced by low, physiological levels of TIMP-2, further highlighting the important stoichiometry of MMPs and their inhibitors (D'Alessio et al., 2008; Yang et al., 2013). In contrast, another study observed increased ERK1/2 activation when MT1-MMP was overexpressed in COS-7, which was

ablated by exogenous TIMP-2 (Gingras et al., 2001). The cytoplasmic domain is involved in ERK activation, but there is debate whether it is solely involved or works in conjunction with the catalytic domain (D'Alessio et al., 2008; Gingras et al., 2001). Regardless, in the context of its proteolytic and non-proteolytic functions, MT1-MMP can associate with a variety of extracellular proteins that aid in ECM remodelling and promote signalling.

1.4.3 Intracellular binding partners

There is conflicting evidence regarding influence of the MT1-MMP cytoplasmic domain on protein-protein binding and its subsequent effects on cell migration, invasion, and signalling. However, the dileucine motif (LL) within the cytoplasmic domain is important for internalization of MT1-MMP through clathrin-dependent mechanisms. Caveolin-dependent internalization has also been observed (Jiang et al., 2001; Uekita et al., 2001). Only 20 amino acids in length, the cytoplasmic tail does not contain sequences that suggest any catalytic activities (Gingras et al., 2001). However, certain residues within the MT1-MMP cytoplasmic tail can be post-transcriptionally modified, particularly phosphorylation of Tyr573 and Thr567. Src-dependent phosphorylation of Tyr573 has been shown to impact tumour cell migration and proliferation, but there is debate about its effect on MT1-MMP catalytic activity (Nyalendo et al., 2007, 2008; Wang and McNiven, 2012). Similarly, phosphorylation of Thr567 enhances invasion and growth of breast and ovarian cancers (Moss et al., 2009; Yang et al., 2017). There is sequence similarity between the cytoplasmic domain and integrin alpha subunits (Dedhar and Hannigan, 1996; Gingras et al., 2001). Further links with integrins exist as during mammary gland branching, the MT1-MMP cytoplasmic domain is believed to regulate expression and activity of β1 integrin and subsequently control cell division (Mori et al., 2013).

A characteristic of cancer cells is altered metabolism by increasing glycolysis even in the presence of adequate oxygen, termed the Warburg Effect (Warburg, 1956). The MT1-MMP cytoplasmic domain can impact cell survival in times of metabolic stress by increased transcription of hypoxia-inducible factor (HIF)-1α target genes (Koziol et al.,

2012; Sakamoto et al., 2011). During processing in the Golgi, the cytoplasmic domain binds to factor-inhibiting HIF-1α (FIH), recruiting its inhibitor amyloid β A4 precursor protein-binding family A member 3 (Mint3), thus deterring FIH-induced repression of HIF-1α. Once stabilized, HIF-1α can alter the expression of multiple genes, most importantly, glycolytic enzymes such as glucose transporter 1, hexokinase 2, lactate dehydrogenase, and monocarboxylate transporter 4 (Hay, 2016). Under normoxic conditions, FIH inhibits HIF-1α; it is typically only during hypoxia that FIH is negatively regulated to shift cellular metabolism. However, MT1-MMP induces the Warburg Effect even under normoxia in cancer cells to increase cell survival (Sakamoto et al., 2011). Similarly, the cytoplasmic domain has also been shown to have a role in MCF-7 cell survival when grown in serum-starved media (Cepeda et al., 2017b). While small, the cytoplasmic domain is involved in MT1-MMP recycling, can be phosphorylated to potentially facilitate cell signalling, and influences cellular metabolism via HIF-1α activation.

1.4.4 Proteolysis of intracellular molecules

Several cell-based proteomic studies have suggested that the MT1-MMP catalytic domain is involved in proteolysis of various intracellular substrates. Cleaved molecules include enolase-β, enolase-γ, fructose-bisphosphate aldolase A, glyceraldehyde 3-phosphate dehydrogenase (GAPDH), and phosphoglycerate phosphokinase 1 (Cauwe and Opdenakker, 2010). Degradation of these metabolic enzymes would stop glucose metabolism at the fructose-1,6-bisphosphate (F1,6BP) stage. If stopped there, metabolism would shift from oxidative phosphorylation to a different pathway such as glycogenesis, again linking MT1-MMP function with metabolic regulation (Hay, 2016). Alternatively, F1,6BP can activate Ras, ultimately linking glycolysis and cell proliferation (Peeters et al., 2017). Apart from metabolism, MT1-MMP accumulates in the centrosome, where it cleaves pericentrin, which coordinates the mitotic spindle (Golubkov et al., 2005), and the breast cancer type 2 (BRCA1) susceptibility protein (Wali et al., 2014). Thus, as with its well-described extracellular roles, MT1-MMP-mediated proteolysis of intracellular proteins also impacts cell growth and survival.

1.4.5 MT1-MMP as a transcription factor

The role of MT1-MMP as a transcription factor is speculative, but related to the fact that active MT1-MMP and MMP-2 have been observed to colocalize in the nucleus (Ip et al., 2007). The functional consequences of this localization are undetermined. However, MT1-MMP is trafficked to nuclei in macrophages (Shimizu-Hirota et al., 2012). There it putatively modulates the expression of over 100 genes through expression/activation of the PI3Kδ/AKT/GSK3β signalling cascades. Many of these genes were linked to immune regulation (Shimizu-Hirota et al., 2012). Evidence that MT1-MMP itself is a transcription factor is nonexistent as associated changes in expression rely on its ability to facilitate signalling cascades and secondary molecules that will eventually function as a transcription factor. However, the reported presence of MT1-MMP in the nucleus suggests interactions with yet to be identified binding partners.

1.5 MT1-MMP proteomic research

Several proteomic approaches have been used to study MT1-MMP protein-protein interactions, with focus often on the investigation of proteolytic substrates. Earlier studies identified these substrates by observation of degradation products following digestion with a soluble MT1-MMP catalytic domain (Ohuchi et al., 1997). However, the use of mass spectrometry technology has provided a high-throughput analysis of cellular interactomes, especially protein-protein interactions. Although methodology changes depending on the approach, protein-protein interaction studies typically use affinity purification – mass spectrometry (AP-MS) (Vermeulen et al., 2008). In brief, a “bait” protein (MT1-MMP, in this case) is purified from control and treatment samples simultaneously with any “prey” proteins bound to it. Following purification, protein samples undergo digestion into peptide fragments before mass spectrometry analysis. Bottom-up proteomics relies on the resulting MS/MS spectra and bioinformatic tools to identify the peptide sequence, and ultimately, the protein. Depending on the need to quantify protein abundance between samples, proteins may be labelled for relative comparison (Nesvizhskii, 2012). The below six studies have utilized mass spectrometry to identify MT1-MMP substrates and binding partner.

Unlabelled AP-MS was used to better understand the link between MMPs and cardiovascular phenotypes commonly observed in animal models. A total of 15 proteins were identified as vascular substrates in human plasma and 12 different proteins in human radial arteries (Hwang et al., 2004; Stegemann et al., 2013). Both studies identified degradation products by mass spectrometry through comparison of total protein following incubation with catalytically active or inactive MT1-MMP. As several protease inhibitors are cleaved by MT1-MMP, incubation with MT1-MMP may indirectly activate other proteases; thus secondary cleavage products may be misinterpreted as MT1-MMP substrates (Hwang et al., 2004). However, advances in technology have created new MS-based approaches for the identification of MMP substrates.

Since mass spectrometry is not inherently quantitative, isotope-coded affinity tagging (ICAT) is a MS technique that labels proteins with biotin-tagged reagents that differ in isotopic composition analysis (Cauwe and Opdenakker, 2010). Using MDA-MB-231 breast cancer cells transfected with MT1-MMP, 17 proteins displayed altered abundance. Interestingly, only two were typical ECM proteins whereas the others included protease inhibitors, chemokines, cytokines, and cell receptors (Tam et al., 2004). Building upon this, researchers investigated the proteome-wide effects of prinomastat, a broad-spectrum MMP inhibitor. In particular, it was studied how treatment of prinomastat alters MMP-mediated ECM degradation and membrane protein shedding (Butler et al., 2008). Over 40 novel substrates were identified within the study, 20 of which were validated following incubation with soluble MT1-MMP. Dickkopft-1, pentraxin, thrombospondin, cathepsin A/B, and galectin-3-binding protein were observed as novel MT1-MMP substrates (Butler et al., 2008). However, intracellular proteins were not considered in either of these studies.

Recent studies of MT1-MMP binding partners utilized similar ICAT techniques for protein quantification, but affinity purify FLAG-tagged MT1-MMP and its binding partners before mass spectrometry identification. Using this approach, 158 and 163 proteins were isolated with MT1-MMP in A375 melanoma (Tomari et al., 2009) and A431 carcinoma cells (Niiya et al., 2009), respectively. In addition to identifying previously known MT1-MMP substrates, non-substrate proteins were also observed and

localized to the membrane, cytoplasm, or secretory pathway. This exemplifies the myriad of possible partners and their localizations.

1.6 Objectives and hypothesis

MT1-MMP has multiple proteolytic and non-proteolytic functions that contribute to proper development as well as pathological diseases. The studies described above utilized mass spectrometry to identify binding partners of MT1-MMP that contribute to its diverse functions. However, previous research used either soluble MT1-MMP domains to identify substrates or correlate changes in expression, protein level, or cellular dynamics after excessive MT1-MMP transfection; neither of which appear to be physiologically relevant. In proteomic studies, the catalytic activity of MT1-MMP is inactivated through amino acid substitution (Niiya et al., 2009; Tam et al., 2004; Tomari et al., 2009) or exogenous inhibitors (Butler et al., 2008; Stegemann et al., 2013). For this reason, studying MT1-MMP binding partners that may act as the source of diverse cellular functions is an attractive route to better understand the proteolytic, but more specifically, the non-proteolytic contributions of MT1-MMP. The aim of this study was to generate a catalog of proteins that associate with MT1-MMP to corroborate previous research regarding the role of MT1-MMP in cell migration, invasion, and survival. In a greater scope, it is important to understand the basic mechanistic function, particularly with respect to binding partners, of relevant proteases within the human degradome.

I hypothesize that if domains of MT1-MMP have different functions, then individual domains will have different binding partners.

Human MCF-7 breast cancer cells were previously generated to either overexpress MT1-MMP (C1) or express a truncated form of MT1-MMP lacking its cytoplasmic domain (ΔCD). In this study, these cells were used to: 1) identify MT1-MMP binding partners using a combination of co-immunoprecipitation and mass spectrometry, 2) compare binding partners between full-length and truncated MT1-MMP expressing cells to determine the role of the cytoplasmic domain in MT1-MMP function, and 3) assess involvement of the cytoplasmic domain of MT1-MMP in cell signalling pathways to better elucidate its role in cell migration.

2 MATERIALS AND METHODS

2.1 Buffers and solutions

All solutions and buffers are dissolved in ddH_2O unless otherwise specified.

2.1.1 Solutions

Phosphate Buffered Saline (PBS), pH 7.4: 154 mM NaCl, 1.05 mM KH_2PO_4, 5.6 mM Na_2HPO_4

2.1.2 Buffers

Nonidet P-40 (NP-40) lysis buffer: 100 mM NaCl, 0.1% NP-40, 10% glycerol, 1 mM ethylenediaminetetraacetic acid (EDTA), 50 mM Tris-HCl pH 8.0

Radioimmunoprecipitation assay (RIPA) lysis buffer: 150 mM NaCl, 1% NP-40, 0.5% sodium deoxycholate, 0.1% sodium dodecyl sulfate (SDS), 50 mM Tris-HCl pH 8.0

SDS running buffer: 25 mM Tris, 192 mM glycine, and 0.1% SDS

Tris Buffered Saline with Tween 20 (TBST, pH 7.5): 50 mM Tris, 150 mM NaCl, 0.05% Tween 20, pH 7.4

Transfer Buffer: 100 mM Tris, 191 mM glycine, 20% methanol

Antibody Stripping Buffer: 2 M glycine pH 2.3

2.2 Cell culture conditions

The human adenocarcinoma breast cancer cell line MCF-7 (ATCC® HTB-22™) was donated by Dr. Postovit, University of Alberta. Cells were incubated at 37ºC with 5% CO_2 in Dulbecco's Modified Eagle Medium (DMEM)/ F-12 media supplemented with 10% fetal bovine serum (FBS), 100 U/mL penicillin, and 100 µg/mL streptomycin. Cells grown in serum-free conditions were maintained in DMEM/F-12 media containing only 1% penicillin/streptomycin. Cells were maintained below 80% confluency and passaged accordingly using 0.25% Trypsin-EDTA (Gibco).

Stable MCF-7 cell lines were previously created as follows by Dr. Mario Cepeda and Jake Pelling (Cepeda et al., 2016, 2017b). MCF-7 cells were selected following transfection with either full length MT1-MMP or truncated MT1-MMP with its cytoplasmic domain removed. Populations were isolated, expanded, and assayed for *MT1-MMP* expression and protein level using qPCR and immunoblotting, respectively. Stable transfection of MCF-7 cells with full-length MT1-MMP created a cell line, henceforth referred to as C1, with a ~2500-fold increase in expression in comparison to MCF-7 parental cells (Cepeda et al., 2016). Transfection with MT1-MMP lacking its cytoplasmic domain created a cell line with a ~100-fold increase in *MT1-MMP* expression and produced a protein of lower molecular weight, henceforth referred to as ΔCD (Cepeda et al., 2017b).

2.3 RNA analysis

2.3.1 RNA extraction and real-time PCR

Real-time PCR (qPCR) analysis was performed to determine mRNA transcript levels between parental MCF-7, C1, and ΔCD cells. RNA was collected 24 hours after cells were seeded at a density of 5 x 10^5 cells/mL using the RNeasy Mini Kit (Qiagen) according to manufacturer's instructions. RNA concentration and quality were determined using a NanoDrop2000 spectrophotometer (Thermo Fisher Scientific). cDNA was synthesized from 1 μg RNA using the High Capacity cDNA Reverse Transcription Kit (Applied Biosystems) according to manufacturer's instructions. Glyceraldehyde 3-phosphate dehydrogenase (*GAPDH*) expression was used as an internal control (Cepeda et al., 2016). cDNA was amplified using primers (sequences provided in Table 1) as well as quantified using SensiFAST SYBR (Bioline) and a CFX96 Real-Time PCR Detection System (BioRad). qPCR was conducted at 95ºC for 2 minutes, followed by a repeated reaction schedule of denaturation at 95ºC for 5 seconds, primer annealing at 60ºC for 10 seconds, and primer extensions at 72ºC for 20 seconds. Transcript levels were calculated and normalized to the internal control. Gene expression relative to parental MCF-7 cell transcript was calculated using the $\Delta\Delta C_t$ method (Livak and Schmittgen, 2001).

Table 1. Primer sequences used for qPCR.

Gene	**Forward** (5' → 3')	**Reverse** (5' → 3')
BSG	GGCTGTGAAGTCGTCAGAACAC	ACCTGCTCTCGGAGCCGTTCA
BST2	GCATGTGCTGCCTGTTGTTAT	TCAGGTGTGCTCTCCCTCAA
CDC42	TAACTCACCACTGTCCAAAGACTC	CCTCATCAAACACATTCTTCAGACC
CDH1	GCCGCTGGCGTCTGTAGGAA	TGACCACCGCTCTCCTCCGA
CDKN1A	GGGCTGGGAGTAGTTGTCTT	ACAGGAGCTGGAAGGTGTTT
EHF	GCACAACGGCACAACCTTC	TGACTTGTGGAACCCAACGG
GAPDH	ACCCACTCCTCCACCTTTGA	CTGTTGCTGTAGCCAAATTCGT
ITGB1	GAAGGGTTGCCCTCCAGA	GCTTGAGCTTCTCTGCTGTT
MMP14	GCAGAAGTTTTACGGCTTGCA	TCGAACATTGGCCTTGATCTC
SLC39A1	GCCTACCCCCAGCGTTATTT	ACAGGTCCCAAAACAGGTCA
SMAD2	TGCACACATCTACACTGGCT	TGAGGGGTGGGGATGGTATT
SMAD4	GTAGAGGCCAGCTTTGTGGT	AATCAATCCAAGCCCGTGAGT
SNAI1	AGGGACTGTGAGTAATGGCTG	AGTTCTGGGAGACACATCGG
TGFB1	TTATTGAGCACCTTGGGCACT	TGGGCTTGTTTCCTCACCTTT
TGFB2	CTATGTTCTGCCAACGCCAG	AACCAACCCCAGAAAGCACG
TGFB3	AGACCCTGTGTTCATTTGGTGT	TACCTCAGTCTATGCGTCTGG
TGFBR1	TCTGTTGCCTTTGGGTCAGC	AATCAAGGGTTTGGGGACCA
TGFBR2	TGTGGGTGGGCTGAGAGTTA	AGAGGTCAATGGGCAACAGC

(Table 1 continued)

Gene	**Forward** (5’ → 3’)	**Reverse** (5’ → 3’)
TGFBR3	CGCGTGCCAGTCTTTTTGTA	TCACATAGGACTCACCCAACA
TP53INP1	TATAGGGGCAGGGCATGAGT	CGAGAAACACATTAAGAAGGCACA

2.4 Protein analysis

2.4.1 Protein collection and immunoblotting

Immunoblotting was performed to assay for changes in protein level between cell lines. Cells were seeded at a density of 5 x 10^5 cells/mL. Twenty-four hours later, cells were washed with PBS and disrupted using RIPA lysis buffer supplemented with phosphatase/protease inhibitor cocktail (Thermo Scientific). Collected protein lysates were shaken on ice for 20 minutes and sonicated three times for 10 seconds each. Protein concentration was quantified using a Pierce bicinchoninic acid (BCA) Protein Assay Kit (Thermo Scientific). Either 10 or 20 μg of protein per sample was mixed with the appropriate amount of Laemmli sample buffer (BioRad) and subjected to sodium dodecyl sulfate polyacrylamide gel electrophoresis (SDS PAGE) at 130 V for approximately three hours in SDS running buffer. Protein was transferred to a polyvinylidene difluoride (PVDF) membrane (BioRad) overnight at 4ºC using 12 V. Membranes were then blocked in either 0.5% or 5% bovine serum albumin (BSA) (Fischer Scientific) dissolved in TBST for 30 minutes at room temperature. Blots were subsequently incubated overnight at 4ºC with a primary antibody (section 2.4.3) followed by an appropriate secondary antibody for one hour at room temperature. Blots were analyzed using a ChemiDoc™ Imaging System (BioRad) and quantified using Image Lab (BioRad) software.

2.4.2 Immunoblot densitometry analysis

Chemiluminescence was analyzed using a ChemiDoc™ Imaging System (BioRad) and Image Lab software (BioRad). Band intensity of a protein of interest was quantified and normalized to β-actin using three independent biological samples (Cepeda et al., 2016). TGF-β1 SLC protein level was shown as a ratio of TGF-β1 SLC signal standardized to β-actin before comparison to parental MCF-7. SMAD2 activation is presented as a ratio between the phospho-SMAD2 and total SMAD2 band intensities within each sample normalized to parental MCF-7 cells.

2.4.3 Antibodies

The following antibodies were used: mouse anti-MT1-MMP (1:200, sc-377097, Santa Cruz), rabbit anti-MT1-MMP (1:1000, AB6004, Millipore), rabbit anti-MT1-MMP (1:2000, ab51074, Abcam), rabbit anti-TGF-β1 (1:2000, ab92486, Abcam), rabbit anti-hyaluronan-mediated motility receptor (HMMR) (1:200, ab124729, Abcam), mouse anti-vitronectin (1:250, ab13413, Abcam), rabbit anti-fragile X mental retardation 1 (FMR1) (1:200, ab17722, Abcam), rabbit anti-phosho-SMAD2 (1:1000, 138D4, Cell Signaling Technology), mouse anti-SMAD2 (1:1000, 610843, BD Transduction Laboratories), mouse anti-β-actin (1:1000, sc-47778, Santa Cruz), and normal rabbit immunoglobulin G (IgG) control (AB-105-C, R&D Systems). Following primary antibody incubation, goat anti-mouse IgG (H+L) (BioRad) and goat anti-rabbit IgG (H+L) (Invitrogen) horseradish peroxidase (HRP) conjugates were used as secondary antibodies for immunoblot analysis (1:10 000). Clarity™ Western Enhanced Chemiluminescence Substrate (BioRad) was used according to manufacturer's instructions to detect secondary antibody.

The MT1-MMP antibody (ab51074) used for immunoprecipitation recognizes the extracellular region of MT1-MMP. Thus, MT1-MMP lacking its cytoplasmic domain was efficiently isolated.

2.4.4 Immunoprecipitation

Immunoprecipitation was used to isolate MT1-MMP and its binding partners in MCF-7, C1, and ΔCD cell lines. Cells were seeded at a density of 4 x 10^5 cells/mL in a 60 mm cell culture dish and incubated for twenty-four hours. On ice, cells were washed with cold PBS before lysate was collected using NP-40 lysis buffer supplemented with phosphatase/protease inhibitor cocktail (Thermo Scientific). Protein lysate was shaken on ice for 20 minutes, homogenized using a 20G syringe, and quantified using a Pierce BCA Protein Assay Kit (Thermo Scientific). Aliquots containing 100 μg of protein were incubated with rabbit anti-MT1-MMP (ab51074) at 25:1 v/v ([ab51074] is 0.174 mg/ml). In parallel, aliquots of 100 μg of protein were incubated with the same volume of rabbit IgG antibody as a negative control. SureBeads Protein A Magnetic Beads (BioRad) were used according to manufacturer's instructions to precipitate the antibody complexes.

Following immunoprecipitation, proteins were eluted from beads with either Laemmli sample buffer for immunoblotting analysis of MT1-MMP and its binding partners, or 200 mM glycine (pH 2.0) for in-solution digestion and subsequent mass spectrometry analysis. To prevent detection of heavy and light IgG chains of the primary antibody used to immunoprecipitate MT1-MMP, rabbit anti-MT1-MMP was used to immunoprecipitate whereas mouse anti-MT1-MMP was used in immunoblot analysis.

2.4.5 In-solution trypsin digestion

Following immunoprecipitation of MT1-MMP from protein lysate, co-immunoprecipitation eluent underwent in-solution digestion before mass spectrometry analysis. Beads used to precipitate MT1-MMP protein complexes were incubated with 200 mM glycine (pH 2.0) for fifteen minutes in a thermoshaker at 56ºC and 400 rpm before neutralization with Tris-HCl (pH 8.0). Samples were reduced with 10 mM dithiothreitol (DTT; dissolved in 100 mM NH_4HCO_3) for one hour at room temperature. Following reduction, samples were alkylated using 100 mM iodoacetamide (dissolved in 100 mM NH_4HCO_3) for one hour at room temperature in the dark. Protein was precipitated with trichloroacetic acid (TCA) extraction, resuspended in 50 mM NH_4HCO_3 (pH 7.8), and quantified using a spectrophotometer (NanoDrop 2000, Thermo Scientific) and protein standards. Samples were then subjected to in-solution digestion with 2% (w/w) sequencing-grade trypsin (Thermo Scientific; resuspended in 50 mM NH_4HCO_3) for 18 hours at 37ºC and 700 rpm. Additionally, 1% (w/w) trypsin was added for 4 hours at 37ºC and 1400 rpm. Resulting peptide samples were purified and concentrated using C18 Spin Columns (Thermo Scientific) according to manufacturer's instructions. Peptide samples were quantified, lyophilized, and resuspended in 0.1% formic acid before analysis by liquid chromatography-tandem mass spectrometry.

2.4.6 Liquid chromatography-tandem mass spectrometry

Liquid chromatography-tandem mass spectrometry (LC-MS/MS) analysis of 3 biological replicates from each cell line were carried out at the Don Rix Protein Identification Facility, Department of Biochemistry (UWO). Every mass spectrometry run included samples immunoprecipitated with an MT1-MMP antibody, identical samples

immunoprecipitated with a rabbit IgG antibody (negative control), as well as a BSA solution that underwent in-solution digestion (positive control). Samples were separated using an ACQUITY UPLC M-Class system (Waters Corporation) connected to an Orbitrap Elite Mass Spectrometer (Thermo Fisher Scientific). Buffer A consisted of water/0.1% formic acid and buffer B consisted of acetonitrile/0.1% formic acid. Samples were trapped for 6 minutes at a flow rate of 5 µL/min using 99% buffer A and 1% buffer B on an ACQUITY UPLC M-Class Symmetry C18 Trapping Column (100 Å, 5 µm, 180 µm x 20 mm, Waters). After trapping, peptides were separated using an ACQUITY UPLC M-Class Peptide BEH C18 Column (130 Å, 1.7 µm, 75 µm x 250 mm) operating at a flow rate of 300 nL/min at 35°C using a 5-40% acetonitrile gradient over 90 minutes. An Orbitrap Elite Mass Spectrometer recorded the mass-to-charge ratio (m/z) of ions over the range of 380-1600. The mass spectrometer was controlled by Xcalibur™ software (Thermo Fisher Scientific) and operated in the data-dependent mode using FT/IT/CID Top 10 scheme.

2.4.7 Protein Identification

Data analysis was performed using PEAKS Studio 10.0 (Bioinformatics Solutions Inc.). MS/MS spectra were searched against the Human Uniprot database with trypsin specificity (updated January 2019 with 20 380 entries; UniProt Consortium, 2019). Missed cleavages were set to 3. Cysteine carbamidomethylation was set as a fixed modification, whereas oxidation (M) and deamidation (NQ) were set as variable modifications (max number of modifications per peptide = 5). All other PEAKS Studio software settings were left as default. Peptide and protein false discovery rate (FDR) was set to 1% (Hughes et al., 2012). FDR values were calculated using the Decoy-Fusion method in PEAKS. Proteins identified by a minimum of one unique peptide and isolated in ≥ 2 biological replicates were retained for downstream analysis (Kuljanin et al., 2017), unless otherwise specified. Proteins identified following rabbit IgG pulldown were considered non-specific background proteins and subsequently removed from the MT1-MMP co-immunoprecipitation datasets. Additionally, structural components of the ribosome and spliceosome were removed. Immunoprecipitation followed by immunoblot analysis was used to confirm selected complexes detected by LC-MS/MS as described in

sections 2.4.1 and 2.4.2. Antibodies specific to hyaluronan mediated motility receptor (HMMR), fragile X mental retardation 1 (FMR1), and vitronectin (VTN) were used to validate mass spectrometry results.

Following PEAKS analysis, the Search Tool for the Retrieval of Interacting Genes/Proteins (STRING) was used to create protein-protein interaction (PPI) networks. STRING (version 11.0) is a well-known public database of protein associations that covers 19 566 protein coding genes from *Homo sapiens* (NCBI taxon ID: 9606) (Szklarczyk et al., 2019). Proteins identified by mass spectrometry were mapped via STRING using co-expression analysis, pathway knowledge from curated databases, and experimentally validated associations (confidence = 0.4). Cytoscape software (version 3.7) was used to construct a PPI network. Within a PPI network, Kyoto Encyclopedia of Genes and Genomes (KEGG) pathway analysis was used to identify enrichment of pathway-specific genes within the network. KEGG is a manually curated database resource with a collection of pathway maps integrating many aspects of the biological system (genes, proteins, RNAs, etc.).

2.5 Statistics

Statistical analysis and graphing of qPCR and immunoblot data was performed using Microsoft Excel (Office 365). Data is present as mean ± SEM. Means were compared using one-way ANOVA followed by Tukey's post-hoc test. Levels of statistical significance are as follows: ****, $p \leq 0.0001$; ***, $p \leq 0.001$; **, $p \leq 0.01$; *, $p \leq 0.05$. KEGG pathway analysis enrichment scores are presented as FDR.

3 RESULTS

In this study, MCF-7 cell lines were used to: 1) identify MT1-MMP binding partners, 2) compare binding partners isolated from full-length and truncated *MT1-MMP* expressing cells, and 3) assess the involvement of the MT1-MMP cytoplasmic domain in cell signalling. Objectives 1 and 2 identified MT1-MMP binding partners that alluded to the role of the cytoplasmic domain on MT1-MMP function. In parallel with proteomic experiments, a different approach was used in Objective 3 to identify changes in expression and protein level between the cell lines. This was done to corroborate previous research that observed an increase in ΔCD, but not C1, cell migration relative to parental MCF-7 cells (Cepeda et al., 2016, 2017b).

3.1 Stable MCF-7 cell lines, C1 and ΔCD, have altered expression of *MT1-MMP*

Cell lines used were repeatedly tested via qPCR and immunoblotting to ensure consistent levels of MT1-MMP over the course of this study. MCF-7 cells were previously transfected with either full length MT1-MMP (Cepeda et al., 2016) or MT1-MMP lacking its cytoplasmic domain (Cepeda et al., 2017b). Parental MCF-7 cells have low abundance of *MT1-MMP* transcript and did not show any detectable levels of MT1-MMP protein (Figure 4). C1 cells created to have a ~2500-fold increase (p<0.0001) in *MT1-MMP* produced a 63 kDa band as expected (Figure 4). The ΔCD cell lines, which expresses ~100-fold increase (p<0.001) of *MT1-MMP* lacking its cytoplasmic domain produced a corresponding smaller (59 kDa) band as expected (Figure 4).

3.2 Immunoprecipitation of MCF-7, C1, and ΔCD cell line lysates with anti-MT1-MMP antibody isolated 248 unique proteins

To identify MT1-MMP binding partners, protein lysate from each cell line was immunoprecipitated with an MT1-MMP antibody. The resulting precipitated complexes were subsequently analyzed with mass spectrometry. As a negative control, cell lysates were immunoprecipitated with a normal rabbit IgG antibody to identify any non-specific antibody interactions. Due to the nature of ultra-sensitive mass spectrometry, these non-specific proteins were removed. Additionally, components of the ribosome were also

Figure 4. Stable transfection of MCF-7 cell lines produce different MT1-MMP expression profiles.

(a) Average expression level of *MT1-MMP* from qPCR analysis of parental MCF-7, C1, and ΔCD cell lines. Relative to parental MCF-7 cell expression, C1 *MT1-MMP* expression is increased 2529-fold ($p \leq 0.0001$) whereas ΔCD is increased 83-fold ($p \leq 0.001$). Log_2 transformed mean fold change ± SEM is presented and was compared using one-way ANOVA and Tukey's post-hoc test; ****, $p \leq 0.0001$; ***, $p \leq 0.001$ (n=4). **(b)** Immunoblot analysis of parental MCF-7, C1, and ΔCD cell lysate show different levels of MT1-MMP protein level. MT1-MMP protein cannot be visualized by immunoblotting in MCF-7 cells, however, stable transfection of full-length MT1-MMP in C1 cells showed a band corresponding to MT1-MMP (63 kDa). ΔCD MT1-MMP transfection results in an increase of MT1-MMP protein, but at a lower molecular weight due to the truncated protein (59 kDa). β-actin was used as a loading control.

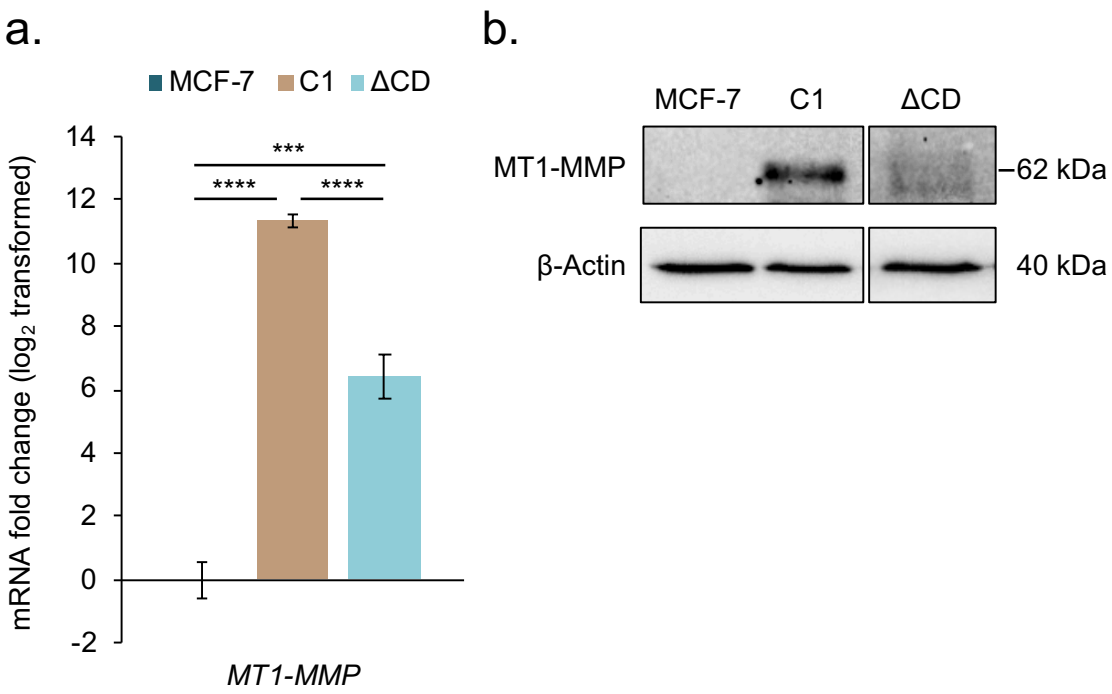
a.
MCF-7
C1
ΔCD
mRNA fold change (log2 transformed)
14
12
10
8
6
4
2
0
-2
***
****
****
MT1-MMP
b.
MCF-7
C1
ΔCD
MT1-MMP
62 kDa
β-Actin
40 kDa

removed due to their overabundance in the rabbit IgG pulldown. Next, a protein was considered a valid binding partner if it was identified by a minimum of one unique peptide and observed in ≥ 2 biological replicates. Prior to filtering and removal of non-specific proteins, 939 proteins were identified in MCF-7 cells, 919 proteins in C1 cells, and 1051 proteins in ΔCD cells following immunoprecipitation with an MT1-MMP antibody (Figure 5a). Following removal of non-specific proteins that were pulled down with the MT1-MMP antibody as well as the rabbit IgG antibody, the catalog of MT1-MMP binding partners was subjected to KEGG analysis.

KEGG analysis identified an enrichment of proteins associated with various pathways. Sorted by FDR, the top 10 enriched pathways and their identified proteins are listed (Appendix A). The pathways include: spliceosome (hsa03040), RNA transport (hsa03013), RNA degradation (hsa03018), mRNA surveillance pathway (hsa03015), protein processing in the endoplasmic reticulum (hsa04141), pathogenic *Escherichia coli* infection (hsa05130), Huntington's disease (hsa05016), endocrine and other factor-regulated calcium reabsorption (hsa04961), non-homologous end-joining (hsa03450), hepatocellular carcinoma (hsa05225), and endocytosis (hsa04144) (Appendix A). Similarly, KEGG analysis of proteins pulled down with the control anti-rabbit IgG identified enrichment in various pathways including the spliceosome (11 of 130 genes, FDR=0.0145; data not shown). Due to the nature of spliceosomal-related proteins having a unique, sometimes solely known function, these proteins were considered background proteins. Therefore, 19 protein were removed from the pool of binding partners.

Following the removal of all non-specific proteins, the final dataset contained 200 proteins isolated in MCF-7 cells, 168 proteins isolated in C1 cells, and 70 proteins isolated in ΔCD cells; a reduction of 79%, 82%, and 93%, respectively, from the original dataset (Figure 5a). When proteins isolated in each cell line were compared, a total of 248 unique proteins immunoprecipitated with MT1-MMP in MCF-7, C1, and ΔCD cells (Figure 5b, Appendix B). STRING analysis of the 248 proteins generated a protein-protein interaction network of 224 nodes (proteins) and 1116 edges (protein-protein interactions; data not shown). Subsequent KEGG pathway analysis of the catalog

Figure 5. Total number of proteins immunoprecipitated with MT1-MMP in parental MCF-7, C1, and ΔCD cell lines.

(a) A total of 939 proteins were identified in parental MCF-7 cells, 919 proteins in C1 cells, and 1051 proteins in ΔCD cells following immunoprecipitation with an MT1-MMP antibody. Following removal of non-specific proteins, 200 proteins were identified as true MT1-MMP interactions in parental MCF-7 cells, 168 protein in C1 cells, and 70 proteins in ΔCD cells. **(b)** Upon comparison of proteins isolated in each cell line, a total of 248 unique proteins immunoprecipitated with MT1-MMP. A complete list of proteins can be found in Appendix B.

a.

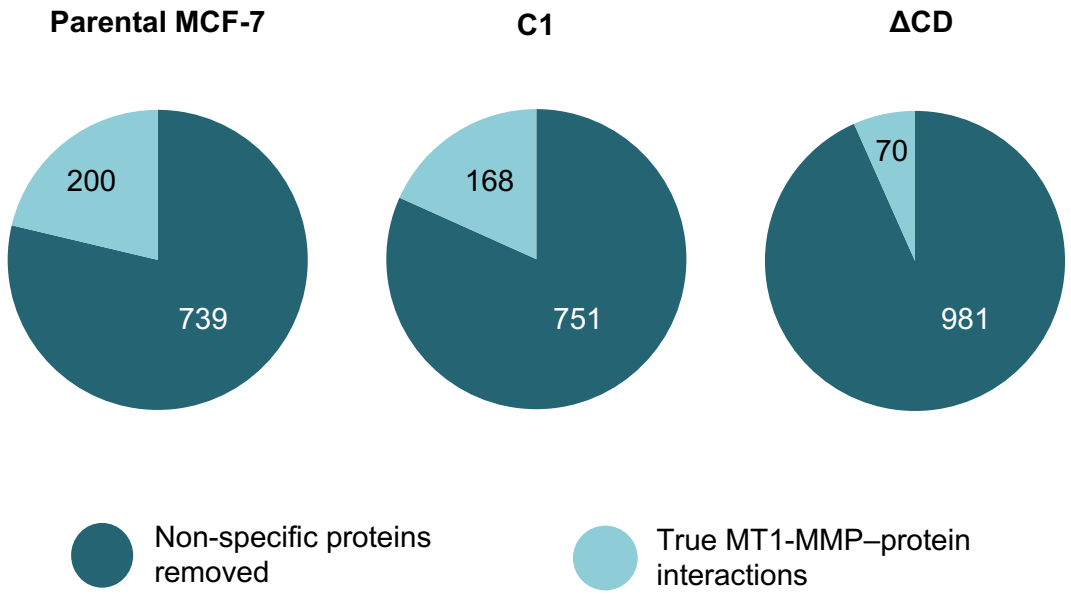
Parental MCF-7
C1
ΔCD
200
739
168
751
70
981
Non-specific proteins removed
True MT1-MMP–protein interactions

b.

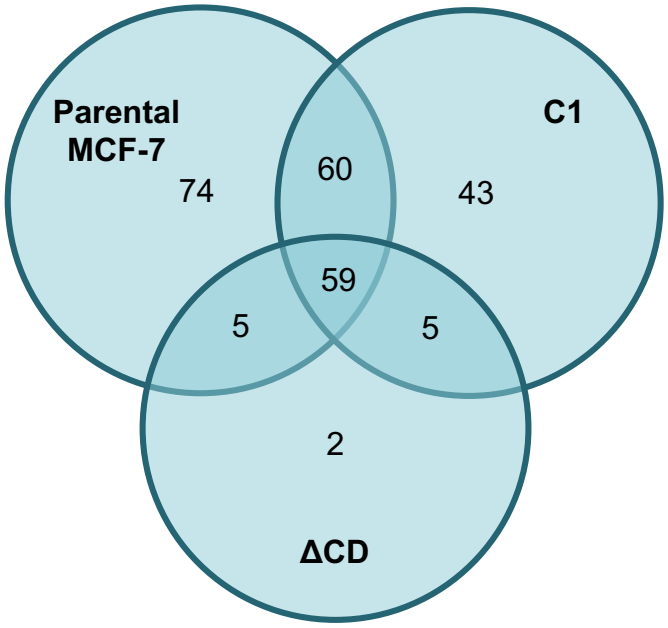
Parental MCF-7
74
60
C1
43
59
5
5
2
ΔCD

of 248 proteins identified enrichment in pathways including: RNA transport, RNA degradation, mRNA surveillance pathway, protein processing in the endoplasmic reticulum, Huntington's disease, endocrine and other factor-regulated calcium reabsorption, adrenergic signaling in cardiomyocytes (hsa04261), non-homologous end-joining, hepatocellular carcinoma, and endocytosis (Table 2).

3.3 Select MT1-MMP binding partners identified by mass spectrometry are validated with immunoblotting

Select proteins identified by mass spectrometry were validated with immunoblotting following immunoprecipitation with an MT1-MMP antibody. Elution of proteins from magnetic beads with Laemmli buffer also elutes the immobilized antibody bound to the beads. As a result, Western blot bands corresponding to the antibody heavy (50 kDa) and light (25 kDa) polypeptide chains appear regardless of primary antibody species due to cross-reactivity. For this reason, mass spectrometry identified proteins that were chosen to be validated had a molecular weight greater than 60 kDa to be accurately visualized. The proteins selected include hyaluronan mediated motility receptor (HMMR), fragile X mental retardation 1 (FMR1), and vitronectin (VTN). As expected, proteins bands corresponding to MT1-MMP were observed in MCF-7 and C1 cell lysate following anti-MT1-MMP immunoprecipitation (Figure 6). Due to oversaturation of the immunoglobin heavy chain chemiluminescent signal (50 kDa), membranes were trimmed at ~60 kDa. As a result, MT1-MMP was poorly visualized in ΔCD cell lysate due to its lower molecular weight (59 kDa). In agreement with HMMR and FMR1 being identified as putative MT1-MMP binding partners by mass spectrometry, bands corresponding to HMMR (84 kDa) and FMR1 (80 kDa) were observed in all cell lysates following anti-MT1-MMP immunoprecipitation, but not rabbit IgG pulldown. While vitronectin was identified by mass spectrometry as a putative binding partner MCF-7 and C1 cells, VTN (62 kDa) was only identified in MCF-7 cell lysate following anti-MT1-MMP immunoprecipitation.

Table 2. Top 10 most significantly enriched KEGG pathways represented by 248 proteins co-immunoprecipitated with MT1-MMP from MCF-7, C1, and ΔCD cell lines[a].

ID: KEGG Pathway	Count[b]	Size[b]	Genes					FDR[a]
RNA transport (hsa03013)	18	159	CASC3 EIF3I FXR2 RAN	EIF2S1 EIF4A1 NUP210 SEC13	EIF2S3 EIF4G1 PABPC1 UPF1	EIF3C FMR1 PABPC4	EIF3CL FXR1 PNN	1.61×10^{-9}
RNA degradation (hsa03018)	11	77	CNOT1 EDC4 XRN2	CNOT2 HSPA9	CNOT3 HSPD1	CNOT7 PABPC1	DDX6 PABPC4	1.1×10^{-6}
mRNA surveillance pathway (hsa03015)	11	89	CASC3 PABPC4 WDR33	CPSF1 PNN	CPSF2 PPP1CA	FIP1L1 PPP1CC	PABPC1 UPF1	2.85×10^{-6}
Protein processing in the endoplasmic reticulum (hsa04141)	12	161	BAG2 HSP90AB1 SEC13	DNAJA1 HSPA1A SSR1	DNAJA2 HSPA5	EIF2S1 RPN1	HSP90AA1 RRBP1	8.25×10^{-5}
Pathogenic *Escherichia coli* infection (hsa05130)	7	53	CTNNB1 YWHAQ	NCL YWHAZ	TUBB2A	TUBB2B	TUBB6	0.00033
Huntington's disease (hsa05016)	10	193	AP2A1 ATP5C1	AP2B1 CLTC	AP2M1 DCTN1	ATP50 NDUFA4	ATP5A1 SLC25A5	0.0071
Endocrine and other factor-regulated calcium reabsorption (hsa04961)	5	47	AP2A1	AP2B1	AP2M1	ATP1A1	CLTC	0.0118

(Table 2 continued)

ID: KEGG Pathway	Count	Size	Genes					FDR
Adrenergic signaling in cardiomyocytes (hsa04261)	8	139	ATP1A1 PPP1CC	ATP2A2 TPM1	CALM1 TPM3	GNAI3	PPP1CA	0.0118
Non-homologous end-joining (hsa03450)	3	13	PRKDC	XRCC5	XRCC6			0.0187
Hepatocellular carcinoma (hsa05225)	8	163	ACTL6A SMARCA4	ARID2 SMARCC2	CTNNB1 SMARCE1	KEAP1	PBRM1	0.0229
Endocytosis (hsa04144)	10	242	AP2A1 CAPZB	AP2B1 CLTC	AP2M1 HSPA1A	ARF5 RAB10	CAPZA TFRC	0.0229

[a] **Abbreviations:** KEGG, Kyoto Encyclopedia of Genes and Genomes; FDR, False Discovery Rate

[b] **Notes:** Count: number of genes isolated within pathway; Size: total number of genes in pathway

Figure 6. Validation of putative MT1-MMP binding partners HMMR, FMR1, and VTN.

Lysates from parental MCF-7, C1, and ΔCD cell line were collected, immunoprecipitated with an MT1-MMP antibody, and immunoblotted to confirm pulldown of proteins identified by mass spectrometry. Hyaluronan mediated motility receptor (HMMR), fragile X mental retardation 1 (FMR1), and vitronectin (VTN) were identified by mass spectrometry to co-immunoprecipitate with MT1-MMP. HMMR and FMR1 were identified in MCF-7, C1, and ΔCD cells whereas VTN was found in MCF-7 and C1 (Appendix B). In parallel, samples were immunoprecipitated with either a rabbit MT1-MMP (IP:MT1-MMP) or normal rabbit IgG (IP: IgG) antibody followed by Western blot analysis. Bands corresponding to HMMR (84 kDa) and FMR1 (80 kDa) were observed in all cell lines. MT1-MMP (63 kDa) protein was visualized in MCF-7 and C1 lysate. Since membranes are trimmed at 60 kDa to limit oversaturation of the heavy chain IgG chemiluminescent signal, the truncated form (59 kDa) of MT1-MMP could not be visualized in ΔCD cell lysate. VTN (62 kDa) was observed only in MCF-7 cells. Pulldown with a rabbit IgG antibody showed no bands corresponding to HMMR, FMR1, MT1-MMP, or VTN protein when probed with their respective antibodies.

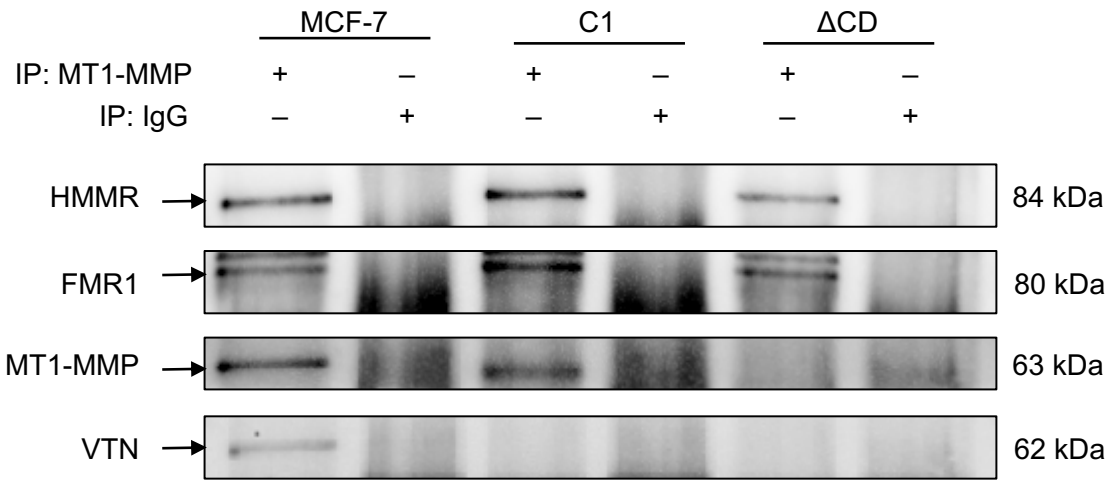
MCF-7
C1
ΔCD
IP: MT1-MMP + – + – + –
IP: IgG – + – + – +
HMMR
84 kDa
FMR1
80 kDa
MT1-MMP
63 kDa
VTN
62 kDa

3.4 Proteins immunoprecipitated from full-length *MT1-MMP* expressing cell lines, but not ΔCD, are involved in various KEGG pathways

Towards identifying any functional consequences of MT1-MMP lacking its cytoplasmic domain, KEGG analysis was used to compare proteins isolated solely in cells expressing full-length MT1-MMP (MCF-7 and C1) with those isolated in ΔCD. The premise of this comparison was to identify potential cytoplasmic binding partners that may be important for cell signalling or MT1-MMP localization that would be absent in ΔCD. A total of 177 proteins were identified following immunoprecipitation of MT1-MMP in MCF-7, C1, or both cell lines in comparison to 71 proteins identified in ΔCD (Figure 5b). KEGG analysis of proteins isolated in MCF-7 and C1 identified enrichment in various pathways (Table 3) such as: protein processing in the ER, RNA degradation, mRNA surveillance, RNA transport, pathogenic *E. coli* infection, non-homologous end-joining, protein export (hsa03060), Huntington's disease, adrenergic signaling in cardiomyocytes, and endocytosis. Except for protein export, these pathways were enriched following KEGG analysis of the original 248 proteins isolated with MT1-MMP pulldown (Table 2). Conversely, KEGG analysis of proteins isolated from ΔCD identified an enrichment of proteins related to RNA transport (7 of 159 genes; FDR=1.3 x 10^{-4}; data not shown). Therefore, enrichment identified in the 248-protein dataset is dependent on the proteins isolated from full-length MT1-MMP expressing cells, and not ΔCD. Marked proteins (*) within the table will be discussed later (section 4.4).

3.5 ΔCD cells have reduced TGF-β1 expression, but not small latency complex protein level

A fundamental embryonic process that can be modulated by MT1-MMP activity is the epithelial-mesenchymal transition. An objective of this research was to assess the involvement of the MT1-MMP cytoplasmic domain in cell signalling pathways to better elucidate its role in cell migration. To determine if expression of genes involved in EMT differed between the cell lines, total RNA was extracted from each cell line to compare transcript levels. Many of the EMT-associated genes chosen, Snail (*SNAI1*), cell division cycle 42 (*CDC42*), cadherin 1 (*CDH1*), integrin subunit β 1 (*ITGB1*), and extracellular matrix metalloproteinase inducer (*BSG*), did not differ between parental MCF-7 cells and

Table 3. Top 10 most significantly enriched KEGG pathways represented by 177 proteins co-immunoprecipitated solely with full-length MT1-MMP expressing cells – MCF-7 and C1[a].

ID: KEGG Pathway	Count[b]	Size[b]	Genes					FDR[a]
Protein processing in the endoplasmic reticulum (hsa04141)	11	161	BAG2 HSP90AB1 SSR1*	DNAJA1 HSPA5	DNAJA2 RPN1*	EIF2S1 RRBP1	HSP90AA1 SEC13*	3.61×10^{-5}
RNA degradation (has03018)	8	77	CNOT1 HSPA9	CNOT2 HSPD1	CNOT3 XRN2	CNOT7	EDC4	3.61×10^{-5}
mRNA surveillance pathway (has03015)	9	89	CASC3 PPP1CA	CPSF1 PPP1CC	CPSF2 UPF1	FIP1L1 WDR33	PNN	3.61×10^{-5}
RNA transport (has03013)	11	159	CASC3 EIF4A1 UPF1	EIF2S1 NUP210	EIF2S3 PNN	EIF3C RAN	EIF3CL SEC13	3.61×10^{-5}
Pathogenic *Escherichia coli* infection (has05130)	6	53	CTNNB1 YWHAZ	NCL	TUBB2A	TUBB2B	TUBB6	0.00045
Endocrine and other factor-regulated calcium reabsorption (has04961)	5	47	AP2A1	AP2B1	AP2M1	ATP1A1	CLTC	0.0026
Non-homologous end-joining (has03450)	3	13	PRKDC	XRCC5	XRCC6			0.0083
Protein export (has03060)	3	23	HSPA5	SRP14*	SRP72*			0.0314

(Table 3 continued)

ID: KEGG Pathway	Count	Size	Genes					FDR
Huntington's disease (has05016)	7	193	AP2A1 DCTN1	AP2B1 NDUFA4	AP2M1	ATP50	CLTC	0.0326
Adrenergic signaling in cardiomyocytes (has04261)	6	139	ATP1A1 TPM1	ATP2A2	GNAI3	PPP1CA	PPP1CC	0.0326
Endocytosis (has04144)	8	242	AP2A1* CLTC*	AP2B1* RAB10*	AP2M1 TFRC	ARF5	CAPZB	0.0326

[a] **Abbreviations:** KEGG, Kyoto Encyclopedia of Genes and Genomes; FDR, False Discovery Rate

[b] **Notes:** Count: number of genes isolated within pathway; Size: total number of genes in pathway

* proteins are discussed in Chapter 4

C1 or ΔCD (Figure 7a). However, a 5-fold reduction of *TGFB1* expression was observed in the ΔCD line ($p \leq 0.05$), but not in the C1 cell line. Immunoblot analysis determined that the reduction of *TGFB1* expression in ΔCD cells did not result in a decrease in TGF-β1 protein. Bands corresponding to TGF-β1 small latency complex (44 kDa) were quantified with no significant difference observed between cell lines (Figure 7b). Quantification of secreted TGF-β1 in media using protein precipitation and immunoblotting was unsuccessful.

3.6 ΔCD cells have altered expression of TGFβ subfamily members and increased SMAD2 phosphorylation

To better understand the decrease of *TGFB1* RNA levels in ΔCD cells, the expression of other TGF-β family members was quantified. In contrast to a decrease of *TGFB1* expression, ΔCD cells had increased levels of *TGFB2*, *TGFB3*, and *TGFBR3* ($p<0.05$) in comparison to parental MCF-7 cells (Figure 8a). No change in expression of TGF-β isoforms or receptors was observed in C1 cells relative to parental MCF-7 cells. Since TGF-β1 and TGF-β2 share similar activation mechanisms of TGF-β signalling through the canonical SMAD pathway, levels of SMAD2 phosphorylation was quantified. Protein bands corresponding to phospho-SMAD2 (60 kDa) were quantified relative to total SMAD2 levels (58 kDa). ΔCD cells displayed a 3.5-fold increase in SMAD2 phosphorylation relative to parental MCF-7 cells, with no change observed in C1 cells (Figure 8b). Additionally, *SMAD2* as well as its cofactor *SMAD4* had increased transcript levels solely in ΔCD cells ($p<0.05$) (Figure 8c).

To corroborate the observation of increased SMAD2 phosphorylation in ΔCD cells, the expression of genes known to be regulated through canonical TGF-β signalling were quantified. Solute carrier family 39 member 1 (*SLC39A1*) (Özdemir et al., 2014), cyclin dependent kinase inhibitor 1A (*CDKN1A*) (Liu et al., 2010), ETS homologous factor (*EHF*) (Yamazaki et al., 2015), bone marrow stromal cell antigen 2 (*BST2*) (Sayeed et al., 2013), and tumour protein P53 inducible nuclear protein 1 (*TP53INP1*) (Liu et al., 2015) are select genes known to be either upregulated or downregulated in response to TGF-β treatment. Thus, corresponding changes in their RNA levels were used to confirm

Figure 7. Cells with MT1-MMP lacking its cytoplasmic domain have an altered profile of TGF-β1 levels.

(a) qPCR analysis of parental MCF-7, C1, and ΔCD cell lines revealed similar expression of genes associated with epithelial-mesenchymal transition. No statistically significant changes were observed in *SNAI1*, *CDC42*, *CDH1*, *ITGB1*, or *BSG* levels. However, ΔCD cells had a significant decrease in *TGFB1* expression relative to parental MCF-7 cells ($p \leq 0.05$). The results of four biological replicates are shown as $\log_2$ transformed mean fold-change ± SEM and were compared using one-way ANOVA and Tukey's post-hoc test; *, $p \leq 0.05$. **(b)** Representative immunoblot image (left) of intracellular TGF-β1 protein level in parental MCF-7, C1, and ΔCD cells. Western blot analysis was used to determine if a reduction of *TGFB1* expression as seen via qPCR resulted in altered TGF-β1 protein levels. No change of intracellular TGF-β1 (44 kDa) sequestered in its small latency complex (SLC) was observed between cell lines following densitometry quantification (right). Band intensities were normalized to β-actin before comparison to parental MCF-7 cells. Means from three biological replicates are presented as mean arbitrary units (a.u.) ± SEM and were analyzed using one-way ANOVA.

a.

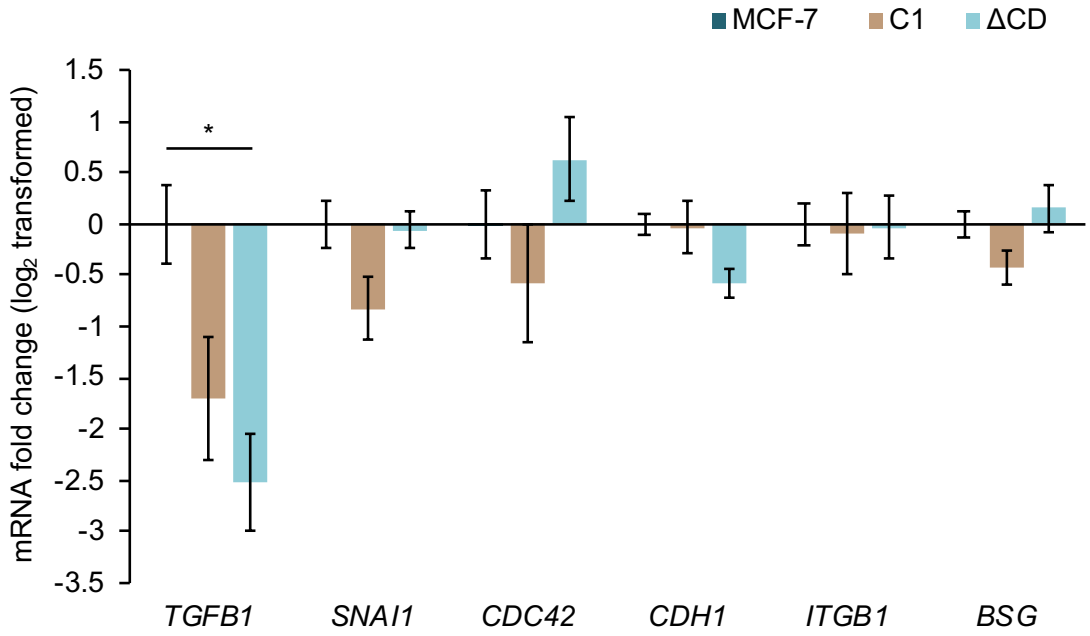
MCF-7
C1
ΔCD
mRNA fold change (log2 transformed)
1.5
1
0.5
0
-0.5
-1
-1.5
-2
-2.5
-3
-3.5
*
TGFB1
SNAI1
CDC42
CDH1
ITGB1
BSG

b.

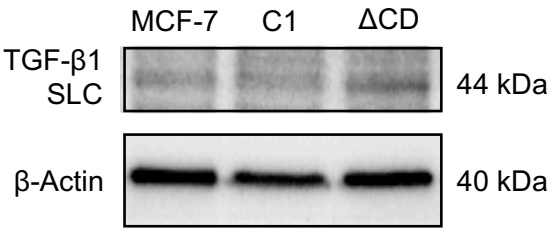
MCF-7
C1
ΔCD
TGF-β1 SLC
44 kDa
β-Actin
40 kDa

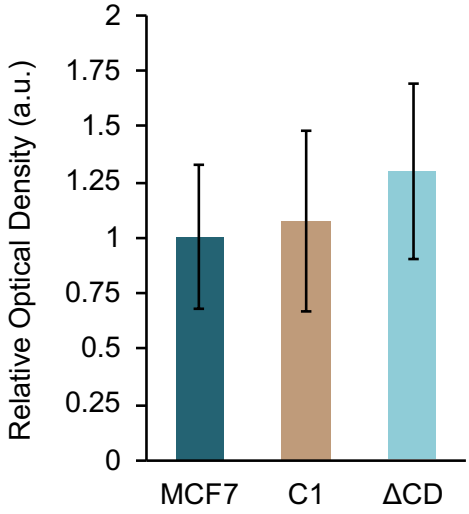
Relative Optical Density (a.u.)
2
1.75
1.5
1.25
1
0.75
0.5
0.25
0
MCF7
C1
ΔCD

Figure 8. Deletion of the cytoplasmic domain of MT1-MMP increased canonical SMAD2-dependent TGF-β signalling.

(a) Expression of different TGF-β isoforms and receptors was assessed using qPCR analysis. *TGFB1* decreased in ΔCD, however, expression of *TGFB2*, *TGFB3*, and *TGFBR3* increased relative to parental MCF-7 cells ($p \leq 0.05$). No change was observed in C1 cells relative to parental MCF-7 cells. The results of three biological replicates are shown as $\log_2$ transformed mean fold-change ± SEM and were compared using one-way ANOVA and Tukey's post-hoc test; *, $p \leq 0.05$. **(b)** Representative immunoblot image (left) of phospho-SMAD2 (60 kDa) and total SMAD2 (58 kDa) protein levels in parental MCF-7, C1, and ΔCD cells. An increase in the relative level of SMAD2 phosphorylation was observed solely in ΔCD cells. Densitometry quantification (right) of three biological replicates are shown, with phospho-SMAD2 normalized to total SMAD2 for each sample before comparison to parental MCF-7. Means are presented as arbitrary units (a.u.) ± SEM and were analyzed using one-way ANOVA and Tukey's post-hoc test; *, $p \leq 0.05$. **(c)** qPCR analysis of *SMAD2* and *SMAD4* in all cell lines. ΔCD cells have significantly higher expression of *SMAD2* and *SMAD4* ($p \leq 0.05$) relative to parental MCF-7 cells. Log_2 transformed mean fold-change ± SEM from three biological replicates were compared using one-way ANOVA and Tukey's post-hoc test; *, $p \leq 0.05$; ***, $p \leq 0.001$.

a.

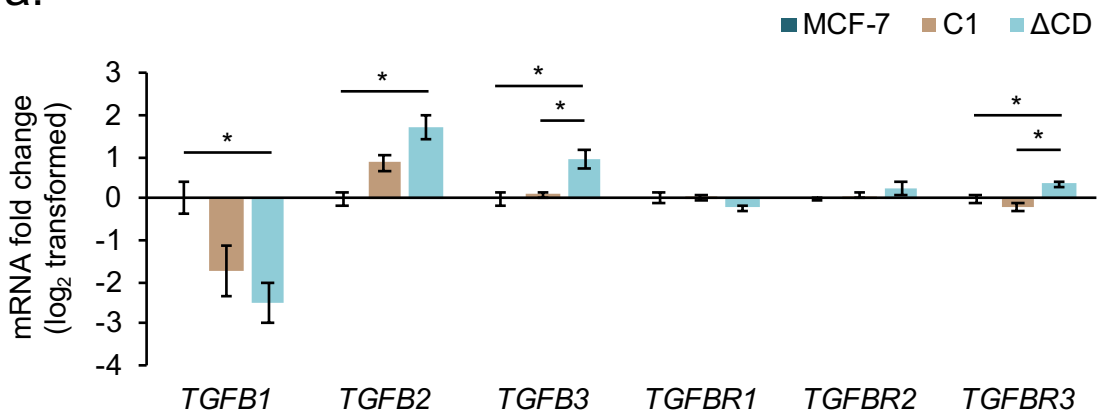
MCF-7
C1
ΔCD
mRNA fold change (log2 transformed)
3
2
1
0
-1
-2
-3
-4
*
*
*
*
*
*
TGFB1
TGFB2
TGFB3
TGFBR1
TGFBR2
TGFBR3

b.

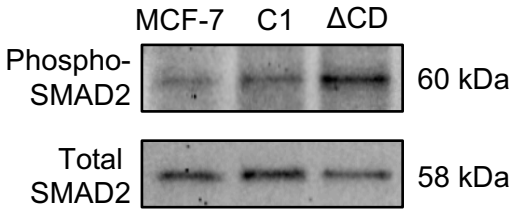
MCF-7
C1
ΔCD
Phospho-SMAD2
60 kDa
Total SMAD2
58 kDa

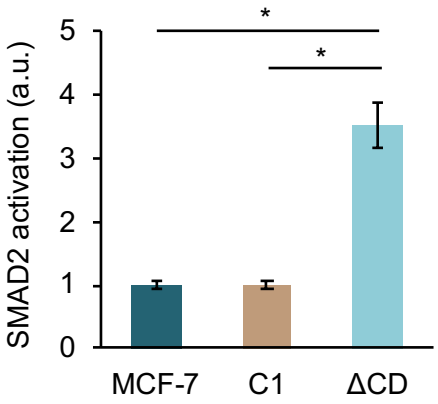
SMAD2 activation (a.u.)
5
4
3
2
1
0
*
*
MCF-7
C1
ΔCD

c.

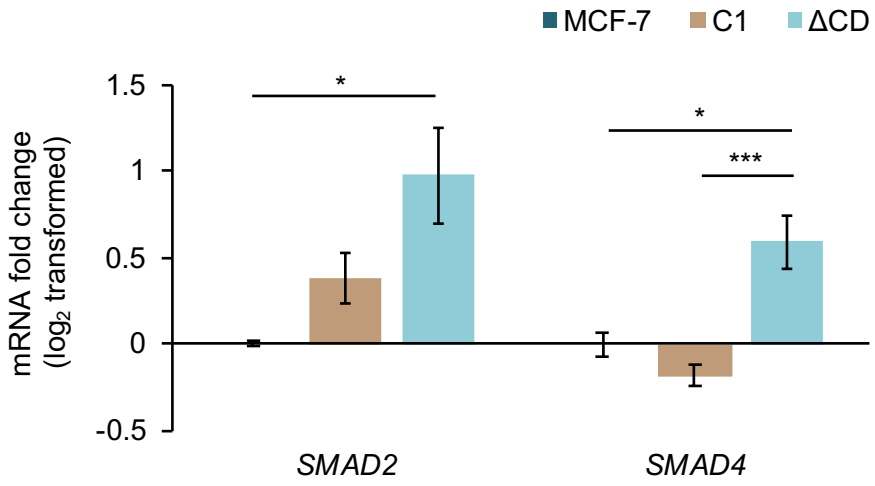
MCF-7
C1
ΔCD
mRNA fold change (log2 transformed)
1.5
1
0.5
0
-0.5
*
*
***
SMAD2
SMAD4

downstream effects of the different TGF-β/SMAD2 levels observed between the cell lines.

As ΔCD cells increased phospho-SMAD2 levels, genes that have been shown to be upregulated through TGF-β signalling – *SLC39A1*, *CDKN1A*, and *EHF* – should have elevated RNA levels in ΔCD cells. Indeed, *SLC39A1* expression increased 1.5-fold ($p<0.01$) in ΔCD cells, but not C1 (Figure 9). In contrast, *EHF* expression was 6.2-fold higher ($p<0.01$) in C1 cells relative to parental MCF-7 cells. *CDKN1A* (aka *P21*) did not change its expression levels in any cell line. Conversely, previous research has linked TGF-β signalling with the downregulation of *BST2* and *TP53INP1*. Accordingly, a decrease in expression was expected in ΔCD cells. *BST2* levels decreased 3.1-fold ($p<0.001$) in C1 and 16.4-fold ($p<0.0001$) in ΔCD cells. No change in *TP53INP1* RNA level was observed in any cell line relative to parental MCF-7 cells.

Figure 9. Observed increase of SMAD-dependent TGF-β signalling in ΔCD cells resulted in increase of *SLC39A1* and decrease of *BST2* expression in ΔCD cells.

Genes previously known to be up- or down-regulated by TGF-β signalling were analyzed with qPCR. *SLC39A1*, *CDKN1A*, and *EHF* have been shown to be upregulated through the canonical TGF-β/SMAD pathway. Increased expression of *SLC39A1* ($p<0.01$) and *EHF* ($p<0.01$) were observed in ΔCD and C1 cells, respectively. No change in *CDKN1A* expression occurred in either cell line. Conversely, *BST2* and *TP53INP1* were previously observed to be downregulated following TGF-β treatment. Expression of *BST2* significantly decreased in C1 ($p<0.001$) and ΔCD ($p<0.0001$) cells, with no change observed in *TP53INP1* expression. Three biological replicates are shown as $\log_2$ transformed mean fold-change ± SEM and were compared using one-way ANOVA and Tukey's post-hoc test; *, $p \leq 0.05$; **, $p \leq 0.01$; ***, $p \leq 0.001$; ****, $p \leq 0.0001$.

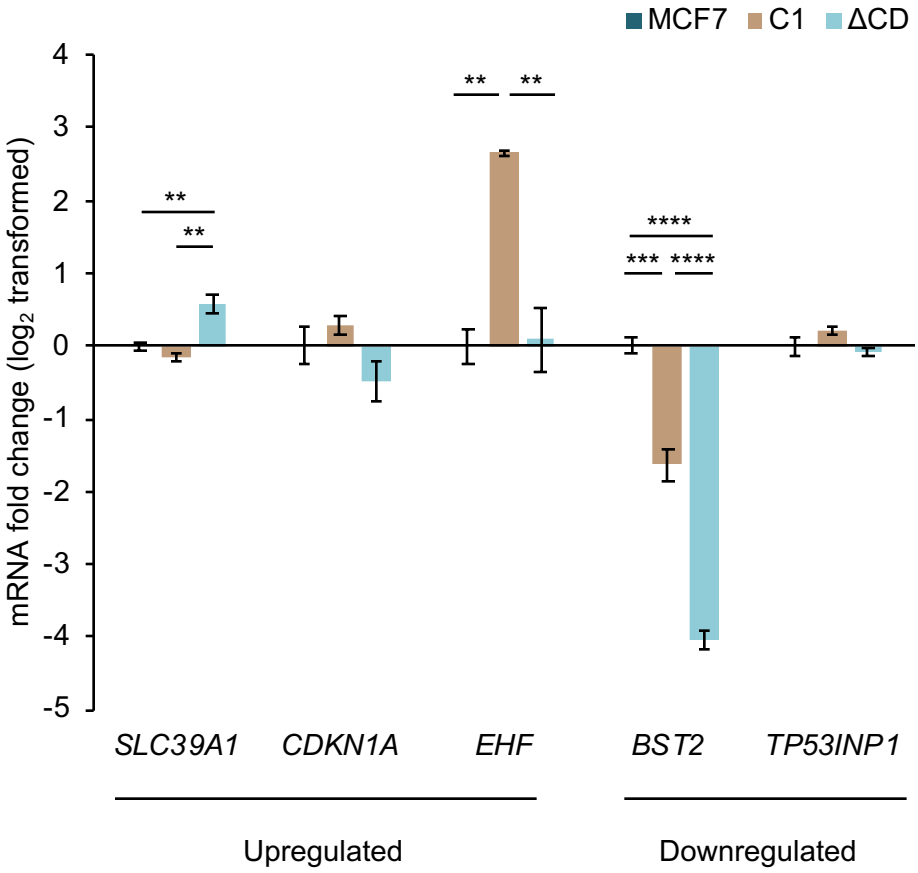
MCF7
C1
ΔCD
mRNA fold change (log2 transformed)
4
3
2
1
0
-1
-2
-3
-4
-5
**
**
**
**
***
****
****
SLC39A1
CDKN1A
EHF
BST2
TP53INP1
Upregulated
Downregulated

4 DISCUSSION

The aim of this study was to generate a catalog of proteins that associate with MT1-MMP to corroborate previous research of MT1-MMP-mediated proteolytic and cell signalling functions. Using MCF-7 breast cancer cells, stable cell lines were previously created that overexpress *MT1-MMP* (C1) or express *MT1-MMP* lacking its cytoplasmic domain (ΔCD). I hypothesized that the diverse functions of MT1-MMP are dependent on domain-specific binding partners that elucidate a cellular response. The first objective of the study was to identify putative MT1-MMP binding partners, and 248 unique proteins were isolated following MT1-MMP pulldown and identified with mass spectrometry. Secondly, comparison of binding partners isolated from full-length and truncated *MT1-MMP* expressing cells identified differences in KEGG pathway enrichment. In particular, the cytoplasmic domain may be required for protein-protein interactions that facilitate MT1-MMP localization. Finally, the cytoplasmic domain of MT1-MMP is involved in cell signalling pathways as indicated by an increase in canonical TGF-β signalling within ΔCD cells.

4.1 Identification of MT1-MMP binding partners and similarities to previous MT1-MMP proteomic research

In this study, 248 proteins (Appendix B) were coimmunoprecipitated with MT1-MMP and identified via mass spectrometry in parental MCF-7, C1, and ΔCD cells. Although 939 proteins were identified in MCF-7 cells, 919 in C1 cells, and 1051 in ΔCD, stringent filtering criteria was used to eliminate non-specific proteins. Firstly, proteins needed to be identified by at least 1 unique peptide and isolated in ≥2 biological replicates. Second, pulldown with a rabbit IgG antibody was used as a negative control to identify proteins that may non-specifically associate with the MT1-MMP rabbit antibody or beads. Third, ribosomes and proteins that were associate with the spliceosome pathway (Appendix A) were removed due to their identification as common contaminants (Gingras et al., 2007). Ribosomal and spliceosome-related proteins were also observed to be enriched in the anti-rabbit IgG pulldown. Following removal of non-specific proteins, the final dataset included ~15% of the total number of proteins that were originally isolated with anti-MT1-MMP immunoprecipitation (Figure 5a). Since label-free

coimmunoprecipitation relies on a single step affinity purification, it is estimated that true interaction partners represent ~10% of originally identified proteins (Nesvizhskii, 2012). The number of true interactions being 15% of the total number of proteins originally isolated in this study is within this magnitude.

In the identification of false positives, many proteins are recognized as common contaminants and subsequently excluded from analysis. Typically, these proteins are highly abundant (e.g. tubulins and actins) or involved in disrupted protein folding (e.g. heat shock proteins and chaperones) (Gingras et al., 2007; Nesvizhskii, 2012). Highly abundant proteins, and those involved in disrupted protein folding, were isolated with MT1-MMP. However, a limitation of affinity purification and mass spectrometry is its inability to decipher a multiplicity of associations (Gingras et al., 2007). These proteins can have dramatically different roles as determined by which distinct, yet biologically relevant, complex they are associated with. For this reason, these proteins (e.g. tubulins, actin, or HSPs) were not removed from the dataset even though they are commonly identified as false positives.

Several studies have identified MT1-MMP binding partners using a bottom-up proteomic approach. From this, approximately 400 unique proteins have been catalogued as potential MT1-MMP binding partners (Butler et al., 2008; Hwang et al., 2004; Niiya et al., 2009; Stegemann et al., 2013; Tam et al., 2004; Tomari et al., 2009). In agreement with previous studies, 26 of the 248 proteins identified here have been reported as MT1-MMP binding partners (Table 4). These proteins include extracellular matrix components (laminin and vitronectin), receptors (transferrin receptor and receptor of activated protein C kinase), and various signalling molecules (G proteins). The catalog of binding partners identified in MT1-MMP proteomic studies contains approximately 400 proteins. However, complete lists of binding partners were not provided in all studies which indicates this catalog is much larger. For instance, Tam et al., (2004) provided only a subset of 17 identified binding partners whereas their original dataset contained over 100 proteins. Similarly, Butler et al., (2008) only considered biochemically validated proteins.

Table 4. Proteins identified in this study that have been previously identified in other proteomic-based MT1-MMP studies.

UniProtKB Accession Number	Protein Name	Reference(s)
O15230	Laminin subunit alpha-5	[1]
O43291	Kunitz-type protease inhibitor 2	[2, 4]
O60884	DnaJ homolog subfamily A member 2	[3]
O95816	BAG family molecular chaperone regulator 2	[3]
P02765	Alpha-2-HS-glycoprotein	[5]
P02786	Transferrin receptor protein 1	[3, 4]
P04004	Vitronectin	[5]
P04843	Dolichyl-diphosphooligosaccharide--protein glycosyltransferase subunit 1	[3]
P05023	Sodium/potassium-transporting ATPase subunit alpha-1	[3]
P08107	Heat shock 70 kDa protein 1A/1B	[4]
P08195	4F2 cell-surface antigen heavy chain	[3]
P08754	Guanine nucleotide-binding protein G(k) subunit alpha	[4]
P10909	Clusterin	[5]
P11021	78 kDa glucose-regulated protein	[3, 4]
P31689	DnaJ homolog subfamily A member 1	[3, 4]
P35221	Catenin alpha-1	[3, 4]
P35222	Catenin beta-1	[4]
P50402	Emerin	[4]
P62873	Guanine nucleotide-binding protein G(I)/G(S)/G(T) subunit beta-1	[3]
P63244	Guanine nucleotide-binding protein subunit beta-2-like 1 (Receptor of activated protein C kinase 1)	[4]
P78371	T-complex protein 1 subunit beta	[3]
Q01650	Large neutral amino acids transporter small subunit 1	[3]
Q13162	Peroxiredoxin-4	[3]
Q13501	Sequestosome-1	[3, 4]
Q9BUF5	Tubulin beta-6 chain	[3]
Q9UIQ6	Leucyl-cystinyl aminopeptidase	[3]

[1] Stegemann et al., 2013; [2] Butler et al., 2008; [3] Tomari et al., 2009; [4] Niiya et al., 2009; [5] Hwang et al., 2004

No accession numbers were provided in Niiya et al., 2009.

Finally, Niiya et al., (2009) did not provide accession numbers of the proteins identified in the study. Due to the historically unpredictable nature of protein naming, a proper comparison could not be completed.

It is important to note that although only ~10% of proteins pulled down in this study have been previously identified, the affinity purification methodology employed in this work differed drastically. In previous studies, the use of tagged MT1-MMP (for easy isolation) or catalytically inactive MT1-MMP (to prevent degradation of binding partners) could alter MT1-MMP–protein complex formation, unlike native MT1-MMP used in this study.

4.2 Validation of select binding partners

As 248 proteins were identified by mass spectrometry as putative MT1-MMP binding partners, I sought to validate the utility of the co-immunoprecipitation. Pulldown of MT1-MMP followed by immunoblot analysis confirmed MT1-MMP interactions with vitronectin, hyaluronan-mediated motility receptor, and fragile X mental retardation protein 1 (Figure 6).

Vitronectin is a multifunctional extracellular glycoprotein commonly involved in cell-ECM adhesion. MT1-MMP mediated degradation of vitronectin was previously observed in human plasma incubated with a soluble MT1-MMP catalytic domain (Hwang et al., 2004). While observed in parental cells, vitronectin was not identified following MT1-MMP pulldown from ΔCD cells by mass spectrometry nor immunoblotting (Appendix B, Figure 6). This is not due to an inability of MT1-MMP to digest vitronectin as MT1-MMP lacking its transmembrane and cytoplasmic domain cleaved vitronectin into two distinct fragments (Ohuchi et al., 1997). Rather, improper localization or recycling of ΔCD MT1-MMP (section 4.4.3) could result in perpetual inhibition by TIMP-2 or other endogenous inhibitors. Although identified by mass spectrometry following MT1-MMP pulldown in C1 cells, no visible band corresponding to vitronectin was observed in the validation assay (Figure 6). Due to increased *MT1-MMP* expression in C1 cells, these cells have higher levels of ECM degradation. For this reason, vitronectin bound to MT1-MMP may be rapidly degraded to a level undetectable by immunoblot analysis.

The hyaluronan-mediated motility receptor belongs to a family of hyaladherins that share the ability to bind hyaluronic acid (HA), an important component of the ECM and tumour microenvironment. Despite its putative extracellular role, there are reports that intracellular HMMR is involved in mitotic spindle integrity and cell cycle progression (Entwistle et al., 1996). In this study, HMMR was isolated in parental MCF-7, C1, and ΔCD cell lines. This alludes that the interaction with MT1-MMP is most likely occurring at the cell surface and supports an extracellular role (Figure 6, Appendix B). This study is the first to report a direct interaction between HMMR and MT1-MMP. However, HMMR forms a complex with CD44 and HA on the cell surface to activate intracellular signalling pathways, in particular MAPK via ERK1/2 activation (Turley et al., 1993; Zhang et al., 1998). The interaction between MT1-MMP and CD44 has been extensively reported, with localization of MT1-MMP to invadopodia and associated increase in cell migration attributed to this interaction (Mori et al., 2002; Ridley et al., 1992). Since MT1-MMP, CD44, and now purportedly HMMR can be clustered to invadopodia, both MT1-MMP hemopexin-mediated binding and proteolytic shedding of HMMR may contribute to the previously observed increase in ERK activation within these cell lines (Cepeda et al., 2016, 2017b).

MT1-MMP not only co-immunoprecipitated with FMR1, but also two homologs that interact with it: fragile X-related protein (FXR) 1 and FXR2 (Zhang et al., 1995; Figure 6, Appendix B). To date, research of FMR1 focuses on its role as a translation regulator of proteins involved in cellular migration, motility, as well as adhesion and EMT (Lucá et al., 2013). In particular, FMR1 modulates the expression of MMP-8 as well as TIMP-2 (Zalfa et al., 2017). For this reason, it is unsurprising that FMR1 is overexpressed in various cancer, correlating with aggressive breast cancer markers. Interaction of MT1-MMP with FMR1 or its homologs have not been previously reported. However, just as MT1-MMP is localized at the leading edge of migrating cells, FMR1 is also asymmetrically distributed with a front-rear polarity in cell migration (Zalfa et al., 2017). Validation of vitronectin, HMMR, and FMR1 co-immunoprecipitation with MT1-MMP further supports that other proteins identified in this study are true interactions.

4.3 Involvement of binding partners in different pathways highlights the diverse function of MT1-MMP

KEGG analysis of MT1-MMP binding partners identified enrichment within various pathways (Table 2). Many of these networks have not been previously shown to involve MT1-MMP functions. Protein involved in endocrine and other factor-regulated calcium reabsorption pathways, pathogenic *Escherichia coli* infection, and Huntington's disease pathways were enriched within the catalog of MT1-MMP pulldown proteins. Upon further examination, many of these proteins are part of cellular processes within the identified pathway. For example, adaptor proteins and clathrin are key proteins involved in endocytosis that may be dysfunctional within Huntington's disease. Since KEGG pathway analysis treats each pathway as a separate entity, it ignores the effect of shared proteins involved in various cascades. For this reason, pathogenic *E. coli* infection, Huntington's disease, and endocrine and other factor-regulated calcium reabsorption pathways are not necessarily indicative of MT1-MMP's function within MCF-7 cells.

Involvement of MT1-MMP in other pathways such as RNA transport, RNA degradation, and mRNA surveillance has also not been reported. However, MT1-MMP pulldown proteins enriched in these KEGG pathways relate to a role in mRNA degradation. Mostly centred around the nucleus, MT1-MMP binding partners (e.g. pinin/PNN) further support that MT1-MMP can be translocated to the nucleus. Although MT1-MMP has no clear nuclear localization sequence (NLS), furin recognition motifs between the pro- and catalytic domain represent a bipartite NLS (Strongin, 2006). MT1-MMP interaction with importin α implies that this method of transport to the nucleus may be occurring. However, it is unknown whether this mechanism would specify between the transport of pro- or active MT1-MMP. Regardless, MT1-MMP colocalizes with MMP-2 in nuclei of liver tumours, correlating with poor survival (Ip et al., 2007). Immunoblot analysis of nuclear MT1-MMP identified the 63 kDa active form as well as the 43 kDa degraded form generated by MMP-2 processing, verifying that MT1-MMP and MMP-2 are catalytically active within the nucleus. Additionally, Ip et al., (2007) observed MT1-MMP transport to the perinuclear region in a caveolin-dependent manner, similar to the nuclear translocation of insulin-like growth factor binding protein-3. Although the function of MT1-MMP within the nucleus isn't fully characterized, isolation of binding

partners involved in mRNA degradation suggest a new potential role of MT1-MMP within the nucleus/perinuclear region.

4.4 The cytoplasmic domain of MT1-MMP is required for protein export, processing in the endoplasmic reticulum, and endocytosis

To better elucidate the role of domain-specific interactions, prey proteins isolated from full-length *MT1-MMP* expressing cells (MCF-7 and/or C1), but not ΔCD cells, were analyzed. KEGG pathway analysis identified enrichment within the 177 proteins isolated in MCF-7 and C1 cells that was not observed in the 71 proteins isolated in ΔCD cells (Figure 5). Of particular interest, there was an enrichment of proteins involved in protein export, protein processing in the endoplasmic reticulum, and endocytosis (Table 3).

4.4.1 Protein export

Approximately 30% of all translated proteins are delivered to the endoplasmic reticulum, most commonly by the signal recognition particle (SRP). Comprised of 6 proteins and a 7S SRP RNA, the SRP can be divided into two distinct domains – Alu domain and S domains. Two different SRP proteins immunoprecipitated with MT1-MMP in the parental MCF-7 and C1 cell lines. Of particular interest, SRP14 is a subunit of the Alu domain whereas SRP72 is a subunit of the S domain (Akopian et al., 2013). No previous research has identified an interaction between MMPs and the SRP. In fact, there has been no reported protease involvement with the SRP. Since pro-MT1-MMP is commonly activated in the trans-Golgi network, this SRP interaction is likely not enzyme/substrate oriented. The lack of SRP components pulled down in ΔCD cells suggests that translation of the complete protein is required for this interaction to occur. As a type-1 transmembrane protein, the cytoplasmic domain is translated last, with the other domains (pro, catalytic, and hemopexin) already present in the ER lumen. Translation of ΔCD MT1-MMP may not be completed properly due to the lack of expected charged amino acid residues that would be found in the cytoplasmic domain. The SRP may detect this anomaly. As a result, while the full-length protein remains bound to the SRP for further functions or processing, the truncated protein is not.

4.4.2 Protein processing within the ER

In comparison with ΔCD, full-length MT1-MMP expressing cells co-immunoprecipitated various proteins associated with quality control in the endoplasmic reticulum (i.e. TRAPα, ribophorin 1, and Sec13). Translocon-associated protein subunit alpha (TRAPα) discriminately binds misfolded proteins for efficient degradation upon unfolded protein response (UPR) stimulation. TRAPα was isolated solely in C1 cells with a ~2500-fold increase in *MT1-MMP* expression. Proper folding of this abnormally high level of protein may be rate-limiting, and thus initiate the UPR. Under homeostatic conditions, however, the TRAP complex associates with the translocon to properly fold newly translated polypeptides (Ménétret et al., 2005). Another commonly associated translocon protein is dolichyl-diphosphooligosaccharide--protein glycosyltransferase subunit 1 (ribophorin 1) that facilitates *N*-glycosylation of newly synthesized proteins (Wilson et al., 2005). MT1-MMP has two potential *N*-glycosylation sites at Asn^{229} in the catalytic domain and Asn^{311} within the linker region (Boon et al., 2016). Although putative sequences are found, inhibition of *N*-glycosylation doesn't affect the glycosylation status of MT1-MMP nor its cell surface localization (Remacle et al., 2006). Instead, ribophorin 1 interaction with MT1-MMP may be related to protein folding in the ER (Wilson et al., 2005).

During translocation through the ER, MT1-MMP matures before transport to the Golgi for further processing. A common mechanism of ER-Golgi transport is via coat protein complex II (COPII)-coated vesicles. Interaction of full-length MT1-MMP with Sec13 indicates that transport from the ER to Golgi occurs in this manner as Sec proteins are constituents of the COPII coat. Membrane proteins transported to the Golgi typically contain an ER-export motif, which is characterized for MT1-MMP (Nufer et al., 2002). The terminal valine of the cytoplasmic domain and dileucine motif near the C-terminus act as ER export signals (Nufer et al., 2002; Ureña et al., 1999). However, MT1-MMP lacking its cytoplasmic domain may still transport to the Golgi for further processing since Sec16, an early mediator of COPII vesicle formation, was pulled down with MT1-MMP in all cell lines (Hughes et al., 2009).

4.4.3 Endocytosis

Endocytosis can regulate MT1-MMP activity by controlling the level of active MT1-MMP on the cell surface as well as by removing TIMP-bound or otherwise inhibited MT1-MMP from the surface. The LLY^{573} motif within the cytoplasmic domain interacts with AP-2 to mediate clathrin-driven endocytosis (Uekita et al., 2001). Previous research of the ΔCD cell line observed that cytoplasmic deletion increased the migration of the cells in multiple assays (Cepeda et al., 2017b). Since ΔCD MT1-MMP mutants are unable to activate MMP-2 nor degrade gelatin (Cepeda et al., 2017b), the increase in cell migration is likely due to non-proteolytic mechanisms. This reduction in catalytic activity may be related to the absence of clathrin-related machinery pulled down in ΔCD cells. Since the MT1-MMP catalytic domain is rapidly inactivated by binding of TIMP-2 and other inhibitors, surface-localized proteolytic function of MT1-MMP relies on a constant supply of active MT1-MMP (Remacle et al., 2006). This supply is not solely dependent on the biosynthetic pathway. Instead, endocytosed MT1-MMP can be recycled back to the membrane during which any bound inhibitors dissociate. It appears that since ΔCD MT1-MMP cannot bind endocytic machinery, ΔCD MT1-MMP is not properly endocytosed via clathrin-coated vesicles. This reduction of endocytosis corroborates previous observations that ΔCD MT1-MMP has punctate localization at the cell surface, yet is unable to activate MMP-2 or degrade gelatin.

Following endocytosis, recycling of MT1-MMP to invasive protrusions of the plasma membrane involves Rab GTPases. Rab GTPases are a family of Ras-related GTPases that determine the specificity of vesicle transport. Rab-4, 5A, 7, and 8 co-localize with MT1-MMP-positive vesicles and have been identified as regulatory components of MT1-MMP exocytosis from the late endosome to invadopodia (Castro-Castro et al., 2016). There are no reports regarding Rab10 and MT1-MMP recycling, however, Rab10 is closely related to Rab8. Rab8 is known to regulate polarized membrane transport to invasive structures in MDA-MB-231 cells (Bravo-Cordero et al., 2007). Intracellular MT1-MMP is compartmentalized in Rab8-positive vesicles to control cell surface activity, but mobilized to the surface when cells are actively degrading the ECM (Bravo-Cordero et al., 2007). This trafficking would mimic other membrane proteins that are

retained intracellularly, but redistributed via Rab10 to the plasma membrane upon stimulation (Sano et al., 2007). Due to the similarity in structure and vesicle localization, Rab8 and Rab10 may share similar roles in the recycling of MT1-MMP to the cell surface, especially since they are upregulated in cancer cells (He et al., 2002; Ip et al., 2007). The cytoplasmic domain is required for proper MT1-MMP endocytosis and recycling through its interaction with AP-2, clathrin, and Rab GTPases.

The cytoplasmic domain has been previously identified as a requirement for proper MT1-MMP endocytosis, this may be due to truncated MT1-MMP being unable to interact with AP-2, clathrin, or Rab GTPases.

4.5 Limitations of affinity-purified mass spectrometry

Although many proteins discovered in this analysis have been previously reported to immunoprecipitated with MT1-MMP, some, such as MMP-2 (Will et al., 1996), CD44 (Kajita et al., 2001), or TIMP-2 (Will et al., 1996), were not isolated here. Due to the sensitivity of mass spectrometry, extensive purification measures are required to remove impurities and reduce the number of false positives. This is done at risk of losing weak interactions that are biologically relevant (Vermeulen et al., 2008). During the mechanical and chemical stresses of co-immunoprecipitation, bait-prey interactions may be lost if the interaction is low-affinity or transient (Gingras et al., 2007). The affinity and strength of an interaction is dictated by the type of bonds that form. For MT1-MMP, hydrogen bonds form between its catalytic domain and substrate whereas covalent or noncovalent bonds can form at other MT1-MMP domains (Overall, 2001). Accordingly, catalytic binding partners such as MMP-2 and TIMP-2 would be more difficult to capture than proteins that bind other MT1-MMP domains.

In addition to loss of protein-protein interactions during purification procedures, commonly identified binding partners may be absent in the final dataset due to cell-type specificity. In previous MT1-MMP proteomic studies, 163 and 158 proteins were coimmunoprecipitated from A431 carcinoma and A375 melanoma cells, respectively. Experimental procedures were identical in these studies, but only 61 proteins were shared between them (Niiya et al., 2009; Tomari et al., 2009). It appears that the sensitivity of

mass spectrometry is affected by sample complexity, with highly abundant proteins being favoured. Although less common than false positives, false negatives typically occur because of this reason; since interactions with lowly abundant proteins can masked by highly abundant protein. Due to low abundance of MMP-2 and TIMP-2 in MCF-7 cells (Cepeda et al., 2017a), the likelihood of pulldown with MT1-MMP is reduced. Similarly, because the mass spectrometer operated using a FT/IT/CID Top 10 data-dependent mode, highly abundant proteins are more likely to be identified than lowly abundant proteins. Cell-type specific expression may explain why commonly reported MT1-MMP binding partners (e.g. MMP-2 and TIMP-2) were not identified in this study as well as previous studies (Niiya et al., 2009; Tomari et al., 2009).

Samples submitted for mass spectrometry are complex and provide a snapshot of MT1-MMP interactions at the time of protein isolation. If the MT1-MMP–protein interaction is weak, it may be lost during affinity purification procedures. In contrast, if the cell has low expression of a binding partner, the interaction may not be occurring at the time of cell lysate collection or it may be masked by higher abundant proteins during mass spectrometry analysis. These issues highlight a disadvantage of unlabelled affinity purification and mass spectrometry analysis: reproducibility between individual sample preparations. In a previous MT1-MMP proteomic analysis, Butler et al., (2008) identified 269 different proteins from 3 biological replicates. However, of those 269 proteins, 65% were identified in only one biological replicate, 28% were identified in two, and 7% were identified in all three. Indeed, even in this present study, known MT1-MMP binding proteins were identified (i.e. collagen 1α and TIMP-3), but only isolated within one biological replicate. Since the criteria of a true interaction required isolation from ≥2 biological replicates, these proteins were subsequently removed.

4.6 The cytoplasmic domain of MT1-MMP attenuates TGF-β signalling in MCF-7 cells

MT1-MMP lacking its cytoplasmic domain has reduced proteolytic activity, yet ΔCD cells, but not C1, were more migratory than parental MCF-7 cells (Cepeda et al., 2016, 2017b). This indicates that MT1-MMP has a non-proteolytic role in cell migration. Increased migration of ΔCD cells is not due to changes in gene expression commonly

observed in epithelial-mesenchymal transition (Figure 7a). However, a decrease in *TGFB1* expression was observed in ΔCD cells. Therefore, an objective of the study was to identify any potential roles of the MT1-MMP cytoplasmic domain regarding cell signalling pathways, in particular TGF-β signalling.

Originally, no change in intracellular small latency complex-bound TGF-β1 protein level was observed (Figure 7b). However, no suitable TGF-β1 antibody, of the three utilized, specifically corresponded with TGF-β1 or its associated complexes. Furthermore, TGF-β1 is a secreted cytokine that is released from inhibitory complexes in the ECM before it can function as a ligand. Thus, whole cell lysate used for immunoblot analysis would not be indicative of extracellular TGF-β1 protein level. For this reason, quantifying the level of intracellular SLC-bound TGF-β1 protein is not representative of TGF-β1 protein level. In an attempt to quantify extracellular TGF-β1 protein level, cell media was protein precipitated and immunoblotted. However, this was not successful. Thus, SMAD2 phosphorylation was used to better understand if a reduction of *TGFB1* resulted in a decrease in canonical TGF-β signalling

Altered levels of TGF-β genes in ΔCD cells ultimately resulted in increased SMAD-dependent TGF-β signalling (Figure 8). Previously observed genes regulated by TGF-β signalling had variable expression in ΔCD cells (Figure 9). However, expected changes in response to increased TGF-β signalling were observed in some genes (e.g. *SLC39A1* and *BST2*). Other genes examined that did not change solely due to increased SMAD-dependent TGF-β signalling may be modulated by multiple signalling pathways.

Altered TGF-β signalling is likely to occur through MT1-MMP-mediated liberation of extracellular TGF-β isoforms from their inhibitory complexes (Nguyen et al., 2016). MT1-MMP can cleave latent TGF-β binding proteins directly, but also indirectly through pro-MMP-2 and pro-MMP-9 activation (Yu and Stamenkovic, 2000). However, MCF-7 cells are naturally deficient in *MMP-2* and *MMP-9* expression. Additionally, MT1-MMP proteolytic activity in ΔCD cells is ablated (Cepeda et al., 2017b). For these reasons, increased SMAD2 phosphorylation is likely not a result of increased free TGF-β ligand that can bind its receptors. Rather, reduced MT1-MMP proteolytic activity in ΔCD cells

maintains TGF-β receptor 3 (TGFβR3, betaglycan) at the cell surface. In contrast, MT1-MMP in parental MCF-7 and C1 cells may shed TGF-β receptors, such as betaglycan, from the cell surface (Velasco-Loyden et al., 2004). When bound to the plasma membrane, betaglycan functions as a coreceptor, enhancing TGFβ affinity with TGFβR2 to facilitate downstream signalling. However, when shed from the membrane, betaglycan has an inverse effect by inhibiting TGF-β availability, especially the TGF-β2 isoform (López-Casillas et al., 1994; Velasco-Loyden et al., 2004). Reduced MT1-MMP catalytic activity in ΔCD cells (Cepeda et al., 2017b) would prevent betaglycan shedding, thus increasing TGF-β signalling relative to parental MCF-7 and C1 cells.

4.7 Future directions

The work presented is a strong foundation on which future data mining of MT1-MMP interacting partners and networks can be accomplished. To begin, although proteins pulled down with MT1-MMP indicate an association, the functional consequences of the interaction are unknown. The comparison of proteins isolated from full-length expressing MT1-MMP cells with proteins isolated in ΔCD cells can help elucidate, but not confirm, the outcome of an interaction. To that end, characterization of domain-specific binding, cellular localization, and the outcome of an interaction regarding cell signalling or degradation by-products should be evaluated first. Future work should aim to better understand the translation of an MT1-MMP–protein interaction to other *in vitro* and *in vivo* approaches. The MCF-7 cell line used in this study has low endogenous expression of *MT1-MMP*. As such, overexpression of *MT1-MMP* may result in nonphysiologically relevant MT1-MMP–protein interactions. An interaction should be confirmed using another cell type, such as MDA-MB 231 cells, that have higher endogenous *MT1-MMP* expression than MCF-7 cells. Additionally, since MT1-MMP remodels the ECM, *in vitro* conditions such as growth on a synthetic ECM may impact the location and outcome of an interaction. Finally, a transition from *in vitro* to *in vivo* studies would provide a more comprehensive understanding of MT1-MMP function as dictated by its interaction with various binding partners.

5 CONCLUSION

Membrane-type 1 matrix metalloproteinase is a multifunctional enzyme involved in a variety of cellular processes. As previous studies have identified binding partners of MT1-MMP that contribute to its diverse function, the aim of this study was to generate a catalog of proteins that associate with MT1-MMP to corroborate previous research regarding the role of MT1-MMP in cell migration, invasion, and survival. Here, 248 proteins were isolated with MT1-MMP in MCF-7 cells, 26 of which have been previously reported as MT1-MMP binding partners. Binding partners identified within this study imply new putative MT1-MMP functions, such as RNA turnover or transport. I hypothesized that these binding partner interactions, and subsequent cellular responses, are MT1-MMP domain-specific. In this study, binding partners isolated from full-length expressing *MT1-MMP* cells were compared with those isolated from cells that express a truncated form of *MT1-MMP* lacking its cytoplasmic domain. KEGG enrichment analysis suggests the cytoplasmic domain may be required for protein-protein interactions that facilitate MT1-MMP function, such as proper processing in the ER, protein export, and endocytosis. However, ΔCD cells have increased SMAD2 phosphorylation, indicating that the cytoplasmic domain of MT1-MMP may attenuate canonical transforming growth factor beta (TGF-β) signalling through an unknown mechanism. By contributing to the expanding catalog of MT1-MMP binding partners, this work suggests new MT1-MMP functions within MCF-7 cells.

References

Abrams, G.A., S.S. Schaus, S.L. Goodman, P.F. Nealey, and C.J. Murphy. 2000. Nanoscale topography of the corneal epithelial basement membrane and Descemet's membrane of the human. *Cornea*. 19:57–64.

Akopian, D., K. Shen, X. Zhang, and S.-O. Shan. 2013. Signal recognition particle: an essential protein-targeting machine. *Annu. Rev. Biochem.* 82:693–721.

Bode, W., C. Fernandez-Catalan, F. Grams, F.X. Gomis-Rüth, H. Nagase, H. Tschesche, and K. Maskos. 1999. Insights into MMP-TIMP interactions. *Ann. N. Y. Acad. Sci.* 878:73–91.

Bode, W., F.X. Gomis-Rüth, and W. Stöckler. 1993. Astacins, serralysins, snake venom and matrix metalloproteinases exhibit identical zinc-binding environments (HEXXHXXGXXH and Met-turn) and topologies and should be grouped into a common family, the "metzincins". *FEBS Lett.* 331:134–40.

Bonnans, C., J. Chou, and Z. Werb. 2014. Remodelling the extracellular matrix in development and disease. *Nat. Rev. Mol. Cell Biol.* 15:786–801.

Boon, L., E. Ugarte-Berzal, J. Vandooren, and G. Opdenakker. 2016. Glycosylation of matrix metalloproteases and tissue inhibitors: present state, challenges and opportunities. *Biochem. J.* 473:1471–82.

Bosman, F.T., and I. Stamenkovic. 2003. Functional structure and composition of the extracellular matrix. *J. Pathol.* 200:423–8.

Bourboulia, D., and W.G. Stetler-Stevenson. 2010. Matrix metalloproteinases (MMPs) and tissue inhibitors of metalloproteinases (TIMPs): Positive and negative regulators in tumor cell adhesion. *Semin. Cancer Biol.* 20:161–8.

Bowden, E.T., M. Barth, D. Thomas, R.I. Glazer, and S.C. Mueller. 1999. An invasion-related complex of cortactin, paxillin and PKCmu associates with invadopodia at sites of extracellular matrix degradation. *Oncogene*. 18:4440–9.

Bravo-Cordero, J.J., R. Marrero-Diaz, D. Megías, L. Genís, A. García-Grande, M.A. García, A.G. Arroyo, and M.C. Montoya. 2007. MT1-MMP proinvasive activity is regulated by a novel Rab8-dependent exocytic pathway. *EMBO J.* 26:1499–510.

Brooks, P.C., S. Silletti, T.L. von Schalscha, M. Friedlander, and D.A. Cheresh. 1998. Disruption of angiogenesis by PEX, a noncatalytic metalloproteinase fragment with integrin binding activity. *Cell*. 92:391–400.

Bruney, L., K.C. Conley, N.M. Moss, Y. Liu, and M.S. Stack. 2014. Membrane-type I matrix metalloproteinase-dependent ectodomain shedding of mucin16/ CA-125 on ovarian cancer cells modulates adhesion and invasion of peritoneal mesothelium. *Biol. Chem.* 395:1221–31.

Buccione, R., J.D. Orth, and M.A. McNiven. 2004. Foot and mouth: podosomes, invadopodia and circular dorsal ruffles. *Nat. Rev. Mol. Cell Biol.* 5:647–57.

Butler, G.S., R.A. Dean, E.M. Tam, and C.M. Overall. 2008. Pharmacoproteomics of a metalloproteinase hydroxamate inhibitor in breast cancer cells: dynamics of membrane type 1 matrix metalloproteinase-mediated membrane protein shedding. *Mol. Cell. Biol.* 28:4896–914.

Castro-Castro, A., V. Marchesin, P. Monteiro, C. Lodillinsky, C. Rossé, and P. Chavrier. 2016. Cellular and molecular mechanisms of MT1-MMP-dependent cancer cell invasion. *Annu. Rev. Cell Dev. Biol.* 32:555–576.

Cauwe, B., and G. Opdenakker. 2010. Intracellular substrate cleavage: a novel dimension in the biochemistry, biology and pathology of matrix metalloproteinases. *Crit. Rev. Biochem. Mol. Biol.* 45:351–423.

Cauwe, B., P.E. Van den Steen, and G. Opdenakker. 2007. The biochemical, biological, and pathological kaleidoscope of cell surface substrates processed by matrix metalloproteinases. *Crit. Rev. Biochem. Mol. Biol.* 42:113–85.

Cepeda, M.A., C.L. Evered, J.J.H. Pelling, and S. Damjanovski. 2017a. Inhibition of MT1-MMP proteolytic function and ERK1/2 signalling influences cell migration and invasion through changes in MMP-2 and MMP-9 levels. *J. Cell Commun. Signal.* 11:167–79.

Cepeda, M.A., J.J.H. Pelling, C.L. Evered, H.S. Leong, and S. Damjanovski. 2017b. The cytoplasmic domain of MT1-MMP is dispensable for migration augmentation but necessary to mediate viability of MCF-7 breast cancer cells. *Exp. Cell Res.* 350:169–83.

Cepeda, M.A., J.J.H. Pelling, C.L. Evered, K.C. Williams, Z. Freedman, I. Stan, J.A. Willson, H.S. Leong, and S. Damjanovski. 2016. Less is more: low expression of MT1-MMP is optimal to promote migration and tumourigenesis of breast cancer cells. *Mol. Cancer*. 15:65–92.

Chang, C.K., W.C. Hung, and H.C. Chang. 2008. The Kazal motifs of RECK protein inhibit MMP-9 secretion and activity and reduce metastasis of lung cancer cells in vitro and in vivo. *J. Cell. Mol. Med.* 12:2781–9.

Chen, W.T. 1989. Proteolytic activity of specialized surface protrusions formed at rosette contact sites of transformed cells. *J. Exp. Zool.* 251:167–85.

Chirco, R., X.W. Liu, K.K. Jung, and H.R.C. Kim. 2006. Novel functions of TIMPs in cell signaling. *Cancer Metastasis Rev.* 25:99–113.

Clark, E.S., and A.M. Weaver. 2008. A new role for cortactin in invadopodia: regulation of protease secretion. *Eur. J. Cell Biol.* 87:581–90.

Clause, K.C., and T.H. Barker. 2013. Extracellular matrix signaling in morphogenesis and repair. *Curr. Opin. Biotechnol.* 24:830–3.

Covington, M.D., R.C. Burghardt, and A.R. Parrish. 2006. Ischemia-induced cleavage of cadherins in NRK cells requires MT1-MMP (MMP-14). *Am. J. Physiol. Renal Physiol.* 290:43–51.

Cui, N., M. Hu, and R.A. Khalil. 2017. Biochemical and biological attributes of matrix metalloproteinases. *Prog. Mol. Biol. Transl. Sci.* 147:1–73.

D'Alessio, S., G. Ferrari, K. Cinnante, W. Scheerer, A.C. Galloway, D.F. Roses, D. V. Rozanov, A.G. Remacle, E.S. Oh, S.A. Shiryaev, A.Y. Strongin, G. Pintucci, and P. Mignatti. 2008. Tissue inhibitor of metalloproteinases-2 binding to membrane-type 1 matrix metalloproteinase induces MAPK activation and cell growth by a non-proteolytic mechanism. *J. Biol. Chem.* 283:87–99.

Dedhar, S., and G.E. Hannigan. 1996. Integrin cytoplasmic interactions and bidirectional transmembrane signalling. *Curr. Opin. Cell Biol.* 8:657–69.

Dumin, J.A., S.K. Dickeson, T.P. Stricker, M. Bhattacharyya-Pakrasi, J.D. Roby, S.A. Santoro, and W.C. Parks. 2001. Pro-collagenase-1 (matrix metalloproteinase-1) binds the α2β1 integrin upon release from keratinocytes migrating on type I collagen. *J. Biol. Chem.* 276:29368–74.

Egawa, N., N. Koshikawa, T. Tomari, K. Nabeshima, T. Isobe, and M. Seiki. 2006. Membrane type 1 matrix metalloproteinase (MT1-MMP/MMP-14) cleaves and releases a 22-kDa extracellular matrix metalloproteinase inducer (EMMPRIN) fragment from tumor cells. *J. Biol. Chem.* 281:37576–85.

Egeblad, M., M.G. Rasch, and V.M. Weaver. 2010. Dynamic interplay between the collagen scaffold and tumor evolution. *Curr. Opin. Cell Biol.* 22:697–706.

Egeblad, M., and Z. Werb. 2002. New functions for the matrix metalloproteinases in cancer progression. *Nat. Rev. Cancer*. 2:161–74.

Ellerbroek, S.M., and M.S. Stack. 1999. Membrane associated matrix metalloproteinases in metastasis. *Bioessays*. 21:940–9.

Endo, K., T. Takino, H. Miyamori, H. Kinsen, T. Yoshizaki, M. Furukawa, and H. Sato. 2003. Cleavage of syndecan-1 by membrane type matrix metalloproteinase-1 stimulates cell migration. *J. Biol. Chem.* 278:40764–70.

Engel, J. 1989. EGF-like domains in extracellular matrix proteins: localized signals for growth and differentiation? *FEBS Lett.* 251:1–7.

Entwistle, J., C.L. Hall, and E.A. Turley. 1996. HA receptors: regulators of signalling to the cytoskeleton. *J. Cell. Biochem.* 61:569–77.

Frantz, C., K.M. Stewart, and V.M. Weaver. 2010. The extracellular matrix at a glance. *J. Cell Sci.* 123:4195–200.

Frantz, S., K. Hu, A. Adamek, J. Wolf, A. Sallam, S.K.G. Maier, S. Lonning, H. Ling, G. Ertl, and J. Bauersachs. 2008. Transforming growth factor beta inhibition increases mortality and left ventricular dilatation after myocardial infarction. *Basic Res. Cardiol.* 103:485–92.

Gingras, A.C., M. Gstaiger, B. Raught, and R. Aebersold. 2007. Analysis of protein complexes using mass spectrometry. *Nat. Rev. Mol. Cell Biol.* 8:645–54.

Gingras, D., N. Bousquet-Gagnon, S. Langlois, M.P. Lachambre, B. Annabi, and R. Béliveau. 2001. Activation of the extracellular signal-regulated protein kinase (ERK) cascade by membrane-type-1 matrix metalloproteinase (MT1-MMP). *FEBS Lett.* 507:231–6.

Golubkov, V.S., S. Boyd, A.Y. Savinov, A. V. Chekanov, A.L. Osterman, A. Remacle, D. V. Rozanov, S.J. Doxsey, and A.Y. Strongin. 2005. Membrane type-1 matrix metalloproteinase (MT1-MMP) exhibits an important intracellular cleavage function and causes chromosome instability. *J. Biol. Chem.* 280:25079–86.

Gross, J., and C.M. Lapiere. 1962. Collagenolytic activity in amphibian tissues: a tissue culture assay. *Proc. Natl. Acad. Sci. U. S. A.* 48:1014–22.

Gururajan, R., J. Grenet, J.M. Lahti, and V.J. Kidd. 1998. Isolation and characterization of two novel metalloproteinase genes linked to the Cdc2L locus on human chromosome 1p36.3. *Genomics*. 52:101–6.

Hara, T., K. Mimura, M. Seiki, and T. Sakamoto. 2011. Genetic dissection of proteolytic and non-proteolytic contributions of MT1-MMP to macrophage invasion. *Biochem. Biophys. Res. Commun.* 413:277–81.

Hawinkels, L.J.A.C., P. Kuiper, E. Wiercinska, H.W. Verspaget, Z. Liu, E. Pardali, C.F.M. Sier, and P. ten Dijke. 2010. Matrix metalloproteinase-14 (MT1-MMP)-mediated endoglin shedding inhibits tumor angiogenesis. *Cancer Res.* 70:4141–50.

Hay, N. 2016. Reprogramming glucose metabolism in cancer: can it be exploited for cancer therapy? *Nat. Rev. Cancer*. 16:635–49.

He, H., F. Dai, L. Yu, X. She, Y. Zhao, J. Jiang, X. Chen, and S. Zhao. 2002. Identification and characterization of nine novel human small GTPases showing variable expressions in liver cancer tissues. *Gene Expr.* 10:231–42.

Holmbeck, K., P. Bianco, J. Caterina, S. Yamada, M. Kromer, S.A. Kuznetsov, M. Mankani, P.G. Robey, A.R. Poole, I. Pidoux, J.M. Ward, and H. Birkedal-Hansen. 1999. MT1-MMP-deficient mice develop dwarfism, osteopenia, arthritis, and connective tissue disease due to inadequate collagen turnover. *Cell*. 99:81–92.

Hughes, C., L. Radan, W.Y. Chang, W.L. Stanford, D.H. Betts, L.M. Postovit, and G.A. Lajoie. 2012. Mass spectrometry-based proteomic analysis of the matrix microenvironment in pluripotent stem cell culture. *Mol. Cell. Proteomics*. 11:1924–36.

Hughes, H., A. Budnik, K. Schmidt, K.J. Palmer, J. Mantell, C. Noakes, A. Johnson, D.A. Carter, P. Verkade, P. Watson, and D.J. Stephens. 2009. Organisation of human ER-exit sites: requirements for the localisation of Sec16 to transitional ER. *J. Cell Sci.* 122:2924–34.

Hwang, I.K., S.M. Park, S.Y. Kim, and S.T. Lee. 2004. A proteomic approach to identify substrates of matrix metalloproteinase-14 in human plasma. *Biochim. Biophys. Acta*. 1702:79–87.

Hynes, R.O. 2009. The extracellular matrix: not just pretty fibrils. *Science*. 326:1216–9.

Ip, Y.C., S.T. Cheung, and S.T. Fan. 2007. Atypical localization of membrane type 1-matrix metalloproteinase in the nucleus is associated with aggressive features of hepatocellular carcinoma. *Mol. Carcinog.* 46:225–30.

Itoh, T., M. Tanioka, H. Yoshida, T. Yoshioka, H. Nishimoto, and S. Itohara. 1998a. Reduced angiogenesis and tumor progression in gelatinase A-deficient mice. *Cancer Res.* 58:1048–51.

Itoh, Y., A. Ito, K. Iwata, K. Tanzawa, Y. Mori, and H. Nagase. 1998b. Plasma membrane-bound tissue inhibitor of metalloproteinases (TIMP)-2 specifically inhibits matrix metalloproteinase 2 (gelatinase A) activated on the cell surface. *J. Biol. Chem.* 273:24360–7.

Itoh, Y., N. Ito, H. Nagase, and M. Seiki. 2008. The second dimer interface of MT1-MMP, the transmembrane domain, is essential for proMMP-2 activation on the cell surface. *J. Biol. Chem.* 283:13053–62.

Itoh, Y., M. Kajita, H. Kinoh, H. Mori, A. Okada, and M. Seiki. 1999. Membrane type 4 matrix metalloproteinase (MT4-MMP, MMP-17) is a glycosylphosphatidylinositol-anchored proteinase. *J. Biol. Chem.* 274:34260–6.

Itoh, Y., and M. Seiki. 2006. MT1-MMP: a potent modifier of pericellular microenvironment. *J. Cell. Physiol.* 206:1–8.

Itoh, Y., A. Takamura, N. Ito, Y. Maru, H. Sato, N. Suenaga, T. Aoki, and M. Seiki. 2001. Homophilic complex formation of MT1-MMP facilitates proMMP-2 activation on the cell surface and promotes tumor cell invasion. *EMBO J.* 20:4782–93.

Jacobsen, J.A., J.L. Major Jourden, M.T. Miller, and S.M. Cohen. 2010. To bind zinc or not to bind zinc: an examination of innovative approaches to improved metalloproteinase inhibition. *Biochim. Biophys. Acta*. 1803:72–94.

James, M.N.G. 2004. Catalytic pathway of aspartic peptidases. *In* Handbook of Proteolytic Enzymes. A.J. Barrett, N.D. Rawlings, and J.F. Woessner, editors. Elsevier, London. 12–19.

Jiang, A., K. Lehti, X. Wang, S.J. Weiss, J. Keski-Oja, and D. Pei. 2001. Regulation of membrane-type matrix metalloproteinase 1 activity by dynamin-mediated endocytosis. *Proc. Natl. Acad. Sci. U. S. A.* 98:13693–8.

Kajita, M., Y. Itoh, T. Chiba, H. Mori, A. Okada, H. Kinoh, and M. Seiki. 2001. Membrane-type 1 matrix metalloproteinase cleaves CD44 and promotes cell migration. *J. Cell Biol.* 153:893–904.

Kalluri, R. 2003. Basement membranes: structure, assembly and role in tumour angiogenesis. *Nat. Rev. Cancer*. 3:422–33.

Kim, S.H., J. Turnbull, and S. Guimond. 2011. Extracellular matrix and cell signalling: the dynamic cooperation of integrin, proteoglycan and growth factor receptor. *J. Endocrinol.* 209:139–51.

Knapinska, A.M., and G.B. Fields. 2019. The expanding role of MT1-MMP in cancer progression. *Pharmaceuticals*. 12:77–92.

Kojima, S., Y. Itoh, S. Matsumoto, Y. Masuho, and M. Seiki. 2000. Membrane-type 6 matrix metalloproteinase (MT6-MMP, MMP-25) is the second glycosyl-phosphatidyl inositol (GPI)-anchored MMP. *FEBS Lett.* 480:142–6.

Koziol, A., M. Martín-Alonso, C. Clemente, P. Gonzalo, and A.G. Arroyo. 2012. Site-specific cellular functions of MT1-MMP. *Eur. J. Cell Biol.* 91:889–95.

Kuljanin, M., D.Z. Dieters-Castator, D.A. Hess, L.M. Postovit, and G.A. Lajoie. 2017. Comparison of sample preparation techniques for large-scale proteomics. *Proteomics*. 17:1600337–46.

Li, Y., G. Cai, S. Yuan, Y. Jun, N. Li, L. Wang, F. Chen, R. Ling, and J. Yun. 2015. The overexpression membrane type 1 matrix metalloproteinase is associated with the progression and prognosis in breast cancer. *Am. J. Transl. Res.* 7:120–7.

Linder, S. 2007. The matrix corroded: podosomes and invadopodia in extracellular matrix degradation. *Trends Cell Biol.* 17:107–17.

Liu, F., X. Kong, L. Lv, and J. Gao. 2015. TGF-β1 acts through miR-155 to down-regulate TP53INP1 in promoting epithelial-mesenchymal transition and cancer stem cell phenotypes. *Cancer Lett.* 359:288–98.

Liu, Q., S. Basu, Y. Qiu, F. Tang, and F. Dong. 2010. A role of Miz-1 in Gfi-1-mediated transcriptional repression of CDKN1A. *Oncogene*. 29:2843–52.

Livak, K.J., and T.D. Schmittgen. 2001. Analysis of relative gene expression data using real-time quantitative PCR and the 2^(-ΔΔC(T)) method. *Methods*. 25:402–8.

Lodillinsky, C., E. Infante, A. Guichard, R. Chaligné, L. Fuhrmann, J. Cyrta, M. Irondelle, E. Lagoutte, S. Vacher, H. Bonsang-Kitzis, M. Glukhova, F. Reyal, I. Bièche, A. Vincent-Salomon, and P. Chavrier. 2016. p63/MT1-MMP axis is required for in situ to invasive transition in basal-like breast cancer. *Oncogene*. 35:344–57.

López-Casillas, F., H.M. Payne, J.L. Andres, and J. Massagué. 1994. Betaglycan can act as a dual modulator of TGF-β access to signaling receptors: mapping of ligand binding and GAG attachment sites. *J. Cell Biol.* 124:557–68.

Lu, P., V.M. Weaver, and Z. Werb. 2012. The extracellular matrix: a dynamic niche in cancer progression. *J. Cell Biol.* 196:395–406.

Lucá, R., M. Averna, F. Zalfa, M. Vecchi, F. Bianchi, G. La Fata, F. Del Nonno, R. Nardacci, M. Bianchi, P. Nuciforo, S. Munck, P. Parrella, R. Moura, E. Signori, R. Alston, A. Kuchnio, M.G. Farace, V.M. Fazio, M. Piacentini, B. De Strooper, T. Achsel, G. Neri, P. Neven, D.G. Evans, P. Carmeliet, M. Mazzone, and C. Bagni. 2013. The fragile X protein binds mRNAs involved in cancer progression and modulates metastasis formation. *EMBO Mol. Med.* 5:1523–36.

Marchesin, V., A. Castro-Castro, C. Lodillinsky, A. Castagnino, J. Cyrta, H. Bonsang-Kitzis, L. Fuhrmann, M. Irondelle, E. Infante, G. Montagnac, F. Reyal, A. Vincent-Salomon, and P. Chavrier. 2015. ARF6-JIP3/4 regulate endosomal tubules for MT1-MMP exocytosis in cancer invasion. *J. Cell Biol.* 211:339–58.

Mauviel, A. 1993. Cytokine regulation of metalloproteinase gene expression. *J. Cell. Biochem.* 53:288–95.

Ménétret, J.F., R.S. Hegde, S.U. Heinrich, P. Chandramouli, S.J. Ludtke, T.A. Rapoport, and C.W. Akey. 2005. Architecture of the ribosome-channel complex derived from native membranes. *J. Mol. Biol.* 348:445–57.

Miyazono, K., H. Ichijo, and C.H. Heldin. 1993. Transforming growth factor-β: latent forms, binding proteins and receptors. *Growth Factors*. 8:11–22.

Miyazono, K., A. Olofsson, P. Colosetti, and C.H. Heldin. 1991. A role of the latent TGF-β 1-binding protein in the assembly and secretion of TGF-β 1. *EMBO J.* 10:1091–101.

Moore, C.S., and S.J. Crocker. 2012. An alternate perspective on the roles of TIMPs and MMPs in pathology. *Am. J. Pathol.* 180:12–6.

Mori, H., A.T. Lo, J.L. Inman, J. Alcaraz, C.M. Ghajar, J.D. Mott, C.M. Nelson, C.S. Chen, H. Zhang, J.L. Bascom, M. Seiki, and M.J. Bissell. 2013. Transmembrane/cytoplasmic, rather than catalytic, domains of Mmp14 signal to MAPK activation and mammary branching morphogenesis via binding to integrin β1. *Development*. 140:343–52.

Mori, H., T. Tomari, N. Koshikawa, M. Kajita, Y. Itoh, H. Sato, H. Tojo, I. Yana, and M. Seiki. 2002. CD44 directs membrane-type 1 matrix metalloproteinase to lamellipodia by associating with its hemopexin-like domain. *EMBO J.* 21:3949–59.

Moss, N.M., Y.I. Wu, Y. Liu, H.G. Munshi, and M.S. Stack. 2009. Modulation of the membrane type 1 matrix metalloproteinase cytoplasmic tail enhances tumor cell invasion and proliferation in three-dimensional collagen matrices. *J. Biol. Chem.* 284:19791–9.

Murphy, G., and H. Nagase. 2008. Progress in matrix metalloproteinase research. *Mol. Aspects Med.* 29:290–308.

Murphy, G.J., G. Murphy, and J.J. Reynolds. 1991. The origin of matrix metalloproteinases and their familial relationships. *FEBS Lett.* 289:4–7.

Nabeshima, K., T. Inoue, Y. Shimao, Y. Okada, Y. Itoh, M. Seiki, and M. Koono. 2000. Front-cell-specific expression of membrane-type 1 matrix metalloproteinase and gelatinase A during cohort migration of colon carcinoma cells induced by hepatocyte growth factor/scatter factor. *Cancer Res.* 60:3364–9.

Nagase, H., R. Visse, and G. Murphy. 2006. Structure and function of matrix metalloproteinases and TIMPs. *Cardiovasc. Res.* 69:562–73.

Nakahara, H., L. Howard, E.W. Thompson, H. Sato, M. Seiki, Y. Yeh, and W.T. Chen. 1997. Transmembrane/cytoplasmic domain-mediated membrane type 1-matrix metalloprotease docking to invadopodia is required for cell invasion. *Proc. Natl. Acad. Sci. U. S. A.* 94:7959–64.

Nesvizhskii, A.I. 2012. Computational and informatics strategies for identification of specific protein interaction partners in affinity purification mass spectrometry experiments. *Proteomics*. 12:1639–55.

Nguyen, H.L., P. Kadam, A. Helkin, K. Cao, S. Wu, G.J. Samara, Q. Zhang, S. Zucker, and J. Cao. 2016. MT1-MMP activation of TGF-β signaling enables intercellular activation of an epithelial-mesenchymal transition program in cancer. *Curr. Cancer Drug Targets*. 16:618–30.

Niiya, D., N. Egawa, T. Sakamoto, Y. Kikkawa, T. Shinkawa, T. Isobe, N. Koshikawa, and M. Seiki. 2009. Identification and characterization of Lutheran blood group glycoprotein as a new substrate of membrane-type 1 matrix metalloproteinase 1 (MT1-MMP): a systemic whole cell analysis of MT1-MMP-associating proteins in A431 cells. *J. Biol. Chem.* 284:27360–9.

Nufer, O., S. Guldbrandsen, M. Degen, F. Kappeler, J.P. Paccaud, K. Tani, and H.P. Hauri. 2002. Role of cytoplasmic C-terminal amino acids of membrane proteins in ER export. *J. Cell Sci.* 115:619–28.

Nyalendo, C., E. Beaulieu, H. Sartelet, M. Michaud, N. Fontaine, D. Gingras, and R. Béliveau. 2008. Impaired tyrosine phosphorylation of membrane type 1-matrix metalloproteinase reduces tumor cell proliferation in three-dimensional matrices and abrogates tumor growth in mice. *Carcinogenesis*. 29:1655–64.

Nyalendo, C., M. Michaud, E. Beaulieu, C. Roghi, G. Murphy, D. Gingras, and R. Béliveau. 2007. Src-dependent phosphorylation of membrane type I matrix metalloproteinase on cytoplasmic tyrosine 573: role in endothelial and tumor cell migration. *J. Biol. Chem.* 282:15690–9.

Oh, J., D.W. Seo, T. Diaz, B. Wei, Y. Ward, J.M. Ray, Y. Morioka, S. Shi, H. Kitayama, C. Takahashi, M. Noda, and W.G. Stetler-Stevenson. 2004. Tissue inhibitors of metalloproteinase 2 inhibits endothelial cell migration through increased expression of RECK. *Cancer Res.* 64:9062–9.

Oh, J., R. Takahashi, S. Kondo, A. Mizoguchi, E. Adachi, R.M. Sasahara, S. Nishimura, Y. Imamura, H. Kitayama, D.B. Alexander, C. Ide, T.P. Horan, T. Arakawa, H. Yoshida, S. Nishikawa, Y. Itoh, M. Seiki, S. Itohara, C. Takahashi, and M. Noda. 2001. The membrane-anchored MMP inhibitor RECK is a key regulator of extracellular matrix integrity and angiogenesis. *Cell*. 107:789–800.

Ohta, S., G.C. Schoenwolf, and G. Yamada. 2010. The cessation of gastrulation: BMP signaling and EMT during and at the end of gastrulation. *Cell Adh. Migr.* 4:440–6.

Ohuchi, E., K. Imai, Y. Fujii, H. Sato, M. Seiki, and Y. Okada. 1997. Membrane type 1 matrix metalloproteinase digests interstitial collagens and other extracellular matrix macromolecules. *J. Biol. Chem.* 272:2446–51.

Okada, Y., T. Morodomi, J.J. Enghild, K. Suzuki, A. Yasui, I. Nakanishi, G. Salvesen, and H. Nagase. 1990. Matrix metalloproteinase 2 from human rheumatoid synovial fibroblasts. Purification and activation of the precursor and enzymic properties. *Eur. J. Biochem.* 194:721–30.

Ortéga, N., F.E. L'Faqihi, and J. Plouët. 1998. Control of vascular endothelial growth factor angiogenic activity by the extracellular matrix. *Biol. Cell*. 90:381–90.

Ota, I., X.Y. Li, Y. Hu, and S.J. Weiss. 2009. Induction of a MT1-MMP and MT2-MMP-dependent basement membrane transmigration program in cancer cells by Snail1. *Proc. Natl. Acad. Sci. U. S. A.* 106:20318–23.

Overall, C.M. 2001. Matrix metalloproteinase substrate binding domains, modules and exosites. Overview and experimental strategies. *Methods Mol. Biol.* 151:79–120.

Overland, A.C., and P.A. Insel. 2015. Heterotrimeric G proteins directly regulate MMP14/membrane type-1 matrix metalloprotease: a novel mechanism for GPCR-EGFR transactivation. *J. Biol. Chem.* 290:9941–7.

Özdemir, B.C., J. Hensel, C. Secondini, A. Wetterwald, R. Schwaninger, A. Fleischmann, W. Raffelsberger, O. Poch, M. Delorenzi, R. Temanni, I.G. Mills, G. van der Pluijm, G.N. Thalmann, and M.G. Cecchini. 2014. The molecular signature of the stroma response in prostate cancer-induced osteoblastic bone metastasis highlights expansion of hematopoietic and prostate epithelial stem cell niches. *PLoS One*. 9:e114530.

Panayotou, G., P. End, M. Aumailley, R. Timpl, and J. Engel. 1989. Domains of laminin with growth-factor activity. *Cell*. 56:93–101.

Park, H.I., Y. Jin, D.R. Hurst, C.A. Monroe, S. Lee, M.A. Schwartz, and Q.X.A. Sang. 2003. The intermediate S1' pocket of the endometase/matrilysin-2 active site revealed by enzyme inhibition kinetic studies, protein sequence analyses, and homology modeling. *J. Biol. Chem.* 278:51646–53.

Park, H.I., J. Ni, F.E. Gerkema, D. Liu, V.E. Belozerov, and Q.X. Sang. 2000. Identification and characterization of human endometase (matrix metalloproteinase-26) from endometrial tumor. *J. Biol. Chem.* 275:20540–4.

Parks, W.C., C.L. Wilson, and Y.S. López-Boado. 2004. Matrix metalloproteinases as modulators of inflammation and innate immunity. *Nat. Rev. Immunol.* 4:617–29.

Peeters, K., F. Van Leemputte, B. Fischer, B.M. Bonini, H. Quezada, M. Tsytlonok, D. Haesen, W. Vanthienen, N. Bernardes, C.B. Gonzalez-Blas, V. Janssens, P. Tompa, W. Versées, and J.M. Thevelein. 2017. Fructose-1,6-bisphosphate couples glycolytic flux to activation of Ras. *Nat. Commun.* 8:922–37.

Pei, D., and S.J. Weiss. 1995. Furin-dependent intracellular activation of the human stromelysin-3 zymogen. *Nature*. 375:244–7.

Pelmenschikov, V., and P.E.M. Siegbahn. 2002. Catalytic mechanism of matrix metalloproteinases: two-layered ONIOM study. *Inorg. Chem.* 41:5659–66.

Pöschl, E., U. Schlötzer-Schrehardt, B. Brachvogel, K. Saito, Y. Ninomiya, and U. Mayer. 2004. Collagen IV is essential for basement membrane stability but dispensable for initiation of its assembly during early development. *Development*. 131:1619–28.

Ra, H.J., and W.C. Parks. 2007. Control of matrix metalloproteinase catalytic activity. *Matrix Biol.* 26:587–96.

Rapraeger, A.C., A. Krufka, and B.B. Olwin. 1991. Requirement of heparan sulfate for bFGF-mediated fibroblast growth and myoblast differentiation. *Science*. 252:1705–8.

Rawlings, N.D., M. Waller, A.J. Barrett, and A. Bateman. 2014. MEROPS: the database of proteolytic enzymes, their substrates and inhibitors. *Nucleic Acids Res.* 42:D503-9.

Reig, G., E. Pulgar, and M.L. Concha. 2014. Cell migration: from tissue culture to embryos. *Development*. 141:1999–2013.

Remacle, A.G., A. V Chekanov, V.S. Golubkov, A.Y. Savinov, D. V Rozanov, and A.Y. Strongin. 2006. O-glycosylation regulates autolysis of cellular membrane type-1 matrix metalloproteinase (MT1-MMP). *J. Biol. Chem.* 281:16897–905.

Ridley, A.J., H.F. Paterson, C.L. Johnston, D. Diekmann, and A. Hall. 1992. The small GTP-binding protein Rac regulates growth factor-induced membrane ruffling. *Cell*. 70:401–10.

Robinson, C.J., and S.E. Stringer. 2001. The splice variants of vascular endothelial growth factor (VEGF) and their receptors. *J. Cell Sci.* 114:853–65.

Rowe, R.G., and S.J. Weiss. 2009. Navigating ECM barriers at the invasive front: the cancer cell-stroma interface. *Annu. Rev. Cell Dev. Biol.* 25:567–95.

Sakamoto, T., D. Niiya, and M. Seiki. 2011. Targeting the Warburg effect that arises in tumor cells expressing membrane type-1 matrix metalloproteinase. *J. Biol. Chem.* 286:14691–704.

Sameshima, T., K. Nabeshima, B.P. Toole, K. Yokogami, Y. Okada, T. Goya, M. Koono, and S. Wakisaka. 2000. Glioma cell extracellular matrix metalloproteinase inducer (EMMPRIN) (CD147) stimulates production of membrane-type matrix metalloproteinases and activated gelatinase A in co-cultures with brain-derived fibroblasts. *Cancer Lett.* 157:177–84.

Sano, H., L. Eguez, M.N. Teruel, M. Fukuda, T.D. Chuang, J.A. Chavez, G.E. Lienhard, and T.E. McGraw. 2007. Rab10, a target of the AS160 Rab GAP, is required for insulin-stimulated translocation of GLUT4 to the adipocyte plasma membrane. *Cell Metab.* 5:293–303.

Sato, H., T. Takino, Y. Okada, J. Cao, A. Shinagawa, E. Yamamoto, and M. Seiki. 1994. A matrix metalloproteinase expressed on the surface of invasive tumour cells. *Nature*. 370:61–5.

Sayeed, A., G. Luciani-Torres, Z. Meng, J.L. Bennington, D.H. Moore, and S.H. Dairkee. 2013. Aberrant regulation of the BST2 (tetherin) promoter enhances cell proliferation and apoptosis evasion in high grade breast cancer cells. *PLoS One*. 8:e67191.

Schenk, S., E. Hintermann, M. Bilban, N. Koshikawa, C. Hojilla, R. Khokha, and V. Quaranta. 2003. Binding to EGF receptor of a laminin-5 EGF-like fragment liberated during MMP-dependent mammary gland involution. *J. Cell Biol.* 161:197–209.

Schlessinger, J., A.N. Plotnikov, O.A. Ibrahimi, A. V. Eliseenkova, B.K. Yeh, A. Yayon, R.J. Linhardt, and M. Mohammadi. 2000. Crystal structure of a ternary FGF-FGFR-heparin complex reveals a dual role for heparin in FGFR binding and dimerization. *Mol. Cell*. 6:743–50.

Seiki, M. 1999. Membrane-type matrix metalloproteinases. *APMIS*. 107:137–43.

Shields, M.A., S. Dangi-Garimella, S.B. Krantz, D.J. Bentrem, and H.G. Munshi. 2011. Pancreatic cancer cells respond to type I collagen by inducing Snail expression to promote membrane type 1 matrix metalloproteinase-dependent collagen invasion. *J. Biol. Chem.* 286:10495–504.

Shields, M.A., S. Dangi-Garimella, A.J. Redig, and H.G. Munshi. 2012. Biochemical role of the collagen-rich tumour microenvironment in pancreatic cancer progression. *Biochem. J.* 441:541–52.

Shimizu-Hirota, R., W. Xiong, B.T. Baxter, S.L. Kunkel, I. Maillard, X.W. Chen, F. Sabeh, R. Liu, X.Y. Li, and S.J. Weiss. 2012. MT1-MMP regulates the PI3Kδ-Mi-2/NuRD-dependent control of macrophage immune function. *Genes Dev.* 26:395–413.

Simizu, S., S. Takagi, Y. Tamura, and H. Osada. 2005. RECK-mediated suppression of tumor cell invasion is regulated by glycosylation in human tumor cell lines. *Cancer Res.* 65:7455–61.

Springman, E.B., E.L. Angleton, H. Birkedal-Hansen, and H.E. Van Wart. 1990. Multiple modes of activation of latent human fibroblast collagenase: evidence for the role of a Cys73 active-site zinc complex in latency and a “cysteine switch” mechanism for activation. *Proc. Natl. Acad. Sci. U. S. A.* 87:364–8.

Stegemann, C., A. Didangelos, J. Barallobre-Barreiro, S.R. Langley, K. Mandal, M. Jahangiri, and M. Mayr. 2013. Proteomic identification of matrix metalloproteinase substrates in the human vasculature. *Circ. Cardiovasc. Genet.* 6:106–17.

Sternlicht, M.D., and Z. Werb. 2001. How matrix metalloproteinases regulate cell behavior. *Annu. Rev. Cell Dev. Biol.* 17:463–516.

Stetler-Stevenson, W.G. 2008. Tissue inhibitors of metalloproteinases in cell signaling: metalloproteinase-independent biological activities. *Sci. Signal.* 1:re6.

Stricker, T.P., J.A. Dumin, S.K. Dickeson, L. Chung, H. Nagase, W.C. Parks, and S.A. Santoro. 2001. Structural analysis of the α2 integrin I domain/procollagenase-1 (matrix metalloproteinase-1) interaction. *J. Biol. Chem.* 276:29375–81.

Strongin, A.Y. 2006. Mislocalization and unconventional functions of cellular MMPs in cancer. *Cancer Metastasis Rev.* 25:87–98.

Strongin, A.Y., I. Collier, G. Bannikov, B.L. Marmer, G.A. Grant, and G.I. Goldberg. 1995. Mechanism of cell surface activation of 72-kDa type IV collagenase. Isolation of the activated form of the membrane metalloprotease. *J. Biol. Chem.* 270:5331–8.

Suenaga, N., H. Mori, Y. Itoh, and M. Seiki. 2005. CD44 binding through the hemopexin-like domain is critical for its shedding by membrane-type 1 matrix metalloproteinase. *Oncogene*. 24:859–68.

Sun, L., M.E. Diamond, A.J. Ottaviano, M.J. Joseph, V. Ananthanarayan, and H.G. Munshi. 2008. Transforming growth factor-β1 promotes matrix metalloproteinase-9-mediated oral cancer invasion through snail expression. *Mol. Cancer Res.* 6:10–20.

Szklarczyk, D., A.L. Gable, D. Lyon, A. Junge, S. Wyder, J. Huerta-Cepas, M. Simonovic, N.T. Doncheva, J.H. Morris, P. Bork, L.J. Jensen, and C. von Mering. 2019. STRING v11: protein-protein association networks with increased coverage, supporting functional discovery in genome-wide experimental datasets. *Nucleic Acids Res.* 47:D607–D613.

Takahashi, C., Z. Sheng, T.P. Horan, H. Kitayama, M. Maki, K. Hitomi, Y. Kitaura, S. Takai, R.M. Sasahara, A. Horimoto, Y. Ikawa, B.J. Ratzkin, T. Arakawa, and M. Noda. 1998. Regulation of matrix metalloproteinase-9 and inhibition of tumor invasion by the membrane-anchored glycoprotein RECK. *Proc. Natl. Acad. Sci. U. S. A.* 95:13221–6.

Tam, E.M., C.J. Morrison, Y.I. Wu, M.S. Stack, and C.M. Overall. 2004. Membrane protease proteomics: Isotope-coded affinity tag MS identification of undescribed MT1-matrix metalloproteinase substrates. *Proc. Natl. Acad. Sci. U. S. A.* 101:6917–22.

Taniwaki, K., H. Fukamachi, K. Komori, Y. Ohtake, T. Nonaka, T. Sakamoto, T. Shiomi, Y. Okada, T. Itoh, S. Itohara, M. Seiki, and I. Yana. 2007. Stroma-derived matrix metalloproteinase (MMP)-2 promotes membrane type 1-MMP-dependent tumor growth in mice. *Cancer Res.* 67:4311–9.

Tchetverikov, I., L.R. Lard, J. DeGroot, N. Verzijl, J.M. TeKoppele, F.C. Breedveld, T.W.J. Huizinga, and R. Hanemaaijer. 2003. Matrix metalloproteinases-3, -8, -9 as markers of disease activity and joint damage progression in early rheumatoid arthritis. *Ann. Rheum. Dis.* 62:1094–9.

Theocharis, A.D., S.S. Skandalis, C. Gialeli, and N.K. Karamanos. 2016. Extracellular matrix structure. *Adv. Drug Deliv. Rev.* 97:4–27.

Tomari, T., N. Koshikawa, T. Uematsu, T. Shinkawa, D. Hoshino, N. Egawa, T. Isobe, and M. Seiki. 2009. High throughput analysis of proteins associating with a proinvasive MT1-MMP in human malignant melanoma A375 cells. *Cancer Sci.* 100:1284–90.

Trepat, X., Z. Chen, and K. Jacobson. 2012. Cell migration. *Compr. Physiol.* 2:2369–92.

Turley, E.A., L. Austen, D. Moore, and K. Hoare. 1993. Ras-transformed cells express both CD44 and RHAMM hyaluronan receptors: only RHAMM is essential for hyaluronan-promoted locomotion. *Exp. Cell Res.* 207:277–82.

Turunen, S.P., O. Tatti-Bugaeva, and K. Lehti. 2017. Membrane-type matrix metalloproteases as diverse effectors of cancer progression. *Biochim. Biophys. Acta Mol. Cell Res.* 1864:1974–1988.

Tuuttila, A., E. Morgunova, U. Bergmann, Y. Lindqvist, K. Maskos, C. Fernandez-Catalan, W. Bode, K. Tryggvason, and G. Schneider. 1998. Three-dimensional structure of human tissue inhibitor of metalloproteinases-2 at 2.1 Å resolution. *J. Mol. Biol.* 284:1133–40.

Uekita, T., Y. Itoh, I. Yana, H. Ohno, and M. Seiki. 2001. Cytoplasmic tail-dependent internalization of membrane-type 1 matrix metalloproteinase is important for its invasion-promoting activity. *J. Cell Biol.* 155:1345–56.

UniProt Consortium. 2019. UniProt: a worldwide hub of protein knowledge. *Nucleic Acids Res.* 47:D506–D515.

Ureña, J.M., A. Merlos-Suárez, J. Baselga, and J. Arribas. 1999. The cytoplasmic carboxy-terminal amino acid determines the subcellular localization of proTGF-α and membrane type matrix metalloprotease (MT1-MMP). *J. Cell Sci.* 112:773–84.

Velasco-Loyden, G., J. Arribas, and F. López-Casillas. 2004. The shedding of betaglycan is regulated by pervanadate and mediated by membrane type matrix metalloprotease-1. *J. Biol. Chem.* 279:7721–33.

Vermeulen, M., N.C. Hubner, and M. Mann. 2008. High confidence determination of specific protein-protein interactions using quantitative mass spectrometry. *Curr. Opin. Biotechnol.* 19:331–7.

Wali, N., K. Hosokawa, S. Malik, H. Saito, K. Miyaguchi, S. Imajoh-Ohmi, Y. Miki, and A. Nakanishi. 2014. Centrosomal BRCA2 is a target protein of membrane type-1 matrix metalloproteinase (MT1-MMP). *Biochem. Biophys. Res. Commun.* 443:1148–54.

Walker, A., J.E. Turnbull, and J.T. Gallagher. 1994. Specific heparan sulfate saccharides mediate the activity of basic fibroblast growth factor. *J. Biol. Chem.* 269:931–5.

Wang, Y., and M.A. McNiven. 2012. Invasive matrix degradation at focal adhesions occurs via protease recruitment by a FAK-p130Cas complex. *J. Cell Biol.* 196:375–85.

Warburg, O. 1956. On the Origin of Cancer Cells. *Science (80-.).* 123:309–314.

Van Wart, H.E., and H. Birkedal-Hansen. 1990. The cysteine switch: a principle of regulation of metalloproteinase activity with potential applicability to the entire matrix metalloproteinase gene family. *Proc. Natl. Acad. Sci. U. S. A.* 87:5578–82.

Will, H., S.J. Atkinson, G.S. Butler, B. Smith, and G. Murphy. 1996. The soluble catalytic domain of membrane type 1 matrix metalloproteinase cleaves the propeptide of progelatinase A and initiates autoproteolytic activation. *J. Biol. Chem.* 271:17119–23.

Wilson, C.M., C. Kraft, C. Duggan, N. Ismail, S.G. Crawshaw, and S. High. 2005. Ribophorin I associates with a subset of membrane proteins after their integration at the sec61 translocon. *J. Biol. Chem.* 280:4195–206.

Wong, H.L.X., G. Jin, R. Cao, S. Zhang, Y. Cao, and Z. Zhou. 2016. MT1-MMP sheds LYVE-1 on lymphatic endothelial cells and suppresses VEGF-C production to inhibit lymphangiogenesis. *Nat. Commun.* 7:10824–41.

Yamazaki, S., N. Nakano, A. Honjo, M. Hara, K. Maeda, C. Nishiyama, J. Kitaura, Y. Ohtsuka, K. Okumura, H. Ogawa, and T. Shimizu. 2015. The transcription factor Ehf Is involved in TGF-β-induced suppression of FcεRI and c-Kit expression and FcεRI-mediated activation in mast cells. *J. Immunol.* 195:3427–35.

Yang, C.C., L.F. Zhu, X.H. Xu, T.Y. Ning, J.H. Ye, and L.K. Liu. 2013. Membrane type 1 matrix metalloproteinase induces an epithelial to mesenchymal transition and cancer stem cell-like properties in SCC9 cells. *BMC Cancer*. 13:171–83.

Yang, J., W.C. Kasberg, A. Celo, Z. Liang, K. Quispe, and M.S. Stack. 2017. Post-translational modification of the membrane type 1 matrix metalloproteinase (MT1-MMP) cytoplasmic tail impacts ovarian cancer multicellular aggregate dynamics. *J. Biol. Chem.* 292:13111–13121.

Yayon, A., M. Klagsbrun, J.D. Esko, P. Leder, and D.M. Ornitz. 1991. Cell surface, heparin-like molecules are required for binding of basic fibroblast growth factor to its high affinity receptor. *Cell*. 64:841–8.

Yu, Q., and I. Stamenkovic. 2000. Cell surface-localized matrix metalloproteinase-9 proteolytically activates TGF-β and promotes tumor invasion and angiogenesis. *Genes Dev.* 14:163–76.

Zalfa, F., V. Panasiti, S. Carotti, M. Zingariello, G. Perrone, L. Sancillo, L. Pacini, F. Luciani, V. Roberti, S. D'Amico, R. Coppola, S.O. Abate, R.A. Rana, A. De Luca, M. Fiers, V. Melocchi, F. Bianchi, M.G. Farace, T. Achsel, J.C. Marine, S. Morini, and C. Bagni. 2017. The fragile X mental retardation protein regulates tumor invasiveness-related pathways in melanoma cells. *Cell Death Dis.* 8:e3169.

Zarrabi, K., A. Dufour, J. Li, C. Kuscu, A. Pulkoski-Gross, J. Zhi, Y. Hu, N.S. Sampson, S. Zucker, and J. Cao. 2011. Inhibition of matrix metalloproteinase 14 (MMP-14)-mediated cancer cell migration. *J. Biol. Chem.* 286:33167–77.

Zhang, S., M.C. Chang, D. Zylka, S. Turley, R. Harrison, and E.A. Turley. 1998. The hyaluronan receptor RHAMM regulates extracellular-regulated kinase. *J. Biol. Chem.* 273:11342–8.

Zhang, Y., J.P. O'Connor, M.C. Siomi, S. Srinivasan, A. Dutra, R.L. Nussbaum, and G. Dreyfuss. 1995. The fragile X mental retardation syndrome protein interacts with novel homologs FXR1 and FXR2. *EMBO J.* 14:5358–66.

Appendices

Appendix A. Top 10 most significantly enriched KEGG pathways represented by 266 proteins co-immunoprecipitated with MT1-MMP in parental MCF-7, C1, and ΔCD.

ID: KEGG Pathway	Count	Size	Genes					FDR
hsa03040: Spliceosome	19	130	CDC5L PCBP1 RBMXL1 SRSF10	DDX5 PLRG1 RP9 SRSF3	DHX15 PRPF19 SART1 SRSF9	EIF4A3 PRPF8 SF3B4 TRA2B	HSPA1A RBMX SNW1	2.53×10^{-11}
hsa03013: RNA transport	19	159	CASC3 EIF3I FXR1 PNN	EIF2S1 EIF4A1 FXR2 RAN	EIF2S3 EIF4A3 NUP210 SEC13	EIF3C EIF4G1 PABPC1 UPF1	EIF3CL FMR1 PABPC4	3.21×10^{-10}
hsa03018: RNA degradation	12	77	CNOT1 DHX36 PABPC4	CNOT2 EDC4 XRN2	CNOT3 HSPA9	CNOT7 HSPD1	DDX6 PABPC1	1.49×10^{-7}
hsa03015: mRNA surveillance pathway	12	89	CASC3 PABPC1 UPF1	CPSF1 PABPC4 WDR33	CPSF2 PNN	EIF4A3 PPP1CA	FIP1L1 PPP1CC	4.87×10^{-7}
hsa04141: Protein processing in the endoplasmic reticulum	12	161	BAG2 HSP90AB1 SEC13	DNAJA1 HSPA1A SSR1	DNAJA2 HSPA5	EIF2S1 RPN1	HSP90AA1 RRBP1	0.00014
hsa05130: Pathogenic *Escherichia coli* infection	7	53	CTNNB1 YWHAQ	NCL YWHAZ	TUBB2A	TUBB2B	TUBB6	0.00045

(Appendix A continued)

ID: KEGG Pathway	Count	Size	Genes					FDR
hsa05016: Huntington's disease	10	193	AP2A1 ATP5C1	AP2B1 CLTC	AP2M1 DCTN1	ATP50 NDUFA4	ATP5A1 SLC25A5	0.011
hsa04961: Endocrine and other factor-regulated calcium reabsorption	5	47	AP2A1	AP2B1	AP2M1	ATP1A1	CLTC	0.0144
hsa04261: Adrenergic signaling in cardiomyocytes	8	139	ATP1A1 PPP1CC	ATP2A2 TPM1	CALM1 TPM3	GNAI3	PPP1CA	0.0167
hsa03450: Non-homologous end-joining	3	13	PRKDC	XRCC5	XRCC6			0.0209

Abbreviations: KEGG, Kyoto Encyclopedia of Genes and Genomes; FDR, False Discovery Rate

Notes: Count: number of genes isolated within pathway; Size: total number of genes in pathway

Appendix B. Final list of 248 MT1-MMP associating proteins identified by LC-MS/MS within MCF-7 cell lines.

UniProtKB Accession Number	UniProtKB Symbol	Protein Name	MCF-7	C1	ΔCD
B5ME19	EIFCL	Eukaryotic translation initiation factor 3 subunit C-like protein	+	–	–
O00468	AGRIN	Agrin	+	–	–
O00567	NOP56	Nucleolar protein 56	+	–	–
O14545	TRAD1	TRAF-type zinc finger domain-containing protein 1	+	–	–
O15230	LAMA5	Laminin subunit alpha-5	+	–	–
O15234	CASC3	Protein CASC3	+	–	–
O60264	SMCA5	SWI/SNF-related matrix-associated actin-dependent regulator of chromatin subfamily A member 5	+	–	–
O60884	DNJA2	DnaJ homolog subfamily A member 2	+	–	–
O75534	CSDE1	Cold shock domain-containing protein E1	+	–	–
O76094	SRP72	Signal recognition particle subunit SRP72	+	–	–
O95047	OR2A4	Olfactory receptor 2A4	+	–	–
O95782	AP2A1	AP-2 complex subunit alpha-1	+	–	–
O95816	BAG2	BAG family molecular chaperone regulator 2	+	–	–
O96019	ACL6A	Actin-like protein 6A	+	–	–
P05198	IF2A	Eukaryotic translation initiation factor 2 subunit 1	+	–	–
P07900	HS90A	Heat shock protein HSP 90-alpha	+	–	–
P07951	TPM2	Tropomyosin beta chain	+	–	–
P08754	GNAI3	Guanine nucleotide-binding protein G(k) subunit alpha	+	–	–
P09493	TPM1	Tropomyosin alpha-1 chain	+	–	–
P10809	CH60	60 kDa heat shock protein mitochondrial	+	–	–
P19338	NUCL	Nucleolin	+	–	–

UniProtKB Accession Number	UniProtKB Symbol	Protein Name	MCF-7	C1	ΔCD
P31689	DNJA1	DnaJ homolog subfamily A member 1	+	–	–
P36873	PP1G	Serine/threonine-protein phosphatase PP1-gamma catalytic subunit	+	–	–
P41091	IF2G	Eukaryotic translation initiation factor 2 subunit 3	+	–	–
P42166	LAP2A	Lamina-associated polypeptide 2 isoform alpha	+	–	–
P49411	EFTU	Elongation factor Tu mitochondrial	+	–	–
P50402	EMD	Emerin	+	–	–
P55265	DSRAD	Double-stranded RNA-specific adenosine deaminase	+	–	–
P60842	IF4A1	Eukaryotic initiation factor 4A-I	+	–	–
P61158	ARP3	Actin-related protein 3	+	–	–
P62136	PP1A	Serine/threonine-protein phosphatase PP1-alpha catalytic subunit	+	–	–
P62873	GBB1	Guanine nucleotide-binding protein G(I)/G(S)/G(T) subunit beta-1	+	–	–
P62879	GBB2	Guanine nucleotide-binding protein G(I)/G(S)/G(T) subunit beta-2	+	–	–
P63104	1433Z	14-3-3 protein zeta/delta	+	–	–
P78371	TCPB	T-complex protein 1 subunit beta	+	–	–
P78527	PRKDC	DNA-dependent protein kinase catalytic subunit	+	–	–
Q02241	KIF23	Kinesin-like protein KIF23	+	–	–
Q13601	KRR1	KRR1 small subunit processome component homolog	+	–	–
Q14498	RBM39	RNA-binding protein 39	+	–	–
Q14694	UBP10	Ubiquitin carboxyl-terminal hydrolase 10	+	–	–
Q15149	PLEC	Plectin	+	–	–
Q15637	SF01	Splicing factor 1	+	–	–
Q5JSZ5	PRC2B	Protein PRRC2B	+	–	–
Q5T200	ZC3HD	Zinc finger CCCH domain-containing protein 13	+	–	–
Q5VZF2	MBNL2	Muscleblind-like protein 2	+	–	–

UniProtKB Accession Number	UniProtKB Symbol	Protein Name	MCF-7	C1	ΔCD
Q6P158	DHX57	Putative ATP-dependent RNA helicase DHX57	+	–	–
Q6P2E9	EDC4	Enhancer of mRNA-decapping protein 4	+	–	–
Q6PJW8	CNST	Consortin	+	–	–
Q8IWZ3	ANKH1	Ankyrin repeat and KH domain-containing protein 1	+	–	–
Q8IY17	PLPL6	Neuropathy target esterase	+	–	–
Q8NE71	ABCF1	ATP-binding cassette sub-family F member 1	+	–	–
Q8TDD1	DDX54	ATP-dependent RNA helicase DDX54	+	–	–
Q92615	LAR4B	La-related protein 4B	+	–	–
Q92928	RAB1C	Putative Ras-related protein Rab-1C	+	–	–
Q96AG4	LRC59	Leucine-rich repeat-containing protein 59	+	–	–
Q96JQ0	PCD16	Protocadherin-16	+	–	–
Q96PK6	RBM14	RNA-binding protein 14	+	–	–
Q99613	EIF3C	Eukaryotic translation initiation factor 3 subunit C	+	–	–
Q9BU76	MMTA2	Multiple myeloma tumor-associated protein 2	+	–	–
Q9BUF5	TBB6	Tubulin beta-6 chain	+	–	–
Q9BWE0	REPI1	Replication initiator 1	+	–	–
Q9BWF3	RBM4	RNA-binding protein 4	+	–	–
Q9BYJ9	YTHD1	YTH domain family protein 1	+	–	–
Q9H0C5	BTBD1	BTB/POZ domain-containing protein 1	+	–	–
Q9H0D6	XRN2	5'-3' exoribonuclease 2	+	–	–
Q9H0U4	RAB1B	Ras-related protein Rab-1B	+	–	–
Q9H307	PININ	Pinin	+	–	–
Q9NR56	MBNL1	Muscleblind-like protein 1	+	–	–
Q9P1U1	ARP3B	Actin-related protein 3B	+	–	–

UniProtKB Accession Number	UniProtKB Symbol	Protein Name	MCF-7	C1	ΔCD
Q9UIQ6	LCAP	Leucyl-cystinyl aminopeptidase	+	–	–
Q9UIV1	CNOT7	CCR4-NOT transcription complex subunit 7	+	–	–
Q9UKV8	AGO2	Protein argonaute-2	+	–	–
Q9UPT8	ZC3H4	Zinc finger CCCH domain-containing protein 4	+	–	–
Q9Y446	PKP3	Plakophilin-3	+	–	–
O00483	NDUA4	NADH dehydrogenase [ubiquinone] 1 alpha subcomplex subunit 4	–	+	–
O43291	SPIT2	Kunitz-type protease inhibitor 2	–	+	–
O43852	CALU	Calumenin	–	+	–
O75909	CCNK	Cyclin-K	–	+	–
O94972	TRI37	E3 ubiquitin-protein ligase TRIM37	–	+	–
P02765	FETUA	Alpha-2-HS-glycoprotein	–	+	–
P02786	TFR1	Transferrin receptor protein 1	–	+	–
P05023	AT1A1	Sodium/potassium-transporting ATPase subunit alpha-1	–	+	–
P07814	SYEP	Bifunctional glutamate/proline--tRNA ligase	–	+	–
P10909	CLUS	Clusterin	–	+	–
P16615	AT2A2	Sarcoplasmic/endoplasmic reticulum calcium ATPase 2	–	+	–
P35221	CTNA1	Catenin alpha-1	–	+	–
P40938	RFC3	Replication factor C subunit 3	–	+	–
P40939	ECHA	Trifunctional enzyme subunit alpha mitochondrial	–	+	–
P43307	SSRA	Translocon-associated protein subunit alpha	–	+	–
P48047	ATPO	ATP synthase subunit O mitochondrial	–	+	–
P53007	TXTP	Tricarboxylate transport protein mitochondrial	–	+	–
P54886	P5CS	Delta-1-pyrroline-5-carboxylate synthase	–	+	–
P55084	ECHB	Trifunctional enzyme subunit beta mitochondrial	–	+	–

UniProtKB Accession Number	UniProtKB Symbol	Protein Name	MCF-7	C1	ΔCD
P62820	RAB1A	Ras-related protein Rab-1A	–	+	–
P62826	RAN	GTP-binding nuclear protein Ran	–	+	–
Q00610	CLH1	Clathrin heavy chain 1	–	+	–
Q01650	LAT1	Large neutral amino acids transporter small subunit 1	–	+	–
Q08J23	NSUN2	tRNA (cytosine(34)-C(5))-methyltransferase	–	+	–
Q10570	CPSF1	Cleavage and polyadenylation specificity factor subunit 1	–	+	–
Q13885	TBB2A	Tubulin beta-2A chain	–	+	–
Q14244	MAP7	Ensconsin	–	+	–
Q14566	MCM6	DNA replication licensing factor MCM6	–	+	–
Q14C86	GAPD1	GTPase-activating protein and VPS9 domain-containing protein 1	–	+	–
Q15773	MLF2	Myeloid leukemia factor 2	–	+	–
Q16891	IMMT	Mitochondrial inner membrane protein	–	+	–
Q7Z6E9	RBBP6	E3 ubiquitin-protein ligase RBBP6	–	+	–
Q86X29	LSR	Lipolysis-stimulated lipoprotein receptor	–	+	–
Q8NF37	PCAT1	Lysophosphatidylcholine acyltransferase 1	–	+	–
Q8TB61	S35B2	Adenosine 3'-phospho 5'-phosphosulfate transporter 1	–	+	–
Q8WXE9	STON2	Stonin-2	–	+	–
Q96FJ2	DYL2	Dynein light chain 2 cytoplasmic	–	+	–
Q9BVA1	TBB2B	Tubulin beta-2B chain	–	+	–
Q9C0J8	WDR33	pre-mRNA 3' end processing protein WDR33	–	+	–
Q9P2E9	RRBP1	Ribosome-binding protein 1	–	+	–
Q9P2I0	CPSF2	Cleavage and polyadenylation specificity factor subunit 2	–	+	–
Q9UBM7	DHCR7	7-dehydrocholesterol reductase	–	+	–
Q9Y5T5	UBP16	Ubiquitin carboxyl-terminal hydrolase 16	–	+	–

UniProtKB Accession Number	UniProtKB Symbol	Protein Name	MCF-7	C1	ΔCD
Q8N163	CCAR2	Cell cycle and apoptosis regulator protein 2	–	–	+
Q9NR30	DDX21	Nucleolar RNA helicase 2	–	–	+
A5YKK6	CNOT1	CCR4-NOT transcription complex subunit 1	+	+	–
O75175	CNOT3	CCR4-NOT transcription complex subunit 3	+	+	–
O95793	STAU1	Double-stranded RNA-binding protein Staufen homolog 1	+	+	–
P04004	VTNC	Vitronectin	+	+	–
P04843	RPN1	Dolichyl-diphosphooligosaccharide--protein glycosyltransferase subunit 1	+	+	–
P08195	4F2	4F2 cell-surface antigen heavy chain	+	+	–
P08238	HS90B	Heat shock protein HSP 90-beta	+	+	–
P11021	GRP78	78 kDa glucose-regulated protein	+	+	–
P11586	C1TC	C-1-tetrahydrofolate synthase cytoplasmic	+	+	–
P12956	XRCC6	X-ray repair cross-complementing protein 6	+	+	–
P13010	XRCC5	X-ray repair cross-complementing protein 5	+	+	–
P35222	CTNB1	Catenin beta-1	+	+	–
P37108	SRP14	Signal recognition particle 14 kDa protein	+	+	–
P38646	GRP75	Stress-70 protein mitochondrial	+	+	–
P42167	LAP2B	Lamina-associated polypeptide 2 isoforms beta/gamma	+	+	–
P47756	CAPZB	F-actin-capping protein subunit beta	+	+	–
P48634	PRC2A	Protein PRRC2A	+	+	–
P51532	SMCA4	Transcription activator BRG1	+	+	–
P52292	IMA1	Importin subunit alpha-1	+	+	–
P55735	SEC13	Protein SEC13 homolog	+	+	–
P61026	RAB10	Ras-related protein Rab-10	+	+	–
P62158	CALM	Calmodulin	+	+	–

UniProtKB Accession Number	UniProtKB Symbol	Protein Name	MCF-7	C1	ΔCD
P63010	AP2B1	AP-2 complex subunit beta	+	+	–
P69905	HBA	Hemoglobin subunit alpha	+	+	–
P84085	ARF5	ADP-ribosylation factor 5	+	+	–
Q00577	PURA	Transcriptional activator protein Pur-alpha	+	+	–
Q09666	AHNK	Neuroblast differentiation-associated protein AHNAK	+	+	–
Q13148	TADBP	TAR DNA-binding protein 43	+	+	–
Q13162	PRDX4	Peroxiredoxin-4	+	+	–
Q14145	KEAP1	Kelch-like ECH-associated protein 1	+	+	–
Q14157	UBP2L	Ubiquitin-associated protein 2-like	+	+	–
Q14203	DCTN1	Dynactin subunit 1	+	+	–
Q14247	SRC8	Src substrate cortactin	+	+	–
Q14596	NBR1	Next to BRCA1 gene 1 protein	+	+	–
Q16698	DECR	2 4-dienoyl-CoA reductase mitochondrial	+	+	–
Q562R1	ACTBL	Beta-actin-like protein 2	+	+	–
Q68CP9	ARID2	AT-rich interactive domain-containing protein 2	+	+	–
Q6NXG1	ESRP1	Epithelial splicing regulatory protein 1	+	+	–
Q6PJT7	ZC3HE	Zinc finger CCCH domain-containing protein 14	+	+	–
Q6UN15	FIP1	Pre-mRNA 3'-end-processing factor FIP1	+	+	–
Q71RC2	LARP4	La-related protein 4	+	+	–
Q7L2E3	DHX30	Putative ATP-dependent RNA helicase DHX30	+	+	–
Q7Z2W4	ZCCHV	Zinc finger CCCH-type antiviral protein 1	+	+	–
Q8NCA5	FA98A	Protein FAM98A	+	+	–
Q8TEM1	PO210	Nuclear pore membrane glycoprotein 210	+	+	–
Q92900	RENT1	Regulator of nonsense transcripts 1	+	+	–

UniProtKB Accession Number	UniProtKB Symbol	Protein Name	MCF-7	C1	ΔCD
Q96B96	TM159	Promethin	+	+	–
Q96CW1	AP2M1	AP-2 complex subunit mu	+	+	–
Q96QR8	PURB	Transcriptional activator protein Pur-beta	+	+	–
Q96T37	RBM15	Putative RNA-binding protein 15	+	+	–
Q9HCE1	MOV10	Putative helicase MOV-10	+	+	–
Q9HCM4	E41L5	Band 4.1-like protein 5	+	+	–
Q9NWB6	ARGL1	Arginine and glutamate-rich protein 1	+	+	–
Q9NX58	LYAR	Cell growth-regulating nucleolar protein	+	+	–
Q9NZN8	CNOT2	CCR4-NOT transcription complex subunit 2	+	+	–
Q9UG63	ABCF2	ATP-binding cassette sub-family F member 2	+	+	–
Q9UKZ1	CNO11	CCR4-NOT transcription complex subunit 11	+	+	–
Q9UQ35	SRRM2	Serine/arginine repetitive matrix protein 2	+	+	–
Q9Y285	SYFA	Phenylalanine--tRNA ligase alpha subunit	+	+	–
Q9Y5A9	YTHD2	YTH domain family protein 2	+	+	–
P17987	TCPA	T-complex protein 1 subunit alpha	–	+	+
P84090	ERH	Enhancer of rudimentary homolog	–	+	+
Q00325	MPCP	Phosphate carrier protein mitochondrial	–	+	+
Q15366	PCBP2	Poly(rC)-binding protein 2	–	+	+
Q969G3	SMCE1	SWI/SNF-related matrix-associated actin-dependent regulator of chromatin subfamily E member 1	–	+	+
P22087	FBRL	rRNA 2'-O-methyltransferase fibrillarin	+	–	+
P61962	DCAF7	DDB1- and CUL4-associated factor 7	+	–	+
Q13347	EIF3I	Eukaryotic translation initiation factor 3 subunit I	+	–	+
Q9BUT9	F195A	Protein FAM195A	+	–	+

UniProtKB Accession Number	UniProtKB Symbol	Protein Name	MCF-7	C1	ΔCD
Q9H0A0	NAT10	N-acetyltransferase 10	+	–	+
O00571	DDX3X	ATP-dependent RNA helicase DDX3X	+	+	+
O15027	SC16A	Protein transport protein Sec16A	+	+	+
O75330	HMMR	Hyaluronan mediated motility receptor	+	+	+
P05141	ADT2	ADP/ATP translocase 2	+	+	+
P06730	IF4E	Eukaryotic translation initiation factor 4E	+	+	+
P06753	TPM3	Tropomyosin alpha-3 chain	+	+	+
P08107	HSP71	Heat shock 70 kDa protein 1A/1B	+	+	+
P11940	PABP1	Polyadenylate-binding protein 1	+	+	+
P16989	YBOX3	Y-box-binding protein 3	+	+	+
P23246	SFPQ	Splicing factor proline- and glutamine-rich	+	+	+
P25705	ATPA	ATP synthase subunit alpha mitochondrial	+	+	+
P26196	DDX6	Probable ATP-dependent RNA helicase DDX6	+	+	+
P26599	PTBP1	Polypyrimidine tract-binding protein 1	+	+	+
P27348	1433T	14-3-3 protein theta	+	+	+
P35251	RFC1	Replication factor C subunit 1	+	+	+
P36542	ATPG	ATP synthase subunit gamma mitochondrial	+	+	+
P43243	MATR3	Matrin-3	+	+	+
P51114	FXR1	Fragile X mental retardation syndrome-related protein 1	+	+	+
P51116	FXR2	Fragile X mental retardation syndrome-related protein 2	+	+	+
P52907	CAZA1	F-actin-capping protein subunit alpha-1	+	+	+
P63167	DYL1	Dynein light chain 1 cytoplasmic	+	+	+
P63244	GBLP	Guanine nucleotide-binding protein subunit beta-2-like 1	+	+	+
P67809	YBOX1	Nuclease-sensitive element-binding protein 1	+	+	+

UniProtKB Accession Number	UniProtKB Symbol	Protein Name	MCF-7	C1	ΔCD
P67936	TPM4	Tropomyosin alpha-4 chain	+	+	+
Q01844	EWS	RNA-binding protein EWS	+	+	+
Q04637	IF4G1	Eukaryotic translation initiation factor 4 gamma 1	+	+	+
Q06787	FMR1	Fragile X mental retardation protein 1	+	+	+
Q07666	KHDR1	KH domain-containing RNA-binding signal transduction-associated protein 1	+	+	+
Q08211	DHX9	ATP-dependent RNA helicase A	+	+	+
Q12905	ILF2	Interleukin enhancer-binding factor 2	+	+	+
Q12906	ILF3	Interleukin enhancer-binding factor 3	+	+	+
Q13283	G3BP1	Ras GTPase-activating protein-binding protein 1	+	+	+
Q13310	PABP4	Polyadenylate-binding protein 4	+	+	+
Q13501	SQSTM	Sequestosome-1	+	+	+
Q14004	CDK13	Cyclin-dependent kinase 13	+	+	+
Q14444	CAPR1	Caprin-1	+	+	+
Q15007	FL2D	Pre-mRNA-splicing regulator WTAP	+	+	+
Q15717	ELAV1	ELAV-like protein 1	+	+	+
Q3MHD2	LSM12	Protein LSM12 homolog	+	+	+
Q6PKG0	LARP1	La-related protein 1	+	+	+
Q7Z417	NUFP2	Nuclear fragile X mental retardation-interacting protein 2	+	+	+
Q86U86	PB1	Protein polybromo-1	+	+	+
Q8NC51	PAIRB	Plasminogen activator inhibitor 1 RNA-binding protein	+	+	+
Q8TAQ2	SMRC2	SWI/SNF complex subunit SMARCC2	+	+	+
Q8WWM7	ATX2L	Ataxin-2-like protein	+	+	+
Q92499	DDX1	ATP-dependent RNA helicase DDX1	+	+	+

UniProtKB Accession Number	UniProtKB Symbol	Protein Name	MCF-7	C1	ΔCD
Q92804	RBP56	TATA-binding protein-associated factor 2N	+	+	+
Q92841	DDX17	Probable ATP-dependent RNA helicase DDX17	+	+	+
Q99700	ATX2	Ataxin-2	+	+	+
Q9BX70	BTBD2	BTB/POZ domain-containing protein 2	+	+	+
Q9C0C2	TB182	182 kDa tankyrase-1-binding protein	+	+	+
Q9H4H8	FA83D	Protein FAM83D	+	+	+
Q9NYF8	BCLF1	Bcl-2-associated transcription factor 1	+	+	+
Q9NZB2	F120A	Constitutive coactivator of PPAR-gamma-like protein 1	+	+	+
Q9UN86	G3BP2	Ras GTPase-activating protein-binding protein 2	+	+	+
Q9Y224	CN166	UPF0568 protein C14orf166	+	+	+
Q9Y2W1	TR150	Thyroid hormone receptor-associated protein 3	+	+	+
Q9Y3I0	RTCB	tRNA-splicing ligase RtcB homolog	+	+	+
Q9Y520	PRC2C	Protein PRRC2C	+	+	+

Curriculum Vitae

Name:	Bradley Bork
Post-secondary Education and Degrees:	The University of Western Ontario London, Ontario, Canada 2012-2017 B.Sc. Honors Specialization in Biology The University of Western Ontario London, Ontario, Canada 2017-present M.Sc.
Honours and Awards:	Four-Year Admission Scholarship, 2012 Dean's Honor List, 2014-2017 Queen Elizabeth II Graduate Scholarship in Science and Technology (OGS), 2017 Queen Elizabeth II Graduate Scholarship in Science and Technology (OGS), 2018 **Declined acceptance* Alexander Graham Bell Canada Graduate Scholarship (NSERC), 2018 Children's Health Research Institute (CHRI) Travel Fund, 2018
Related Work Experience	Undergraduate Researcher The University of Western Ontario 2016-2017 Teaching Assistant, Developmental Biology 3338A The University of Western Ontario 2017-2019
Publications:	Willson, J.A., **Bork, B.S.**, Muir, C.A. and Damjanovski, S. (2019). Modulation of RECK levels in *Xenopus* A6 cells: effects on MT1-MMP, MMP-2, and pERK levels. *J. Biol. Res. (Thessalon).* 26:16-26
Presentations: Oral	**Bork, B.S.** and Damjanovski, S. (2018). MT1-MMP mediated cell signalling in MCF-7 cells: more than just an enzyme. Biology Graduate Research Forum. London, ON. **Bork, B.S.** and Damjanovski, S. (2019). Identifying membrane-type 1 matrix metalloproteinase (MT1-MMP) binding partners in MCF-7 cells. Biology Graduate Research Forum. London, ON

Posters at International Conferences:

Bork, B.S., Muir, C.A. and Damjanovski, S. (2018). Membrane-Type 1 Matrix Metalloproteinase (MT1-MMP) cytoplasmic domain alters TGF-β signalling in MCF-7 breast cancer cells. The American Society for Cell Biology Annual Meeting. San Diego, CA (USA).

Muir, C.A., **Bork, B.S.**, Neff, B.D. and Damjanovski, S. (2018). Elevated embryonic incubation temperature alters cardiogenesis gene expression and heart function in Atlantic salmon (*Salmo salar*). The American Society for Cell Biology Annual Meeting. San Diego, CA (USA).